Use of Oncolytic Adenovirus expressing Interferon (IFN) Alpha as a tool to improve IFN-based chemoradiation regimen to treat pancreatic cancer

A DISSERTATION
SUBMITTED TO THE FACULTY OF THE GRADUATE SCHOOL
OF THE UNIVERSITY OF MINNESOTA
BY

Amanda Oliveira Salzwedel

IN PARTIAL FULFILLMENT OF THE REQUIREMENTS
FOR THE DEGREE OF
DOCTOR OF PHILOSOPHY

Advisor: Masato Yamamoto MD, PhD
Co-Advisor: Julia Davydova MD, PhD

February 2018

Acknowledgments

First of all, I would like to thank my mentor Dr. Masato Yamamoto for all his hard work, time, and dedication in guiding me through this process. His admirable example as a mentor, scientist, and doctor was a true inspiration throughout my PhD helping me not only to become a better scientist, but also a better person. Thank you, Dr. Yamamoto, for carrying out the role of a mentor so well, recognizing the strengths and weakness of each person on your team and working with each of them so that they could achieve their full potential. Thank you for knowing how to lead and teach by example, always motivating us to give our best when developing our work and our career. I also would like to acknowledge my co-adviser, Dr. Julia Davydova. Her friendship, kindness, and dedication pushed me to improve myself and were also key to my achievements. Her continuous feedback during lab meetings and private meetings always brought insightful suggestions that greatly contributed to the development of my projects. Thank you for always contributing with a different and valid point of view to our research. I am very grateful you highly recommended me to Dr. Yamamoto. Thank you for believing in my potential as a scientist. I have no words to express the extent of my gratitude for having the opportunity to have Dr. Yamamoto and Dr. Julia Davydova mentoring me during my Ph.D.

I also thank my committee members: Dr. Colin Campbell, Dr. David Brown, Dr. Sundaram Ramakrishnan, and Dr. Julia Davydova for participating and contributing to the completion of my work. Your feedback was always constructive and much appreciated.

Finally, I would like to thank my family and my husband Matthew for their constant support during my Ph.D. Their endless motivation and dedication to me were essential for me to get to this point. I would not have done it without them.

I dedicate this thesis to my parents Humberto and Silési who gave me the greatest gift of all—they always believed in me. Everything that I am and have achieved in my life I owe to them.

Abstract

Pancreatic Ductal Adenocarcinoma (PDAC) may soon become the third-leading cause of cancer-related death in the United States. Aside from curative resection of tumors, there is no highly effective therapy to treat PDAC. Because patients are usually diagnosed in the late stage of the disease, more than 80% of them are not eligible to undergo surgery, which results in a post-diagnosis survival rate of three to four months, and an extremely low five-year survival rate of 6%. Despite discouraging current clinical outcomes, clinical trials treating PDAC patients with adjuvant therapy combined with IFN-α (IFN), Fluorouracil (5-FU), Cisplatin (CDDP), and radiation have shown to improve patients' two-year survival rates by 20-41%, and improve their five-year survival rates by 35%. These clinical trials show that IFN-therapy is now one of the few therapeutic regimens that can significantly improve the short- and long-term survival of PDAC patients.

Despite its high efficacy, the drawbacks of IFN therapy included high IFN systemic toxicity, which resulted in increased patient drop-out rates in clinical trials, and low levels of the cytokine in tumors, which hampered the chemo-radio-sensitization capability of IFN during therapy. To attempt to improve the efficacy and overcome the drawbacks of IFN therapy, we studied the use of IFN-expressing replication competent oncolytic adenovirus (OAd) vectors in combination with chemoradiation mimicking the aforementioned chemoradiation and IFN-based clinical trials. Because IFN therapy can stimulate a tumor-specific immune response, we first evaluated the anti-tumor effect of oncolytic adenovirus vector expressing hamster IFN (OAd-hamIFN) in a syngeneic immunocompetent PDAC hamster model. To further understand the interaction between IFN-expressing OAd and chemotherapy, radiation, and chemoradiation, and to evaluate the therapeutic effect of the virus used in treatments mimicking the IFN therapy, we also tested the effect of a human IFN-expressing oncolytic adenovirus (OAd-IFN) in immunodeficient mice bearing human PDAC xenografts. To increase infectivity of OAd-hamIFN in hamster pancreatic cancer cell lines, we included the RGD-4C (Arginive-Glycine-Aspartic) motif in the HI loop of OAd-hamIFN fiber. This modification is known to shift viral tropism from the Coxsackie and Adenovirus Receptor (CAR) to integrins αvβ3 and αvβ5, which are widely expressed in hamster pancreatic cancer cell lines. To increase infectivity of OAd-IFN in human

pancreatic cancer cells lines, we replaced the adenovirus type 5 fiber with the chimeric adenovirus 5/3 fiber, which consisted of the fiber of adenovirus type 5 with the knob of adenovirus type 3. This modification has been proven to shift viral tropism from CAR receptor, which shows low expression in human pancreatic cancer cells, to Desmoglein type-2 and CD46 proteins, which are widely expressed in human pancreatic cancer cell lines. To improve spreading in tumors and oncolytic effect of both OAd-hamIFN and OAd-IFN in PDAC cells, and to achieve replication-dependent expression of IFN, we included the Adenovirus Death Protein (ADP) and respective IFN genes in the adenovirus (Ad) E3 region. To restrict the replication of human IFN expressing OAd vector (OAd-IFN) in human PDAC cells, we added the cyclooxygenase-2 (Cox-2) promoter upstream of the Ad E1 region, which is the region responsible for initiating viral replication.

Combinations of 5-FU, radiation, and 5-FU + Radiation with OAd-hamIFN in hamster PDAC cells, or with OAd-IFN in human PDAC cells, resulted in highly synergistic and cytotoxic combinations *in vitro*. Studies in the syngeneic hamster PDAC model showed that including OAd-hamIFN in combination with therapeutics used in IFN therapy improved treatment efficacy, and that using the virus in treatment mimicking the IFN therapy (OAd-hamIFN + 5-FU + Radiation) was the most effective treatment strategy in the study. When we analyzed the effect of OAd-IFN in combination with 5-FU + CDDP in human PDAC cells, the combinations were antagonistic and weakly cytotoxic. But adding radiation to the treatment (OAd-IFN + (5-FU + CDDP) + Radiation) overcame the chemotherapy antagonism, which resulted in highly synergistic and extremely potent treatments *in vitro* and in mice bearing PDAC xenografts.

Because radiation eliminated the antagonism of chemotherapy to the virus *in vivo*, we tested different radiation protocols in combination with OAd-IFN in mice bearing PDAC tumors. We concluded that administering radiation before infecting tumors with OAd-IFN improved treatment efficacy and that using radiation before OAd-IFN infection should potentiate the effect of Cox-2 controlled IFN-expressing OAds in combination with chemoradiation.

In summary, our data strongly support including an IFN expressing OAd in treatments mimicking IFN therapy. As this therapy is one of the few therapeutic regimens shown to improve patients' short- and long-term survival rates, developing a virus-based IFN treatment protocol may result in a highly effective means to treat PDAC.

Table of Contents

List of Tables

List of Figures

Background Figures:

Figures in Chapter I

Figures in Chapter II

1. Background

1.1. History of virotherapy

The years leading up to the twentieth century marked the beginning of modern medicine. Charles Darwin introduced the theory of evolution and Gregor Mendel began the field of genetics by describing basic concepts of genetic inheritance. Louis Pasteur and Robert Koch founded modern microbiology, and Claude Bernard enunciated principles about the internal environment of the body that contributed to the development of the fields of physiology, biochemistry, and pathology. These advances in biological sciences were accompanied by innovations in the field of human medicine with the invention of the stethoscope, use of x-rays, development of anesthesia, and the treatment of infections. Despite considerable scientific, technological, and biological progress, there were no reports of appreciable improvements in the treatment of human malignances such as cancer. Cancer treatment was restricted to primitive surgical procedures, and the use of non-effective therapeutic approaches like the use of castor oil and arsenic (1, 2). Despite further advances in the treatment of malignances with emerging chemotherapies and the use of radiotherapy in the 1940s, these methods still were not effective in improving the long-term survival rates of patients affected by many types of cancers, including pancreatic cancer. There still is a pressing need to find alternative and efficacious methods to treat cancer.

The relationship between viruses and human diseases has two contrasting aspects: 1) oncogenic viruses can induce carcinogenesis (3, 4); and 2) other viruses can be effective in treating cancer. Using viruses to treat cancer was not premeditated, but coincidental. The development of the field of virotherapy began at the end of the nineteenth century with the observation that leukemia patients who became naturally infected with influenza had a brief remission in the course of their disease. Although complete leukemia remission was never reported, viruses started to be considered as a promising therapeutic modality to treat malignancies (1, 5). Incidences occurred where patients with leukemia (5, 6), Hodgkin's disease (7, 8) , and Burkitt's lymphoma (9) would also show disease regression when concomitantly and naturally infected with the measles virus. Similar case reports were also

described in cancer patients who were naturally infected with the hepatitis virus. In fact, infection of Hodgkin's disease patients with the hepatitis virus is historically cited as one of the first attempts to use a virus as a therapy to treat cancer (1). With the evolution and experimentation in the virotherapy field, viruses causing serious disease such as West Nile, Uganda, dengue, and yellow fever viruses were casually tested in cancer patients. Because of the lack of efficacy and safety when using these viruses, there was a gradual shift in the virotherapy field to study the efficacy of adenoviruses, poxviruses, picornaviruses, paramyxoviruses, and herpes viruses in treating malignancies. Talimogene laherparepvec (Imlygic or T-VEC), is a herpes simplex virus that was modified and tested in the treatment of melanoma (10-12). In 2015, Imlygic was the first vector approved by the Food and Drug Administration for use in treating melanoma patients in the United States, and it is also being used in Europe (13).

In summary, the widespread testing and use of viruses in treating malignancies greatly advanced and built the foundation of virotherapy as a modality to treat cancer. Through extensive experimentation and observation in the field, there are several important key points about using viruses to treat cancer: a) viruses can be used to eliminate tumors and can be well tolerated by the patients; b) successful tumor regression is usually seen in younger patients with compromised immune systems (e.g., leukemia or lymphoma patients).

1.2. History of adenovirus use in virotherapy

Using adenoviruses to treat cancer began in the early 1950s when the adenovirus—A.K.A. adenoidal-pharyngeal-conjunctival virus—was identified as an oncolytic agent in pre-clinical models (1). Contrary to previously used viruses such as the hepatitis and West Nile viruses, which provoked life-threatening side effects in patients, oncolytic adenoviruses (OAd) only induced mild common cold-like symptoms (14). The safety of the adenovirus in patients rapidly promoted this viral agent for use in clinical trials to treat cervical cancer (15). Viral administration was safe when given intravenously, intravascularly, and intra-arterially to women presenting with epidermoid carcinoma of the cervix. But although the use of OAd resulted in remarkable localized tumor necrosis, the immune system quickly

eradicated the virus, and none of the trials showed a significant increase in the rate of patient survival (16, 17). This was the first indication of the impact of pre-existing immunity against adenovirus in the treatment efficacy.

To date, there are 67 identified serotypes of adenovirus, and they are subdivided into groups A through G. Groups A, F, and G have been associated with gastrointestinal tract diseases; groups B, D, and E with conjunctivitis outbreaks; and groups B, C, and E with upper respiratory tract infections (18-20). Human adenoviruses have been studied extensively over the years, and there is extensive knowledge about their replication cycle, genome, structure, cells, and pre-clinical models susceptible to viral replication. Human Adenovirus type 5 (Ad5), which belongs to group C, is the most genetically modified and classically used serotype in cancer virotherapy (21).

A review of the literature in this area thoroughly describes the use of tissue-specific promoters to restrict viral replication to specific cancer types; retargeting of viral infection by fiber modification; elimination of antibody neutralization by modifying highly antigenic regions of the virus; and modifying the viral genome to eliminate regions responsible for initiating viral replication in healthy tissues (21-28). After the aforementioned clinical trials where wild type Ad5 was used to treat cervical cancer, a variety of genetically modified adenovirus vectors were tested in multiple clinical trials targeting pancreatic cancer, ovarian cancer, head and neck cancer, and other cancer types (21, 29-32). Although many of these trials did not provide enough evidence for the United States Food and Drug Administration to approve OAd for treating the targeted cancers, in 2005 the State Food and Drug Administration in China approved a genetically modified Ad5 based vector (H101) as a drug to treat head and neck cancer (33). This was the first time in the history of OAd use that a replication-controlled OAd vector was proven to be efficacious in treating a solid tumor. Despite steady and exponential progress in the virotherapy field, the fatal death and negligent administration of a genetically modified adenovirus to correct a metabolic syndrome in a teenager caused the quick cessation of OAd use and skepticism in the field (34-36).

2. Adenovirus

2.1. Structure and replication cycle

Human adenoviruses are non-enveloped, double-stranded DNA viruses belonging to the Adenoviridae family **(Figure 1)**. The viruses measure 70-90 nm and possess an icosahedral capsid encasing a tightly packed 36kB viral genome (37). As mentioned above, there are 67 identified adenovirus serotypes, which are subdivided into groups A–G. Human Adenovirus type 5 (Ad5), which belongs to group C, is the most genetically modified and classically used serotype in cancer virotherapy (21). Hexon is the most abundant protein in the viral capsid (approximately 240 units total), and its expression in the late phase of the virus-replication cycle is commonly used to track viral replication in vitro and in vivo (24, 38). Viral fibers are individually connected to each of the 16 penton bases present in the capsid. The adenovirus fiber is a homotrimer with each subunit consisting of three domains: the amino-terminal tail, which is connected to the penton base protein; the shaft, which is comprised of a 15 residues motif repeated 22 times; and the knob, which established the primary contact between the virus and the cellular receptor (39-41).

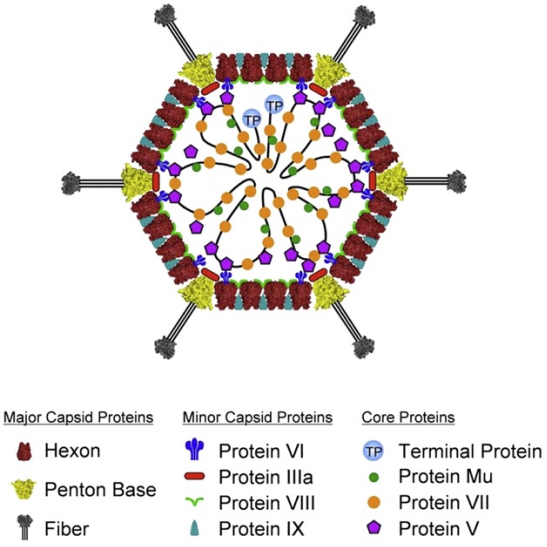

Figure 1: Human adenovirus structure. Figure reproduced from reference (37)

Except for adenoviruses belonging to group B, which bind to CD46 surface proteins (42), all other adenovirus groups bind to the coxsackievirus and adenovirus receptor (CAR)(43). After high affinity binding between the fiber knob and adenovirus receptor (CAR or CD46), there is a secondary binding interaction between the RGD (Arg-Gly-Asp) motif located on the penton base of the adenovirus capsid and cellular integrins, fibronectins, or vitronectins receptors. There are over 20 known integrins that can be recognized by the RGD motif. Among these, the most common ones are αvβ3, αvβ5, αvβ6, and αvβ8. Of the fibronectin and vitronectin receptors, the most common ones recognized by the RGD motif are: α5β1, ,α8β1, and α_vβ1-8 (44). Complete binding of virus to the receptor induces viral-clathrin mediated endocytosis followed by fusion of clathrin coated pit and cellular lysosomes (late endosome formation). Acidification of late endosome induces capsid uncoating by conformational changes in the viral capsid proteins leading to shedding of the penton base, pIIIa protein, fiber, and peripentonal hexons. Protein pVI, which contains an amphipathic domain in its N-terminal tail, interacts with the endosomal membrane and releases uncoated capsid into the cellular cytoplasm. The uncoated capsid interacts with cellular microtubules and it is presumed that the motor proteins (e.g., dynein and kinesin) direct viral capsid to the nuclear pore (37). Filament protein CAN/Nup214 and nuclear histone H1 bind to the capsid hexon protein and stably dock the capsid in the nuclear pore complex (NPC). Retrograde movement of capsid driven by microtubular motor proteins pull the capsid in the opposite direction of the NPC, which results in capsid disruption and viral DNA release. The exact method of transport of viral DNA through the NPC is controversial, but there is evidence that the histone H1 and hsc70 mediate the process (45, 46). Once inside the nucleus, the transcription process starts. The adenovirus genome is divided into early genes (E1, E2, E3, and E4), late genes (L1, L2, L3, and L5), the VA-RNA region. The L5 region is also classified as the fiber region in the adenovirus genome (47). Both extremities of the adenoviral genome (or the Inverted Terminal Repeats (ITRs)), are covalently bound to the Terminal Protein (TP) and possess an origin of replication. The NF-1 and Oct-1 cellular transcription factors bind to the 5' origin of replication and contribute to the formation of a transcription pre-initiation complex that enhances the start of viral DNA replication.

The replication process starts by the expression of genes from the adenoviral E2 region encoding for TP precursor (pTP), adenovirus DNA polymerase (Ad-pol), and DNA-binding protein (DBP). In conjunction with the NF-1 and Oct-1 factors, the DBP binds and helps in the remodeling of the pre-initiation complex. Protein-primed DNA synthesis starts by the covalent addition of a dCMP residue to the pTP. After some intermediary processes and covalent modifications of the TP by the Ad-pol, the polymerase detaches from the pTP region. After it detaches, there is an increased rate of polymerization and proofreading by the Ad-pol enzyme that continues the process of viral DNA extension and replication. In the final stages of replication, the pTP is cleaved by a viral protease resulting in TP, which follows attached to recently formed viral DNA. This step completes the replication process, and the newly formed viral DNA is ready to be encapsidated (48). The encapsidation process occurs when freshly formed capsids are transported through the nuclear pore by the protein VI, which is a structural protein located below the 12 vertices of the adenoviral capsid. The protein VI possesses nuclear localization signals in its C-terminus region, and works as an adaptor that facilitates hexon import through the nucleus (49).

2.2. Adenovirus early gene expression

Expression of adenovirus early genes (E1-E4) is essential to initiate and complete successful viral replication in host cells. Each of the adenovirus's early regions is controlled by an individual promoter. Expression of the adenovirus's E1 region results in the transactivation of the subsequence promoter regions (E2, E3, and E4) and tightly orchestrates the progression of the viral cell cycle. Proteins E1A, E1B 19K, and E1B 55K are some main products of adenoviral E1 region. E1A binds to the cellular Rb and releases the E2F transcription factor. Free E2F drives the cell cycle to the S-phase and boosts the cell's capacity for DNA replication and, consequently, protein production (50). Proteins E1B 19K and E1B 55K, respectively, inhibit and target for degradation cellular Bcl-2 and p53 proteins (51, 52). Because Bcl-2 is a pro-apoptotic protein, and p53 is a tumor suppressor that also induces apoptosis, the degradation of both proteins will ensure that the infected host cell progresses to the S-phase without undergoing apoptosis. As discussed above, the E2 region of the adenovirus genome is responsible for expressing the viral DNA polymerase. The E3 region encodes for many different gene products, most of which are

related to inhibiting the host immune system's identification of virus infected cells. The E3-gp19K protein, for example, prevents the loading of intrinsic cellular peptides (including viral peptides) into the class I major histocompatibility-mediated antigen presentation complex (MHC-I). As a result, the identification and elimination of infected cells by the cytotoxic T lymphocytes (CTLs) is blunted (53, 54). Another important function of the adenoviral E3 region is the expression of the Adenoviral Death Protein (ADP). ADP is a palmitoylated integral membrane glycoprotein that is expressed early on in the viral cell cycle, but is greatly amplified during later stages of infection. ADP expression is correlated with increased cell lysis and viral spreading (54). Although it is not clear how ADP causes cell lysis, the protein is found in the nuclear membrane and Golgi complex. Because the final viral assembly and DNA encapsidation occurs in the nucleus (49), it is possible that ADP lysis of the nuclear membrane makes the process of viral release more efficient. High ADP expression becomes particularly important in designing oncolytic vectors to kill cancer cells. Since most of the E3 region's genes are not essential, it is possible to induce massive ADP expression by deleting most genes from this region and reintroducing ADP to the same location (54).

The E4 region contains a variety of genes that modulate transcription, cell cycle, cell signaling, and interfere with cellular DNA repair (55). The E4 region also contains genes that are not essential to viral replication and that can be replaced by other transgenes (e.g., enzymes, cytokines, prodrugs, and others). Although both the E3 and E4 regions can lead to high expression of transgenes, the E4 region has been found to produce comparatively higher yields of expression (55, 56).

2.3. Adenovirus late gene expression

The adenovirus's late-phase genes—L1, L2, L3, L4, and L5— encode capsid proteins or proteins that are responsible for capsid assembly. The Major Late Promoter (MLP), which is minimally active during the first phase of adenovirus replication, controls the expression of these genes. With the expression of the Iva2 and pIX (minor capsid proteins), transcription through the MLP becomes fully activated, and the MLP strongly expresses the remaining major and minor capsid proteins and adenovirus fiber (57). During late gene

expression, protein synthesis in the host cells is heavily suppressed because the adenovirus tripartite leader (TPL) shuts down the host's cellular cap-dependent mRNA translation. At this stage, the cell's protein translation machinery becomes exclusively dedicated to producing adenovirus proteins. Adenovirus TPL is composed of three introns (TPL 1–3), and mediates the nuclear export, translation, and stability of late viral mRNAs that will in turn be translated into adenoviral-structural proteins in a cap-independent manner (58). Viral structural proteins are comprised of hexon, fiber, penton, polypeptides core proteins V and VII, as well as minor polypeptide proteins: IIIa, VI, VIII, IX, and X-XII. Besides playing a role in the agglutination of cells and the induction of the host's antibody response, these proteins are essential to maintaining viral structure and infectivity (59).

2.4. Adenovirus VA-RNA

The adenovirus-associated RNA (VA-RNA) are non-coding RNA transcripts that are abundantly expressed during adenovirus replication. RNA concentrations can reach up to 10^8 DNA copies per cell and measure 150–200 nucleotides long. Approximately 80% of all adenoviruses, including Ad5, encode two distinct VA-RNA transcripts (VA-RNAI and VA-RNAII) and both VA RNAs are transcribed by the cellular RNA Polymerase III. The expression of VA-RNA is essential during viral replication because its absence during replication can result in about a about 60-fold decrease in viral yield in infected cells. Beginning at 18hrs post-infection, the VA-RNAI and VA-RNAII accumulate in the cytoplasm, and their peak expression happens by the end of the lytic cycle (24hrs post-infection) (60).

Although the VA-RNAs have several proposed functions, their main function is to inhibit the shutdown of protein translation in the host cell through RNA-activated protein kinase (PKR)(60). Expression of PKR is induced by type I Interferons (IFN-α and IFN-β), which orchestrate an anti-viral cellular response against DNA and RNA viruses. The IFNs act in a species-specific manner and exert their actions through cell-surface receptors (IFNAR-1 and IFNAR-2) (61, 62). The presence of double-stranded RNA in the cellular cytosol results in the transcriptional activation of the type I IFN promoters and the expression of IFN response genes. As the result, production of type I IFN by the infected cells is

stimulated, and newly expressed IFN acts in a paracrine and autocrine manner to stop the viral infection from progressing to neighboring cells.

Although IFN-stimulated expression of MHC-I, PKR, Mx GTPase protein, and inducible nitric oxide synthase all contribute to protecting the cell against viral infection, the stimulation of PKR is markedly important in this process (61). PKR can inhibit protein translation in the host cells by performing serine phosphorylation in the cytosolic eIF-2 (63). Phosphorylation of eIF-2 affects the formation of the translation initiation complex in cells, which, in turn, shuts down protein translation. The VA-RNA produced by the adenovirus can co-localize with the translation-initiation complex in infected cells and inhibit the phosphorylation of eIF-2. It also helps in preferential protein translation from viral RNA, which then forces the cell to progress with a massive production of viral proteins and newly formed virions regardless of IFN anti-viral effects (60, 61).

2.5. Oncolytic Adenoviruses (OAds)

Because OAds display a lytic-replication cycle—meaning that they disrupt the host's cells by the end of replication—they are an attractive tool for cancer therapies since they can cause debulking and elimination of solid tumors (21, 24, 38). During oncolysis, OAds release tumor-specific peptides into the host's immune system, which stimulates formation of an anti-tumor immune response (21, 64). Conditionally Replicating Adenoviruses (CRADs) are replication-competent OAds that are designed to replicate and kill a specific type of target cell (eg. cancer cells) (21, 65). Targeted replication of CRADs in cancer cells can be achieved by introducing a cancer-specific promoter upstream of the E1 region of the viral genome. Because there is differential expression of this promoter in cancer tissue as compared to normal tissue, CRADs restrict their replication to cancer cells avoiding normal cells (21). Another way to target the replication of CRAds in cancer cells is to delete the adenovirus's E1A and E1B region. Because protein coded by these two regions induce E2F release from Rb, and target p53 for degradation, modified vectors will restrict their replication to cells that are deficient in Rb and p53. Since most cancer cells lack Rb and p53, but normal cells do not, CRADs target their replication in cancer cells (21, 65-67). It also is possible to modify the fiber in OAds to target receptors that are differentially

expressed in cancer cells, or to gain infectivity to a cell type that lacks its natural receptor (CAR). For example, pancreatic cancer cells show a very low expression of CAR, but show a higher expression of mesothelin or desmoglein type-2 receptors. Substituting the knob of the Ad 5 fiber for the knob of Ad type 3 can shift the tropism of Ad5 from CAR to the mesothelin or desmoglein type-2 receptors, which can increase the infectivity of modified Ad5 to pancreatic cancer cells (21, 38, 56).

3. Immune response vs adenovirus-based therapy

3.1. Effect of preexisting immune response in adenovirus-based therapy

Evoking an immune response against adenovirus may or may not be beneficial during cancer treatment. One potential obstacle when using the virus to treat cancer is that many patients have pre-existing anti-adenovirus neutralizing antibodies. The presence of these antibodies can reduce treatment efficacy because they neutralize and eliminate a considerable number of viral particles during therapy (68). Despite this limitation, there are reports showing that the presence of anti-adenovirus antibodies in patients before or during treatment using the virus does not affect therapy efficacy. For example, in the Cellgenesis prostate cancer clinical trial based on the use of a Prostate Specific Antigen (PSA) replication controlled OAd, levels of adenovirus-specific antibody titers in patients did not correlate with decreased therapeutic efficacy or increased patient PSA levels (69). These data showed that although anti-adenovirus antibodies were present, the viral therapy was effective and the PSA levels were diminished after therapy. Another example is a recent clinical trial and subsequent report describing the intravenous administration of a chimeric adenovirus vector (Psioxus) for the treatment of colon cancer (70). In this trial, although treatment with the Psioxus vector elicited an antibody response, the patients still experienced a reduction in tumor size.

3.2. Effect of innate immune response during Adenovirus-based therapy

The earliest sensors that trigger an innate immune response against the adenovirus are the a) binding of the adenovirus fiber to the CAR receptors; and b) binding of the RGD motif in the adenovirus penton base to the cellular integrins or fibronectin receptors. When the

virus fiber binds to CAR receptors, there is clustering of junctional adhesion molecule-like protein (JAML) and the activation of phosphoinositide 3-kinase (PI3K), which eventually leads to the activation of the NF-κB pathway and the production of pro-inflammatory chemokines and leukocyte recruitment (71). When the RGD motif binds to cellular integrins, especially the αvβ3, it leads to the production of IL-1 beta, which can also be stimulated when viral DNA binds to the Toll-Like Receptor 9 (TLR9) in the late endosomes. The downstream pathway of TLR9 activation stimulates the NF-κB pathway, which, in turn, produces chemokines and cytokines, including IL-1.

Of the many ways that the innate immune response can fight a pathogen, the stimulation of IFN-type I (IFN) and the Interleukin-1 (IL-1) pathways are the main innate immune responses to eliminate virus infection. The chemokines and cytokines that are induced by the IFN and IL-1 pathways induce the expression of P-selectin, E-selectin, and α-integrins in blood vessels (72). These cytokines also induce the opening of blood-vessel fenestration, which leads to the extravasation of cellular pro-inflammatory infiltrate to the infected areas. The pro-inflammatory infiltrate is usually comprised of leukocytes, $CD11b^+$ neutrophils, NK cells, and macrophages. This cellular infiltrate eliminates infection and infected cells.

In most cases, treatment with adenovirus vectors also can lead to high levels of infectious particles trapped in the liver. As a result, liver-resident macrophages (Küpffer cells) phagocyte the virus and release pro-inflammatory cytokines and chemokines such as tumor necrosis factor-alpha (TNF-α), IP-10, and RANTES. Depending on the dose of adenovirus used to treat the patient, and the level of viral particles that the patient retains in his or her liver, the induction of cytokines can be extremely elevated and lead to acute liver failure (35, 73).

Although the activation of an innate immune response can be extremely beneficial in the treatment of cancer patients (74), it also can lead to fast viral clearance (80%) in the host or cancer patient within the first 24 hours after infection. On the other hand, the stimulation of an innate immune response against the virus can boost treatment efficacy when CTLs and Natural Killer (NK) cells are recruited to the infection site by chemokines, and these

cells eliminate virally infected cells, which in the case of OAd therapy, are cancer cells (21). Also, when using an oncolytic adenovirus during treatment, virus-induced oncolysis can broaden the repertoire of cancer-specific peptides presented to the immune system, stimulate CD8 tumor-specific T-cells, and cause immunological awakening at the cancer site (75). Although tumors are immunosuppressed environments, OAd oncolysis results in the expression of chemokines and cytokines, which, in turn, coordinate the activation of NK cells and the formation of cellular immunity at the cancer site (75, 76). Oncolysis also can make tumors resistant to PD-1/PD-L1 immunotherapy, susceptible to this therapeutic approach (75). Patients who develop an anti-tumor immune response, especially with tumor CTLs and NK cells, are reported to have delayed disease recurrence and a better ability to fight metastases and micrometastases (74).

3.3. Effect of acquired immune response in adenovirus-based therapy

During infection, professional antigen-presenting cells (APC), such as dendritic cells and macrophages, phagocytize viral particles and present their viral specific peptides on their class II major histocompatibility-mediated antigen presentation complex (MHC-II). APCs then migrate to the draining lymph nodes and prime and activate native T cells against the viral peptides. Activated T-cells (CD4+ and CD8+) leave the lymph nodes and scan the body to identify viral antigenic epitopes presented in the MHC-I of infected tissues. When activated T-cells recognize an antigen, they produce IFN-γ and express pro-inflammatory cytokines such as IL-1, IL-6, and TNFα which aids in the recruitment and activation of leucocytes. The activation of B cells through phagocytosis or by contact with activated T-cells results in the production of high titers of adenovirus-specific antibodies and the formation of adenovirus specific memory B cells (77, 78). Because as much as 80% of the human population has been exposed to at least one of the 67 adenoviruses serotypes during their lifetime (77), most of the population has adenovirus-specific memory B cells against at least one serotype of the virus. Therefore, the treatment of cancer patients using adenovirus vectors results in the rapid production of high titers of anti-adenovirus antibodies that might or may not interfere with therapeutic efficacy.

There are several ways to avoid the deleterious effects of a patient's pre-existing immunity to the adenovirus and improve treatment efficacy. Because most of the anti-adenovirus antibodies recognize viral capsid proteins, covalent modifications of capsid immunodominant peptides with FDA-approved Polyethylene-Glycol (PEG) can inhibit the immediate production of antibodies (79). Encapsulation of the virus vector with inert polymers can also achieve the same goal (80, 81). Immunosuppression with dexamethasone (82), cyclosporine (83), cyclophosphamide (84), deoxyspergualin (85), and Tacrolimus (86) are also pharmacological alternatives that can be administered to patients before they are treated with an adenovirus vector.

As previously mentioned, although there are many ways to decrease the effect of a preexisting immune response against the adenovirus during therapy, there is no clear clinical indication that the presence of anti-adenovirus neutralizing antibodies can eliminate the efficacy of adenovirus-based cancer therapies (69, 70). Despite the lack of persuasive clinical evidence, however, it is true that the presence of anti-adenovirus neutralizing antibodies have the potential to eliminate a great number of the viral particles when a virus vector is administered intravenously. The role of neutralizing antibodies during adenovirus therapy is controversial. Some reports, for example, indicate that the presence of antibodies can increase liver toxicity by stimulating elevated antibody mediated virus phagocytoses by Küpffer cells in the liver, which can result in high expression of pro-inflammatory cytokines leading to liver failure. Contrary to that, other reports show that the presence of antibodies actually mitigates virus-induced liver toxicity (77).

4. *In vivo* models to study human oncolytic adenovirus therapy

4.1. Mouse models

While mice models are widely used to test the efficacy of the adenovirus in cancer treatment, mice are not permissive to human adenovirus replication (87-89). Infection of murine cancer cells with human adenovirus type 5 (Ad5) is reported to result in 1000-fold lower viral yields compared to infection of human cancer cells with Ad5 (88, 89). There also is evidence that viral DNA and RNA are greatly reduced in mice cells, as is the

expression of viral early and late genes (88). Published studies showed that intravenous administration of Ad5 in mice resulted in detectable lysis of liver cells, but replication of the virus was incomplete and there was no increase in adenovirus titers in the blood over time. Although the adenovirus's natural site of replication in humans is considered to be the lungs, studies trying to assess Ad5 replication in mice showed that the virus displayed transient or very low levels of replication in murine lung cells (89). The main disadvantage of using mice to study adenovirus-based therapies is the inability to clearly analyze the toxicity of an adenovirus vector in normal tissue. This limitation, however, does not invalidate using mice in adenovirus cancer research. Immunodeficient mice can be engrafted with human cancer cell lines or patient-derived tumors, which allows an isolated assessment of adenovirus-therapy efficacy in these tissues without the interference of the immune response. In this scenario, mice can provide an *in vivo* assessment of the inhibition or potentiation of drugs in viral replication, the spreading of the virus in human tumors, and the susceptibility of human tumors to adenovirus therapy. On the other hand, in case studies involving the tumor microenvironment are conducted, it is necessary to be aware that although human cancer cells are injected in the animals, mice fibroblasts and other mice derived cells will be composing most of the tumor microenvironment.

4.2. Hamster models

Golden Syrian hamsters (*Mesocricetus auratus*) are one of the few animals considered to be permissive for human adenovirus replication (87, 90). Intranasal infection of hamsters with Ad5 showed that there is a sustained viral replication in the lungs followed by a gradual increase in viral titers in the blood over time (91). Previous studies that assessed replication of the virus *in vitro* also confirmed productive adenovirus replication and expression of late gene products in a variety of hamster cells (89). Unlike mice, hamsters can be used to assess virus toxicity in normal tissues during adenovirus-based treatments. Hamsters can also be extremely useful when analyzing the effectiveness of adenovirus therapy in cancer treatment, especially pancreatic cancer. Since hamsters have a very low variability in their major histocompatibility complex genes (Hm-1)(92) (especially if they are inbred for research), use of hamster pancreatic cancer cells lines such as HP1, HAPT-1, H2T, PC1, and WD to grow tumors in these animals results in a syngeneic

immunocompetent model of pancreatic cancer (93, 94). This model allows the assessment of adenovirus replication in noncancerous tissues; safety of adenovirus replication controlled by specific promoters; the effect of anti-adenovirus immune response during treatment; and the effect of anti-tumor immune response during therapy. It is also possible to generate more clinically translatable data and have a clearer understanding of how to manipulate OAd-based therapies to achieve maximum effect in cancer patients. While a syngeneic immunocompetent cancer model is extremely resourceful, the availability of reagents to assess the immunological response in hamsters still is very limited. Although this is not an insurmountable obstacle, it still poses limitations on the thoroughness of immunological analyses that can be done using these animals.

5. Pancreatic cancer

Pancreatic cancer may soon be the third leading cause of cancer-related death in the United States (95). In 2017, about 53,670 people will be diagnosed with pancreatic cancer, and 43,090 will die from the disease. Pancreatic cancer accounts for 3% of all cancers in the U.S. and about 7% of all cancer deaths. The risk factors associated with the disease are both changeable and non-changeable. The changeable risk factors include smoking, excess weight and obesity, and exposure to heavy metals, and carcinogenic substances. The non-changeable risk factors are age (the average age of detection is 71), race (African–Americans are at greater risk than Caucasians), family history, genetic inherited syndromes (possessing KRAS, P53, P16, and other shared pancreatic-cancer mutations), diabetes, pancreatitis, liver cirrhosis, and stomach problems (e.g., infection with *Helicobacter pylori)* (96).

The early stages of pancreatic cancer are usually asymptomatic. The majority of patients are diagnosed when the disease spreads and starts to compromise the functions of other organs. Although levels of cancer markers CA 19-9 and carcinoembryonic antigen (CEA) are closely correlated with pancreatic cancer, detectable levels are mostly found in advanced cases of the disease. And even though a tumor may have spread beyond the pancreas, not all patients show elevated levels of these markers (96-98).

Pancreatic cancer can be divided in subtypes (96, 99):

Pancreatic Ductal Adenocarcinoma (PDAC): PDAC causes 90% of pancreatic cancer cases. It originates from the cells lining the pancreatic duct and is usually malignant and aggressive.

Acinar Cell Carcinoma: Acinar Cell Carcinoma is a rare form of pancreatic adenocarcinoma. Its tumors are characterized by excessive production of pancreatic lipase.

Intraductal Papillary-Mucinous Neoplasm (IPMN): IPMN is a cystic tumor that grows from the main pancreatic duct. It appears to be benign in its early stages, but can progress to adenocarcinoma.

Mucinous Cystadenocarcinoma: Mucinous Cystadenocarcinoma is a rare, malignant, cystic tumor that is filled with mucin. It occurs in only one area of the pancreas and is usually in the tail. This type of tumor is found mostly in women.

Pancreatic Neuroendocrine Tumors (NETs): NETs are pancreatic cancer tumors that often release hormones into the bloodstream. They are classified as gastrinomas, glucagonoma, insulinomas, somatostatinomas, VIPomas, PPomas, and carcinoid tumors. NETs can be detected by tracking their respective hormone levels in the bloodstream.

5.1. Pancreatic cancer staging

The system used most often to stage pancreatic cancer is the American Joint Committee on Cancer (AJCC) TNM system (96, 100). This system is the first criteria applied to the disease and it considers:

- The size of primary tumor **(T)** and whether it has spread beyond the pancreas into nearby organs.
- The spread of the tumor to regional lymph nodes (**N**).
- Evidence of metastasis **(M)** to other organs. The most common metastasis sites are the liver, lungs, and the peritoneum.

5.1.1. The T categories

- **TX:** The main tumor cannot be assessed.

- **T0:** No evidence of a primary tumor.
- **Tis:** Carcinoma in situ (the tumor is confined to the top layers of pancreatic duct cells).
- **T1:** The tumor has not spread beyond the pancreas and is two centimeters (cm) or less wide.
- **T2:** The tumor has not spread beyond the pancreas but is larger than 2 cm.
- **T3:** The tumor has spread beyond the pancreas into nearby surrounding structures but not into major blood vessels or nerves.
- **T4:** The tumor has spread beyond the pancreas into nearby large blood vessels or nerves.

5.1.2. N categories

- **NX:** The regional lymph nodes cannot be analyzed.
- **N0:** The cancer has not spread to nearby lymph nodes.
- **N1:** The cancer has spread to nearby lymph nodes.

5.1.3. M categories

- **M0:** The cancer has not spread to distant lymph nodes or other organs (e.g., the liver, lungs, or brain).
- **M1:** The cancer has spread to distant lymph nodes or other organs.

Once the **T**, **N**, and **M** categories have been assessed, the information is combined to calculate overall stage of the pancreatic cancer (0, I, II, III, or IV).

Stage	Stage grouping	Stage description
0	Tis, N0, M0	The tumor is confined to the top layers of pancreatic duct cells and has not invaded deeper tissues. It has not spread outside the pancreas. These tumors are sometimes referred to as pancreatic carcinoma in situ or pancreatic intraepithelial neoplasia III (PanIn III).

IA	T1, N0, M0	The tumor is confined to the pancreas and is 2 cm wide or smaller (T1). The cancer has not spread to nearby lymph nodes (N0) or distant sites (M0).
IB	T2, N0, M0	The tumor is confined to the pancreas and is larger than 2 cm wide (T2). The cancer has not spread to nearby lymph nodes (N0) or distant sites (M0).
IIA	T3, N0, M0	The tumor is growing outside the pancreas but not into major blood vessels or nerves (T3). The cancer has not spread to nearby lymph nodes (N0) or distant sites (M0).
IIB	T1-T3, N1, M0	The tumor is either confined to the pancreas or is growing outside the pancreas but has not spread into major blood vessels or nerves (T1-T3). The cancer has spread to nearby lymph nodes (N1) but has not spread to distant sites (M0).
III	T4, Any N, M0	The tumor is growing outside the pancreas and into nearby major blood vessels or nerves (T4). The cancer may or may not have spread to nearby lymph nodes (Any N). It has not spread to distant sites (M0).
IV	Any T, Any N, M1	The cancer has spread to distant sites (M1).

Table 1. Pancreatic Cancer Staging. Table copied from reference (96)

5.2. Other prognostic factors contributing to pancreatic cancer staging

Physicians issue a prognosis that predicts the outcome of a disease based on the staging and the patient's condition at the diagnosis. Several factors play a role in determining a prognosis, or future outcome, of pancreatic-cancer patients. Besides the staging of pancreatic cancer, the determination of tumor grade after a biopsy and surgery will greatly affect the prognosis and the chances that the patient will be cured.

5.2.1. Tumor grading

The tumor grade reflects how abnormal the pancreatic tumor cells appear under the microscope. Higher grade tumors are correlated with a poor prognosis. The scale used to define tumor grade goes from G1 (lowest grade; cells closely resembling natural morphology) to G4 (higher grade; cells are abnormal and do not resemble the natural morphology) (96). Microscopic cellular abnormalities include a) the presence of a highly

pleomorphic nucleus and basophilic cytoplasm with the presence of vacuoles; b) the presence of a polymorphic nucleus, more than one nucleus, or peripheral dislocation of cellular nucleus; and c) high frequency of mitoses (96, 101). For NET tumors, the proliferation marker ki67 is an added parameter to determine the tumor grade.

5.2.2. Surgical resection margins

Surgery still is the most favorable treatment to increase pancreatic cancer patients' long-term survival and cure. Depending on how much the disease has spread in a patient, surgery can be **curative** (complete tumor resection) or **palliative** (removal of tumor masses to alleviate pressure in other organs). Most patients are diagnosed in the late stage of the disease, and by then tumors are locally advanced or metastastic. In these cases, the tumors are classified as unresectable, and patients receive palliative surgery. If curative surgery is performed, tumors are classified as:

- **Resectable:** The tumor is restricted to the pancreas or has spread just beyond the pancreas. In these cases, the entire tumor mass can be removed.
- **Borderline resectable:** The tumor is located near blood vessels and cannot be completely removed, but has the potential of being completely removed.

For patients who undergo surgery, the staging of pancreatic cancer will also consider whether the surgery can remove the entire tumor, or, if after removal of the tumor, there still is residual disease in the resection margins (96). In both cases, the margin of tumor resection is submitted for microscopic analysis to evaluate whether cancer cells are present. The margins of tumor resection are classified as:

R0: The tumor was completely removed and there is no microscopic indication of tumor cells in the resection border.

R1: The tumor was visibly removed, but there is microscopic indication of tumor cells in the resection border.

R2: The surgeon could not perform a complete removal of the tumor, and there is visible indication of large numbers of tumor cells in the resected area.

Patients with R0 and R1 resection margins have better prognoses than patients with R2 margins.

5.3. Pancreatic cancer survival rates

There are several ways to determine a cancer patient's chances of survival. Depending on the parameter used, chances of survival can be classified as:

- The **survival rate** is the percentage of people diagnosed with pancreatic cancer who survived for a determined period of time in a determined study. Survival rate is not a predictor of treatment success or completion.
- The **relative survival rate** is the ratio of the proportion of observed survival in a cohort of cancer patients to the proportion of expected survival in a comparable cohort of cancer-free patients.
- **Median survival** is the amount of time that 50% of pancreatic cancer patients have died and 50% have survived.
- **Overall Survival (OS)** the amount of time between the cancer diagnosis or beginning of a treatment to the patient's death. OS is often used in clinical trials as an indication of how well a treatment works.
- **Progression free survival (PFS)** is the amount of time between the beginning of treatment to disease progression or the patient's death. PFS is used to evaluate the effectiveness of drugs in clinical trials.
- **Disease free survival** is the amount of time between the end of treatment to when the patient starts to show signs of disease progression or has died.

For all combined stages of pancreatic cancer, the current one-year relative survival rate is 20%, and the five-year rate is 6% (95, 96, 102). Advanced stage and spreading of the disease by the time of diagnosis are the main contributors to these poor survival rates. By the time of diagnosis, less than 20% of patients are eligible for surgery, which is the most effective treatment for the disease. In cases where surgery can be performed, the average survival period is 23–36 months, and the overall five-year survival rate is about 10%. But

if the tumor can be completely removed and there is no sign that the cancer has spread, the five-year survival rate is reported to be 20–35% (102).

5.4. Pancreatic cancer mutations

Current knowledge about pancreatic carcinogenesis suggests that multifocal, microscopic pancreatic intraepithelial neoplasms (PanINs), intraductal papillary mucinous neoplasms (IPMNs), and mucinous cystic neoplasms (MCNs) are precursor lesions for pancreatic-cancer formation (103-105). PanINs, IPMNs, and MCNs are usually asymptomatic and the progression of these lesions into malignant pancreatic cancer is outlined in **Figure 2.** The most predominant and well-studied precursor lesion that precedes pancreatic ductal adenocarcinoma (PDAC) is PanINs. PanINs are noninvasive, asymptomatic, and microscopic lesions (usually <5 mm) that are comprised of columnar or cuboidal cells with varying degrees of cytological dysmorphia. PanINs are usually classified as 1) PanINs A and B—low-grade lesions with lower levels of cellular atypia; 2) PanINs-2—intermediate grade lesions with mild to moderate levels of cellular atypia; and 3) PanINs-3 or high grade PanINs, which show a high degree of cellular atypia and are usually referred as “carcinoma in situ”.

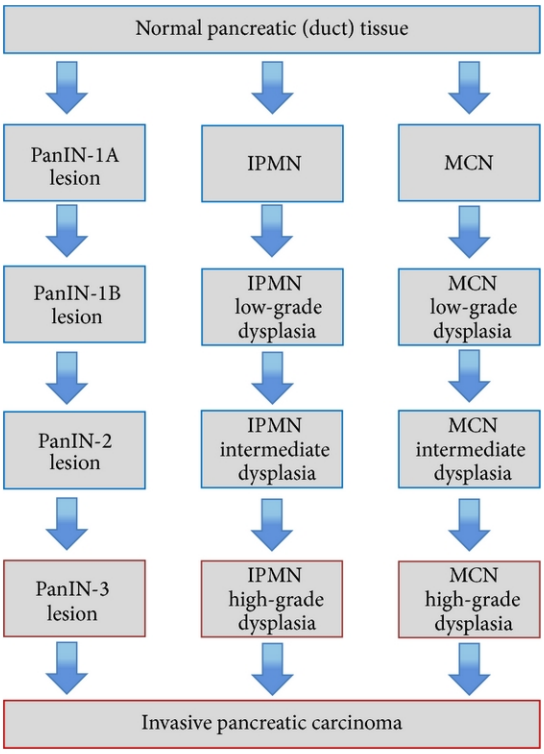

Figure 2 Pancreatic Cancer Precursor Lesions. Progression of precursors legions that lead to transformation and carcinogenesis of a normal pancreas. (Figure extracted from reference (105)).

One of the main driving forces in converting PanINs to invasive PDACs is the activation of the small GTPase protein KRAS. KRAS alternates between two states: the GTP-bound active and GDP-bound inactive. The guanine nucleotide exchange factors (GEFs) are responsible for activating KRAS by exchanging GDP for GTP, and the GTPase-activating proteins (GAPs) inactivate KRAS by hydrolyzing the GTP to GDP (106).

In humans, point mutations at the KRAS codons G12 (exon 2), G13 (exon 2), and Q61 (exon 4) are activating mutations that impair the intrinsic activity of GAPs to hydrolyze GTP to GDP, which, in turn, activating cell proliferation. Mutations in codon G12 are most prevalent in PDACs present in 98% of all KRAS mutations in PDAC. The mutation occurs in codon 12 (GGT-GAT) and results in a single amino-acid change from glycine (G) to aspartic acid (D), which makes KRAS constantly bound to GTP and in a constant activated state (106, 107). Constitutively activated KRAS activates pro-carcinogenic pathways such as Raf/Mek/Erk, PI3K/Pdk1/Akt, and the Ral guanine nucleotide exchange factor (108,

109). Unregulated stimulation of these pathways results in sustained proliferation and survival of cancer cells; metabolic reprogramming; remodeling of the tumor microenvironment; evasion of the immune response; and increased cell migration and metastasis. All these effects are hallmarks of cancer and contribute to the progression of PanINs to invasive PDAC (106). In fact, KRAS mutations can be found as early as in PanINs-1A. After KRAS activation, cancer cells undergo enhanced genomic instability, which leads to loss of functioning in tumor suppressors P53 (70 % of PDACs), P16 (98% of PDACs), SMAD4 (50% of PDACs), and BRCA1 and BRCA2 (6.6 % of PDACs) (107, 110-114).

5.5. Type I IFN pathway in pancreatic cancer cells

Besides modulating the immune response against pathogens, stimulation of the type I IFN pathway leads to the expression of Interferon Activated Response Elements (ISRE) and later expression of anti-viral genes such as PKR, MX1, OAS, TRIM5, ZAP, APOBEC3G, EPSTI1, XAF1, GBP, and IFITM3 (115). During viral infection, these genes are responsible for stopping viral replication in infected cells and halting the spread of the infection to neighboring cells. Pancreatic cancer cells have defective type I IFN pathways (116, 117) and, therefore, are susceptible to viral infection. The susceptibility of PDAC cells to viral infection has been connected with the lack of MX1, EPSTI1, XAF1, and GBP1 IFN inducible anti-viral genes (118), but not all PDAC cells have disrupted type I IFN pathways (117). Despite an active IFN-induced anti-viral response in some PDAC cells (117, 119), this response does not impede adenovirus replication in these cells (24, 56, 120). Even though the type I IFN pathway might not be completely disrupted in some pancreatic cancer cells, the adenovirus is inheritably resistant to the anti-viral effects caused by IFN. As mentioned above, the expression of VA-RNA by the adenovirus promotes preferential viral RNA translation in cells with active PKR that are stimulated by IFN (117, 119).

Type I IFN induces higher expression of MHC-I on the cell surface, thereby increasing the presentation of viral-specific peptides to cytotoxic CD8+ lymphocytes (CTL), which then leads to the increased elimination by the lymphocytes of virally infected cells. The

adenovirus's E3 gp19K protein inhibits the loading of MHC-I with cellular peptides or the transport of loaded MHC-I to the cell surface, which avoids the CTLs' elimination of infected cells (121, 122).

Adenovirus E3 gp19K also can suppress infected cell recognition by natural killer (NK) cells by performing intracellular sequestration of stress-induced MHC-I chains A and B, which are part of the complex of receptors recognized by NK cells (123). Despite adenovirus ability to suppress recognition by natural killer cells, Aoki and colleagues have shown that an IFN-expressing adenovirus still could stimulate a NK response against pancreatic cancer tumors leading to tumor reduction in adenovirus untreated tumors even though virus had the capacity of evade the NK response against infected cells (119).

5.6. Use of Oncolytic Adenoviruses to treat pancreatic cancer

There are several cases where oncolytic adenoviruses or CRADs have been employed in clinical trials as therapy against PDAC. ONXY-015 (*dl1520*) was the first replication-competent oncolytic adenovirus used in clinical trials to treat PDAC (124). ONYX-015 was designed to selectively replicate in pancreatic-cancer cells by deleting the E1B 55 kD protein, which inhibits the function of tumor suppressor p53. Although the use of ONXY-015 reduced PDAC tumor size in PDAC pre-clinical models (125), the effectiveness of ONXY-015 to treat PDAC was not significant even when the virus was combined with gemcitabine (32). While the virus was injected in primary PDAC tumors, there was no proof of viral replication in tumors, and patients developed high levels of neutralizing antibodies (126). The virus's lack of replication in PDAC tumors could be explained by the fact the PDAC cells express low levels of CAR receptors. As ONXY-015 is based on the adenovirus type 5, which uses CAR to infect cells, it is possible that the virus did not achieve high infectivity in PDAC. Despite that, ONXY-015 was approved as a therapy to treat head and neck cancer in China (33).

5.7. Treatment of Pancreatic cancer

5.7.1. Surgery

In cases where surgery can be performed on PDAC patients, surgery procedures can be described as:

- The **Whipple procedure (pancreaticoduodenectomy)** is the most common operation performed on patients. During this operation, the surgeon removes the head of the pancreas and sometimes the body as well. The surgeon may also elect to remove nearby structures such as parts of the small intestine, bile duct, stomach, gallbladder, and lymph nodes near the pancreas.
- **Distal pancreatectomy** consists of removing only the tail of the pancreas.
- T**otal pancreatectomy** which is the complete removal of the pancreas.

5.7.2. Standard of care

For many years, the approved standard of care to treat PDAC was gemcitabine as a monotherapy (127). But in January of 2017, the approved standard of care was changed to Gemcitabine plus Capecitabine. Although treatment with Gemcitabine-based therapies were never proven to extend the long-term survival of patients, treatment with Gemcitabine plus Capecitabine resulted in an overall survival period of 28.8 months, while treatment with gemcitabine alone extended the survival period to only 25 months. For this reason, the standard of care changed to the use of Gemcitabine plus Capecitabine (128).

Despite an already-approved standard of care to treat PDAC, several therapeutic protocols are being tested in PDAC clinical trials. Though many of these protocols have failed to improve survival periods of PDAC patients, adjuvant therapies using FOLFIRINOX, nab-paclitaxel combined with Gemcitabine, and IFN-alpha combined with chemoradiation have shown promising results. Adjuvant therapy is a form of treatment where surgery is performed before treatment with other therapeutic agents such as chemotherapy or radiation.

5.7.3. FOLFIRINOX and nab-paclitaxel plus Gemcitabine in adjuvant PDAC therapy

Clinical trials that have tested the use of FOLFIRINOX (Folinic acid, Irinotecan, Fluorouracil, and Oxaliplatin) in an adjuvant setting have shown that the therapy improved short-term survival of PDAC patients compared to treatment with gemcitabine alone (129, 130). Despite its apparent effectiveness, however, FOLFIRINOX is highly toxic and tolerated by only younger patients (130, 131). Clinical trials that assessed the effectiveness of adjuvant therapy and treatment with nab-paclitaxel plus Gemcitabine also showed improved patient survival compared to use of Gemcitabine alone. While effective, the survival of patients who were treated with nab-paclitaxel plus Gemcitabine was not different than the survival of patients treated with FOLFIRINOX. Furthermore, treatment with nab-paclitaxel (albumin bound paclitaxel) plus Gemcitabine was also extremely toxic to patients, and long-term survival was not improved by using neither nab-paclitaxel plus Gemcitabine nor FOLFIRINOX in therapy (132, 133).

5.7.4. IFN-α combined with chemotherapy and radiation in adjuvant PDAC therapy (IFN-therapy)

Phase II clinical trials where patients were treated with adjuvant therapy and subcutaneous IFN-α (IFN) combined with radiation, 5-FU, and Cisplatin reported an increase in the two-year survival of patients by 16–40% (134-136), and an increase in their five-year survival by 35% (134, 137, 138). Another Phase II trial that added Gemcitabine to the same treatment protocol reported 55% and 26% increase in the one and two-year survival of patients respectively (136). Most therapies to treat PDAC such as FOLFIRINOX, nab-paclitaxel plus Gemcitabine, and even Gemcitabine plus Capecitabine showed improvement in only the patients' short-term survival rates. To date, IFN-therapy is one of the few therapeutic regimens that can show an impressive increase in patients' long-term survival. While trial results have been encouraging, strong IFN systemic toxicity and low levels of cytokine in tumors were identified as the therapy's main drawbacks (139-141). Most of the effects of IFN toxicity included extreme fatigue, leucopenia, severe thrombocytopenia, flu like-symptoms, and gastrointestinal disturbances. Although

seemingly benign, the toxicity effects were rated as grade III and IV, and most patients that displayed IFN toxicity had to be hospitalized and dropped out of the trials (135, 137, 142-144).

IFN-α (IFN) is a cytokine secreted mainly by lymphocytes (NK cells, B cells, and T cells), macrophages, and fibroblasts. Besides inducing an anti-viral state in infected cells and having immunostimulatory properties, IFN has several anti-cancer therapeutic properties. The cytokine is known to inhibit proliferation, induce apoptosis, reduce angiogenesis, and potentiate the killing effect of chemotherapy and radiation in cancer cells (139). Because IFN was reported to have a high degradation rate in the blood of patients during treatment, low levels of the cytokine in tumors constituted one of the major setbacks to IFN-therapy efficacy (139-141). Despite the reported IFN systemic toxicity and lower IFN levels in tumors, use of IFN in combination with chemoradiation in an adjuvant setting still is one of the most promising therapeutic regimens to treat PDAC. In addition to contributing to longer patient survival, a multicenter Phase III clinical trial showed that patients who were treated with IFN-therapy developed a cancer-specific immune response (137, 144). Although no correlation was found between increased survival and the development of an anti-tumor immune response in that trial, long term follow-up of phase II clinical trials developed by the Virginia Manson group showed that 28% of the patients survived for at least 10 years. Of these patients, nine lived more than ten years and seven are still alive without any indication of disease (145). Because the development of an anti-tumor immune response is known to reduce tumor recurrence and improve patients' long-term survival, it is possible that stimulation of anti-tumor immune response played a role in helping these patients experience extended survival periods after being treated with the IFN therapy.

6. Mechanism of action of therapeutics used in IFN therapy

6.1. Ionizing radiation

Ionizing radiation is the most commonly used form of radiation given to patients during cancer therapy. X-rays and gamma rays are the most often used types of electromagnetic ionizing radiation in cancer treatment (146). X-rays are produced by the high-energy acceleration of electrons followed by the abrupt stop of those electrons in a tungsten or gold surface that results in a release of energy. X-rays have a short wavelength and their delivered energy can be classified as "packages of energy," or photons. One photon carries 124 KeV of energy, which is enough to break chemical bonds between molecules. The potency of X-rays is mostly a function of the size of the photons, not the amount of energy absorbed (147).

Gamma-rays are penetrating electromagnetic radiation that is derived from the radioactive decay of atomic nuclei. During nuclear decay, radiation—comprised of alpha-particles, beta-particles, and neutrinos—is emitted. The delivery of energy also forms photons, which are part of the highest observed range of photon energy (146). While X-ray energy ranges from 100eV–124KeV, gamma-ray energy is greater than 100 KeV. Although gamma-ray photons are more likely to cause biological changes compared to X-rays, X-ray energy can also cause extensive damage to DNA and cellular structures.

The biological effectiveness of radiation depends on the linear energy transfer (LET), total dose, fractionation, and radiosensitivity of the cells to radiation treatment (148). Radiation particles are either negatively charged (electrons), or positively charged (protons, alpha rays, and other heavy ions) and both can deposit high amounts of energy on the targeted areas causing accentuated cellular damage. The potent cellular damage caused by these particles results from their capacity to transfer energy right after they pass though matter (146).

Radiation is classified as either directly or indirectly ionizing. X-rays and gamma rays are considered directly ionizing if they transfer energy and disrupt the atomic structure in cells causing chemical and biological changes. During radiotherapy, which uses a linear

accelerator, the indirectly ionizing effect—or the Compton process—predominates. In this process, the energy photon interacts with a free electron that absorbs the energy photon and is ejected from its orbital path. The remaining non-absorbed energy is then deflected with less energy to the surrounding areas. During radiation, several fast-moving electrons are produced, and they are responsible for the biological indirect effect of radiation by breaking chemical bonds, damaging cellular structures, interacting with other compounds (e.g., water), and causing DNA damage (147). Emitted photons can also ionize water molecules, and, as a result, high levels of free oxoniumyl radicals (H_2O^+) are formed. These ion radicals have an unpaired electron in their outer shell, which makes them react to DNA bases causing extensive damage. Radiation-induced DNA damage can cause single-strand break (SSB), base damage, and double-strand break (DSB) in cancer cells. Because cancer cells highly depend on DNA replication, DSB has the most deleterious effect on cells and results in cell apoptosis (146, 147).

6.2. Radiation in IFN therapy

In IFN-based clinical trials, patients were given radiation in a fractionated manner. Patients received 45–54 Gray (Gy) in 25 fractions of approximately 1.8–2Gy five days a week for five–six weeks (134, 135, 149). The concept of fractionated radiation takes into consideration the 4Rs: **repair**, **redistribution**, **reoxygenation**, and **repopulation** (147).

Repair Phase

Radiation can cause potentially lethal damage (PLD), sub-lethal damage (SLD), and lethal damage (LD) to cellular DNA. When radiation is fractionated during a treatment period, PLD and SLD mainly accumulate in cellular DNA. To efficiently repair this damage, cells need to activate DNA-repair pathways and induce cell-cycle arrest. Because cancer cells often have mutations in their DNA-repair pathways, and lack important tumor-suppressor genes (e.g., TP53, p16, and BRCA genes), they are unable to undergo cell-cycle arrest and cannot efficiently repair the DNA damage. Consequently, the administration of fractionated radiation results in the extended accumulation of non-repaired DNA damage in cells that leads to mitotic crisis and cell apoptosis. This is the **repair** phase of fractionated radiation.

Redistribution Process

Cells are most sensitive to radiation DNA damage when they are in the G2/M phase of the cell cycle, and are particularly resistant to damage when they are in the S-phase of the cycle. During radiation, some cells are G2/M phase and others are in the S-phase. The fractionation of radiation allows the cells that are in the S-phase of the cell cycle to have time to progress to G2/M stage and be susceptible to radiation damage. This happens during the radiation interval—the 24-hour interval between successive administrations of fractionated-radiation doses. This is the **redistribution** process, and its goal is to increase the cell population that can be affected by radiation.

Reoxygenation Process

Oxygen is a potent inducer of DNA damage during radiation because of the formation of free radicals. Free radicals can cause extensive DNA damage and also disrupt cell structures which results in apoptosis. There is a gradient distribution of oxygen in tumors, meaning that the borders of the tumors are more oxygenated than their internal parts. Between the border of a tumor and its center there is a gradual decrease in oxygen concentration, and the center is most of the time hypoxic. A tumor can also go through an acute hypoxic stage (when its capillaries momentarily close and do not provide oxygenated blood) and can also experience a chronic stage of hypoxia (where oxygenated blood does not reach the center of the tumor because of inefficient vascularization). By spacing the radiation doses, there is the possibility that transiently closed vessels can reopen and provide oxygen to hypoxic cells increases. Radiation kills cells that are near capillaries more effectively, relieving the capillary pressure and allowing a flow of oxygenated blood to the more-internal parts of the tumor. As these cells are destroyed, the pressure on nearby capillaries is relieved, and oxygenated blood can irrigate the tumor's hypoxic areas more efficiently making these cells susceptible to free oxygen species formation during radiation. This is the **reoxygenation** process.

Repopulation Process

After radiation, cancer cells can undergo a high rate of cell growth and quickly repopulate the tumor. But, highly replicating cells are especially sensitive to radiation, which can enhance the efficacy of fractionation radiation in eliminating these cells. Because the fractionation of radiation is given over a period of time, most of cells that have the capacity of repopulating the tumor are affected leading to the inability of these cells to contribute to increase in tumor volume. This is the **repopulation** process (147, 150).

7. Chemotherapies used in IFN-therapy

7.1. 5-FU, Gemcitabine, and Cisplatin chemotherapies

During the five to six weeks of radiation in the IFN-based clinical trials, chemotherapy treatment consisted of the administration of a bolus dose of Cisplatin at the beginning of the week, subcutaneous IFN three times during the week, and continuous administration of 5-FU. After a period of rest, patients then received continuous doses of 5-FU or, depending on the clinical trial in question, Gemcitabine for additional four weeks(135, 136). All these chemotherapy drugs are considered DNA-damaging drugs since 5-FU and Gemcitabine are base analogs and Cisplatin can bind to nucleophilic groups in DNA hampering DNA replication and repair. Using these drugs in conjunction with radiation attempts to maximize deleterious DNA damage in cancer cells.

7.2. Fluorouracil (5-FU)

5-Fluoro-Uracil (5-FU) is a fluoropyrimidine or a fluorinated base analog of uracil with a fluorine atom at the C-5 position instead of a hydrogen **(Figure 3) (151, 152)**. 5-FU enters cells through the same facilitated-transport mechanism as uracil, and is converted into several active metabolites: fluorodeoxyuridine monophosphate (FdUMP), fluorodeoxyuridine triphosphate (FdUTP), and fluorouridine triphosphate (FUTP). These metabolites are responsible for the biological activity of 5-FU in cells, which includes inhibiting thymine production by the enzyme thymidylate synthase (TS), and interfering with DNA and RNA functions (152). Inactivation of 5-FU happens in the liver where

dihydropyrimidine dehydrogenase (DPD) converts 5-FU to its inactive form dihydrofluorouracil (DHFU).

7.2.1. 5-FU inhibition of thymidylate synthase and DNA damage

Normally, thymidylate synthase (TS) catalyzes the reductive methylation of deoxyuridine monophosphate (dUMP) into deoxythymidine monophosphate (dTMP) using reduced folate (CH_2 THF) as a methyl donor. dTMP is the source to produce *de novo* thymidylate, which is used to produce thymine in cells. Thymine is used in DNA repair and newly formed DNA molecules. To catalyze this reaction, TS forms a ternary complex with the nucleotide dUMP and CH_2 THF, but when FdUMP is present, the 5-FU metabolite forms a stable ternary complex with the TS nucleotide binding site and with reduced folate blocking the access of dUMP to the TS and inhibiting thymidylate (dTMP) production. This leads to thymine deprivation in cells, which, in turn, prevents the synthesis of new DNA molecules and DNA repair. Because cancer cells are highly dependent on DNA synthesis to support their growth, and are most of the time unable to induce cell cycle arrest due to the lack of tumor suppressor genes, 5-FU treatment causes cells to undergo mitosis crisis and apoptosis (151, 152).

In addition, the depletion of dTMP caused by TS inhibition results in the reduction of deoxythymidine triphosphate (dTTP) and perturbation in the levels of deoxynucleotides dATP, dGTP, and dCTP. Deoxynucleotide imbalances can disrupt DNA synthesis and repair, resulting in lethal DNA damage. When a deoxynucleotide imbalance occurs, dUMP also accumulates in cells, which leads to higher conversion of deoxyuridine triphosphate (dUTP). A high ratio of dUMP/dUTP makes nucleotide excision DNA repair inefficient, and results in increased incorporation of false-nucleotide bases (5-fluoronucleotides) in DNA. The many cycles of misincorporation, inefficient base-excision repair, and DNA-repair inhibition results in DNA strand breaks and cell death.

7.2.2. 5-FU impact on RNA

The 5-FU metabolite 5-FUTP is extensively incorporated into RNA and it disrupts normal RNA processing and function. 5-FUTP misincorporation inhibits the conversion of pre-

RNA into mature rRNA, disrupts the post-transcriptional modification of tRNA, the assembly and activity of snRNA/protein complexes, and inhibits the splicing of pre-RNA (152-155). 5-FU metabolites also inhibit the post-transcriptional conversion of uridine to pseudouridine impacting RNA, rRNA, tRNA, and snRNA because each of these RNA molecules require pseudouridine. Finally, 5-FU also interferes with RNA processing and function by inhibiting the polyadenylation of mRNA, which significantly interferes with its function (156, 157). It is not known whether 5-FU interference with DNA is stronger than its interference with RNA. But it is possible that both effects contribute to cell death. Despite this uncertainty, it is possible that using 5-FU in combination with other DNA-damaging drugs might result in more pronounced negative effects in DNA, making DNA damage in treatments with 5-FU the main cause of cancer-cell death.

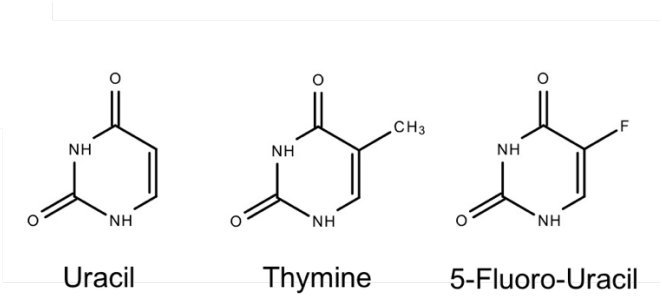

Figure 3. Drawing made using Chemspider (http://www.chemspider.com/). Figure adapted from reference 132.

7.3. Cisplatin (CDDP)

Cisplatin (CDDP) is a divalent, inorganic, water soluble, platinum-containing complex that is highly reactive to nucleophilic groups present in the cellular DNA (158). The drug is transported through the cellular membrane by passive diffusion, and becomes activated when cis-chloro ligands are replaced by water molecules **(Figure 4).** This replacement process forms an aquated form of CDDP that is trapped intracellularly. Activated CDDP is a highly reactive species and shows high avidity for nucleophilic groups in the cell (159, 160). The interaction between CDDP and cytosolic nucleophilic groups in glutathione (GSH), methionine, metallothionein, and proteins can inactivate CDDP. If this step is not a rate limiting process, activated CDDP reaches the nucleus, and interacts with nucleophilic

groups in DNA and nuclear proteins (161). In the nucleus, CDDP reacts with the nucleophilic N7-sites of purine bases in the cellular DNA and causes intra- and inter-strand cross-linkage of purine bases (159, 160). Relatively speaking, intra-strand cross-linkages are the most cytotoxic lesions and are highly correlated with increased apoptosis (162, 163). The interaction between CDDP and DNA causes distortions in the DNA strand and attracts proteins that recognize DNA damage. These damage-recognition proteins include the hMSH2 or hMutSa proteins, which are components of the mismatch-repair (MMR) complex. The interaction between CDDP and DNA also attracts non-histone chromosomal high-mobility proteins (HMG1 and HMG2), RNA polymerase I binding factor (hUBF), and TATA binding protein (TBP) transcription factors. When CDDP–DNA adducts extensively accumulate in the cell, the cell up-regulates p53 and undergoes cell-cycle arrest (159). As mentioned above, cancer cells have a mutated p53 or lack this tumor-suppressor protein. Thus, these cells are unable to induce cell cycle arrest and start DNA repair. Thus, there is accumulation of CDDP–DNA adducts in cells leading to mitosis crisis and apoptosis.

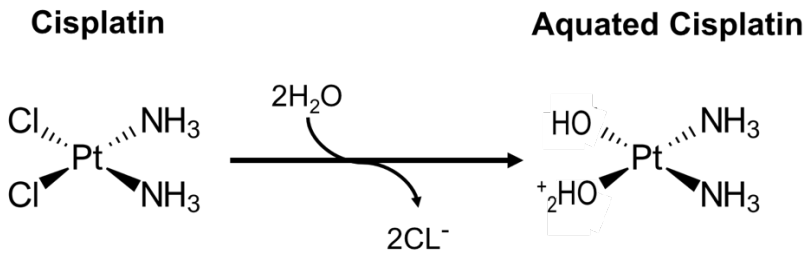

Figure 4. Cisplatin and its activated aquated form.

7.4. Gemcitabine

Gemcitabine (2',2'-difluoro-2'-deoxycytidine, or dFdC) is a nucleoside analog of deoxycytidine **(Figure 5)**. It is derived from the drug cytosine arabinoside (Ara-C), which was classically used as a chemotherapy drug for acute myeloid leukemia, acute lymphocytic leukemia, chronic myelogenous leukemia, and non-Hodgkin's lymphoma (164, 165). Gemcitabine is a pro-drug, and, once it is transported into a cell through nucleoside transporters, it is phosphorylated by deoxycytidine kinase (dCK) into gemcitabine monophosphate (dFdCMP) and dFdCMP and is then converted into

gemcitabine di- and triphosphates (dFdCDP and dFdCTP). dFdCDP and dFdCTP are Gemcitabine's active metabolites (165) and they perform several inhibitory functions in cells.

The dFdCTP metabolite inhibits DNA polymerase and is incorporated into DNA. Incorporation of this metabolite into DNA results in chain-elongation termination and prevents DNA damage repair by DNA repair enzymes (166, 167). dFdC and dFdCTP may also be incorporated into RNA, although the effects of the incorporation in RNA are unclear (165). These gemcitabine metabolites also induce self-potentiation of Gemcitabine in cells (168). They prolong the maintenance of high intracellular concentrations of gemcitabine metabolites and increase the probability of their successful incorporation into nucleic acids, mainly DNA. This process occurs by reducing the competition between the cell's natural nucleic acid related metabolites and the gemcitabine metabolites. The dFdCDP metabolite, for example, inhibits the enzyme ribonucleotide reductase (RR) (169, 170), while the other metabolites can inhibit the enzymes cytidine triphosphate synthetase (CTP synthetase) (171) and deoxycytidylate deaminase (dCMP deaminase). These inhibitory processes decrease the competing deoxyribonucleotide pools necessary for DNA synthesis (171, 172). Finally, gemcitabine can inhibit topoisomerase I, leading to topoisomerase I-mediated DNA break formation, which significantly contributes to the drug's cytotoxicity (173). Apoptosis is the main mechanism of cancer-cell death caused by gemcitabine (174, 175). Apoptosis occurs because cancer cells cannot induce cell-cycle arrest, mobilize DNA repair pathways, and produce deoxynucleotides for DNA synthesis.

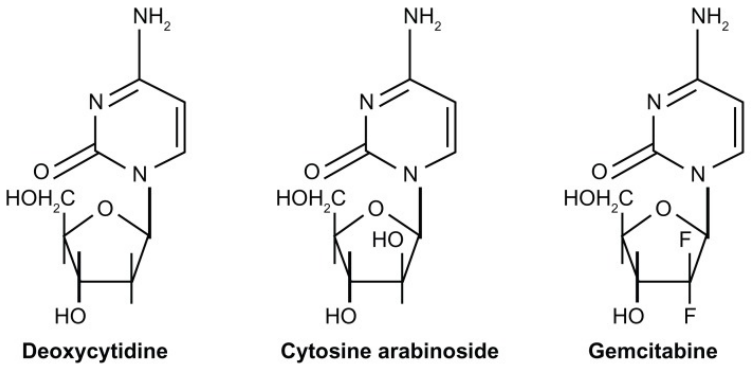

Figure 5. Structures of deoxycytidine, Cytosine arabinose (Ara-C), and Gemcitabine. Figure from reference (176).

7.5. IFN-α

Interferon alpha (IFN) is a pleiotropic cytokine that can induce negative regulatory effects on the growth of normal and malignant cells *in vitro* and *in vivo* (152, 177). As mentioned above, IFN has therapeutic properties that can be used in cancer treatment. Some of these therapeutic properties include

- Direct anti-proliferative effects in cancer cells by prolonging cell-cycle completion;
- Induction of genes that cause RNA degradation;
- Inhibition of protein synthesis;
- Down-regulation of oncogene expression;
- Induction of tumor-suppressor genes;
- Antagonism of epidermal growth factor (EGF) and platelet-derived growth factor (PDGF);
- Downregulation of cell-surface receptors for growth factors;
- Inhibition of tumor neovascularization by downregulation of vascular endothelial growth factor (VEGF);
- Basic fibroblast growth factor; and
- Matrix metalloproteinase-9 (178-183).

IFN is also a radiosensitizer and was used in several clinical trials in conjunction with radiation (142, 143, 184). It also is a chemosesnitizer to 5-FU, Cisplatin, and Gemcitabine

(183). In the case of 5-FU, IFN can synergistically potentiate 5-FU's cytotoxic effect by potentiating single- and double-stranded DNA breaks in cancer cells by boosting the misincorporation of 5-fluoropyrimidides (FdUTPs) to DNA (152, 177, 185-187).

With regard to the stimulation of an anti-tumor immune response, IFN can enhance the immunogenicity of tumors. IFN increases the expression of MHC-I in tumor cells; induce the differentiation, maturation, and function of dendritic cells (DC); enhance the survival of T cells; stimulate the generation of CD8+ memory cells; enhance macrophage activity; and activate natural killer cells (179, 188-190).

8. Effect of chemotherapy in replication of oncolytic vectors

Several treatments are based on using chemotherapy in combination with oncolytic viral vectors (191). Although these treatments have been effective, there still is a question whether chemotherapies can affect viral replication in cells. Studies that have explored the inhibition of chemotherapies to oncolytic vectors have found that administering 5-FU, irinotecan (CPT-11), or methotrexate (MTX) in combination with Herpes simplex virus 1 (HSV-1), and use of 5-FU combined with rinderpest virus (RPV) reduced viral replication in cancer cells (191, 192). Despite these findings, using chemotherapies 1716 and Mitomicyn C (MMC) in combination with HSV resulted in synergistic combinations and had no effect on viral replication in lung-cancer cells (193). When HSV is used in virotherapy, the vectors are modified to exclude its virulence factors (e.g., viral ribonucleotide reductase (RR) and γ34.5, which induce E2F release in cells). As a result, selective replication of modified HSV occurs in cancer cells because these cells usually express homologs of these virulence factors or have high levels of free E2F. As treatment of cancer cells with chemotherapy can upregulate expression of these HSV virulence factor homologs in cells, in these cases, using chemotherapies in combination with HSV can actually enhance viral replication in infected cells (191).

Use of the oncolytic adenovirus vector (OAd) ONYX-015 in combination with Cisplatin (CDDP) or 5-FU was shown to enhance an anti-tumor response in carcinoma cells (194). Also, a Phase II clinical trial for head-and-neck cancer showed that combining CDDP and 5-FU with ONYX-015 is effective (195). ONYX-015 was also clinically tested in

combination with 5-FU and folinic acid (leucovorin) (196), MAP chemotherapy (i.e., mitomycin C [MMC], doxorubicin [Adriamycin; ADR], and CDDP) (197), irinotecan, 5-FU (198), and gemcitabine (32) showing to be effective in some treatments. In these cases, ONYX-015 by itself did not produce an objective anti-tumor response in all treated tumors, but marked anti-tumor response was observed in some cases, especially when chemotherapy alone had previously failed in the patient (199). In contrast, combinations of 5-fluorouracil (5-FU) and oncolytic adenoviruses vectors (OAds) have been shown to inhibit viral replication in pancreatic cancer cells (200).

9. Study of the Combination Index between therapeutic agents

Cancer can be treated in several ways, and treatments usually gravitate towards surgery, chemotherapy, radiation, and, most recently, immunotherapy and gene therapy. Whatever the treatment method, it usually is not limited to a single therapy (monotherapy). Except for curative resection through surgery, treatments usually consist of **combination therapy**, that is, a combination of two or more nonsurgical therapeutic methods. As discussed above, **adjuvant combination therapy** consists of surgery followed by chemotherapy, radiation, immunotherapy, gene therapy, or even a combination of two or more of these therapeutic modalities. **Neo-adjuvant combination therapy** starts with treatment using nonsurgical therapeutic modalities (e.g., chemotherapy, radiation, immunotherapy, and others) followed by surgery. This method is usually employed when the tumor size needs to be reduced before surgery can be performed.

Because each therapeutic approach has a specific mechanism of action, multiple drugs can attack different targets in a single cell. And since tumors are formed by multiple subpopulations of heterogeneous cells—each one being in a different mitotic stage or presenting a different level of drug resistance—combining drugs with different mechanisms of action can result in more effective cancer treatment. In IFN therapy, for example, DNA-damaging agents such as CDDP and 5-FU are combined with radiation, which is also DNA damaging. All these therapeutic agents can cause DNA damage in a different manner, and when they are combined with IFN-α, there is a potentiation of their DNA damaging effects by the chemoradiosensitization properties of IFN.

Today, however, combining therapeutic agents is not done randomly. Combination treatment usually considers the drugs' individual mechanisms of action and their collective interaction to kill cancer cells. A drug interaction can be synergistic, additive, or antagonistic. A **synergistic interaction** occurs when combining two drugs results in a more potent effect compared to the individual effect of each drug. In cases of synergistic interaction, it is possible to replicate or potentiate the level of a therapy by using a lower dose of each drug in combination. Synergism is highly desirable for cancer therapy because it can more efficiently eliminate cancer cells using lower doses of each therapeutic component, which will also reduce the therapy's toxicity. An **additive effect** occurs when combining two drugs results in an effect equivalent to the sum of the individual effects of each drug. Finally, an **antagonistic effect** occurs when combining two drugs decreases the individual effects of each drug. Calculating the **Combination Index (CI)** between drugs can determine how they will interact.

9.1. Isobologram

S. Loewe developed the isobologram in 1927 (201), and this is a commonly used method to determine the drug-combination index. Following Loewe's work, Grabovsky and Tallarida are now studying and further developing the isobologram concept (202-204). Although their method is efficient, it allows only for the determination of the CI between two drugs. The effectiveness of the method, therefore, is necessarily limited in cases of multiple drug therapies—such as IFN therapy—since it cannot determine the CI for combinations of more than two drugs. As discussed above, IFN therapy concomitantly uses two chemotherapy drugs in combination with IFN and radiation.

The isobologram assumes that all drugs used in combination have a constant relative potency, which means that at any effect level the equally effective doses (a of Drug A and b of Drug B) show a constant-dose ratio: $a/b = R(203)$. The isobologram's graphical representation displays the linear relationship (isobole) between two drugs. In the graph below, for example, each drug and its respective concentrations are displayed in either the x or y axis, and the linear relationship between them signifies the point where the two drugs have an equivalent magnitude of effect (203, 204). Combinations of different drug doses

can lie below the isobole (synergistic), on it (additive), or above it (antagonistic) (**Figure 6)**.

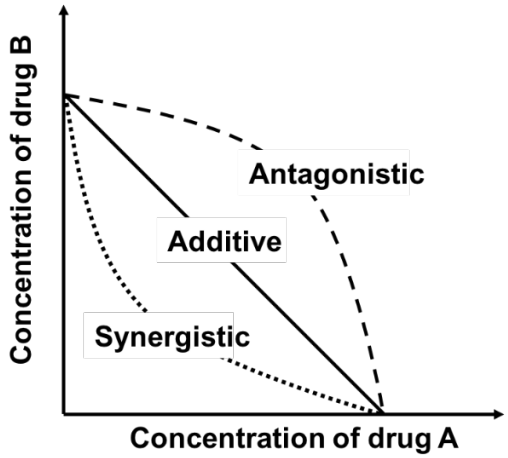

Figure 6. Isobologram graphical representation.

One drawback of using isobolograms is that, when drugs show a variable relative potency, it results in the representation of a nonlinear isobole of additivity instead of a linear isobole. In such a case, experimental results could be mistaken for synergism or antagonism. Despite this possible limitation, using isobolograms in analyzing the Combination Index is not incorrect. Several published articles address this limitation and propose ways to analyze data despite this apparent pitfall (202, 203).

9.2. Chou–Talalay method of combination analysis

The Chou– Talalay method of combination analysis, which Chou and Talalay developed in 1974, is a more advanced method of analyzing drug combinations because it can determine the Combination Index between two or more drugs. Combination analysis is performed using the Median–Effect Equation (MEE) of the mass-action law , which was developed by Chou-Talalay in 1974 through the derivation of more than 300 rate equations of enzyme dynamics, followed by mathematical induction and deduction **(Figure 7) (205)**. The MEE equation developed by Chou represents the **"unified theory"** of the four basic equations: (a) the Michaelis–Menten equation, which described the rate of enzyme kinetics; (b) the Hill equation, which determines ligand binding saturation; (c) the Henderson–Hasselbalch

equation, which describes the derivation of pH as a measure of acidity; and (d) the Scatchard equation, which results in the Scatchard plot for analysis of receptor bound and unbound ligands (205-209). Although these four equations have different physicochemical meanings, they share the same mathematical form (the MEE equation). That is why the MEE equation is called the "unified theory" **(Figure 7).**

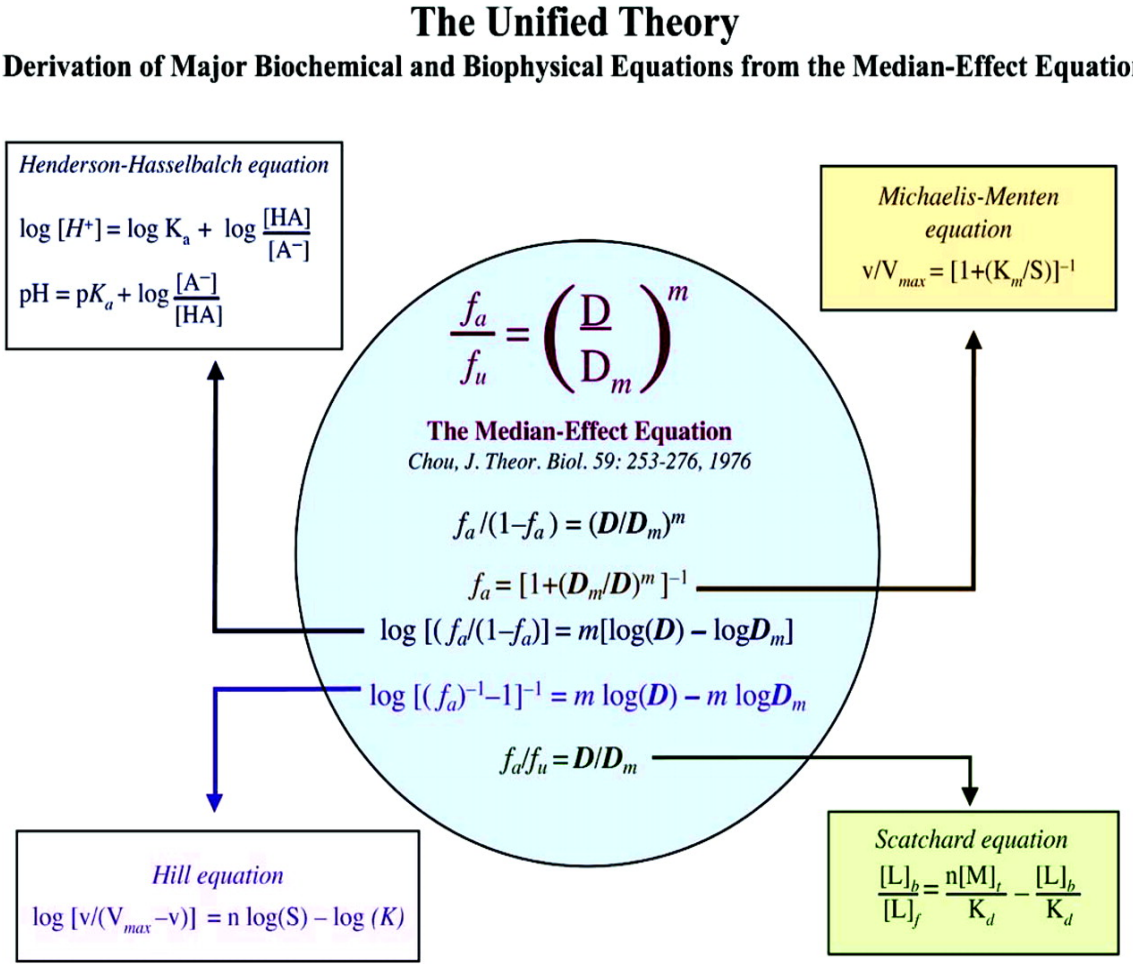

Figure 7. Representation of the Median-Effect Equation (MEE) and its derivations. Figure 7 is extracted from reference (205). The rearrangement of the MEE equation (or taking its logarithmic form) results in the Michaelis–Menten, Hill, Henderson–Hasselbalch, and Scatchard equations. In the MEE, (fa) is the fraction of affected; (fu) is the fraction of unaffected; (D) is the dose of the drug; (Dm) is the median-effect dose or potency of the drug; and m is the sigmodicity (shape) of the dose-effect curve (m=1, hyperbolic; m>1, sigmoidal; and m <1, flat sigmoidal).

The MEE was used to develop the computer program **Compusyn** and the **Combination Index theorem**, which is used to determine the **Combination Index (CI)** between drugs

(Figure 8). The combination-index theorem can establish the interaction between multiple drugs because the fraction of affected and unaffected—the EC50—of each drug is provided as a monotherapy after *in vitro* testing. Combination Indexes less than 1 (CI<1) are classified as synergistic; equal to 1 (CI=1) are additive; and greater than 1 (CI>1) are antagonistic. **Table 2** shows the range of CI classifications. Before CI studies, the ED50 of each drug as a monotherapy has to be determined.

Median-Effect equation

$$\frac{(f_a)}{(f_u)} = \left(\frac{(D)}{(D_m)}\right)^m$$

$$\frac{(f_a)_{1,2}}{(f_u)_{1,2}} = \frac{(f_a)_1}{(f_u)_1} + \frac{(f_a)_2}{(f_u)_2} = \frac{(D)_1}{(D_m)_1} + \frac{(D)_2}{(D_m)_2}$$

When M ≠ 1

$$\left[\frac{(f_a)_{1,2}}{(f_u)_{1,2}}\right]^{1/m} = \left[\frac{(f_a)_1}{(f_u)_1}\right]^{1/m} + \left[\frac{(f_a)_2}{(f_u)_2}\right]^{1/m} = \frac{(D)_1}{(D_m)_1} + \frac{(D)_2}{(D_m)_2}$$

$$\left[\frac{(f_a)_{1,2}}{(f_u)_{1,2}}\right]^{1/m} = \frac{(D)_1}{(D_m)_1} + \frac{(D)_2}{(D_m)_2} + \frac{(D)_1(D)_2}{(D_m)_1(D_m)_2}$$

$$CI = \frac{(D)_1}{(D_x)_1} + \frac{(D)_2}{(D_x)_2} = \frac{(D)_1}{(D_m)_1[f_a/(1-f_a)]^{1/m_1}} + \frac{(D)_2}{(D_m)_2[f_a/(1-f_a)]^{1/m_2}}$$

Figure 8. The Combination Index Theorem. Figure 8 shows the derivations of the MEE that resulted in the development of the Combination Index Theorem. In these derivations, numbers 1 and 2 are the theoretical representation of two different drugs used in combination, and x is the log [(D)1 + (D)2]. The other variables are as described for the MEE equation.

Range of Combination Index	Description
<0.1	Very strong synergism
0.1–0.3	Strong synergism
0.3–0.7	Synergism
0.7–0.85	Moderate synergism
0.85–0.9	Slight synergism
0.9–1.10	Nearly additive
1.10–1.20	Slight antagonism
1.20–1.45	Moderate antagonism
1.45–3.3	Antagonism
3.3–10	Strong antagonism
>10	Very strong antagonism

Table 2. Range of Combination Indexes and their respective interpretations.

Compusyn not only displays the CI between drugs, but also provides combinations of drug pairs by **isobologram**, the **Dose-reduction Index (DRI) table and plot**, the **Median-Effect plot**, the **Combination-Index plot**, and the **polygonogram** (205).

9.2.1. Isobologram

As mentioned above, the isobologram analyzes the interaction between two drugs. Thus, when analyzing the CI of more than two drugs, the isobologram only partially represents the interaction among them. For example, if drugs A, B, and C are used in combination, the isobolograms of A and B; A and C; and B and C will give only an approximated representation of the interaction of all three drugs when they are used in combination. Compusyn, however, constructs the isobologram using Chou and Talalay's Combination

Index theorem **(Figure 9)**. Despite that, it will also give the interaction of only two drugs in combination.

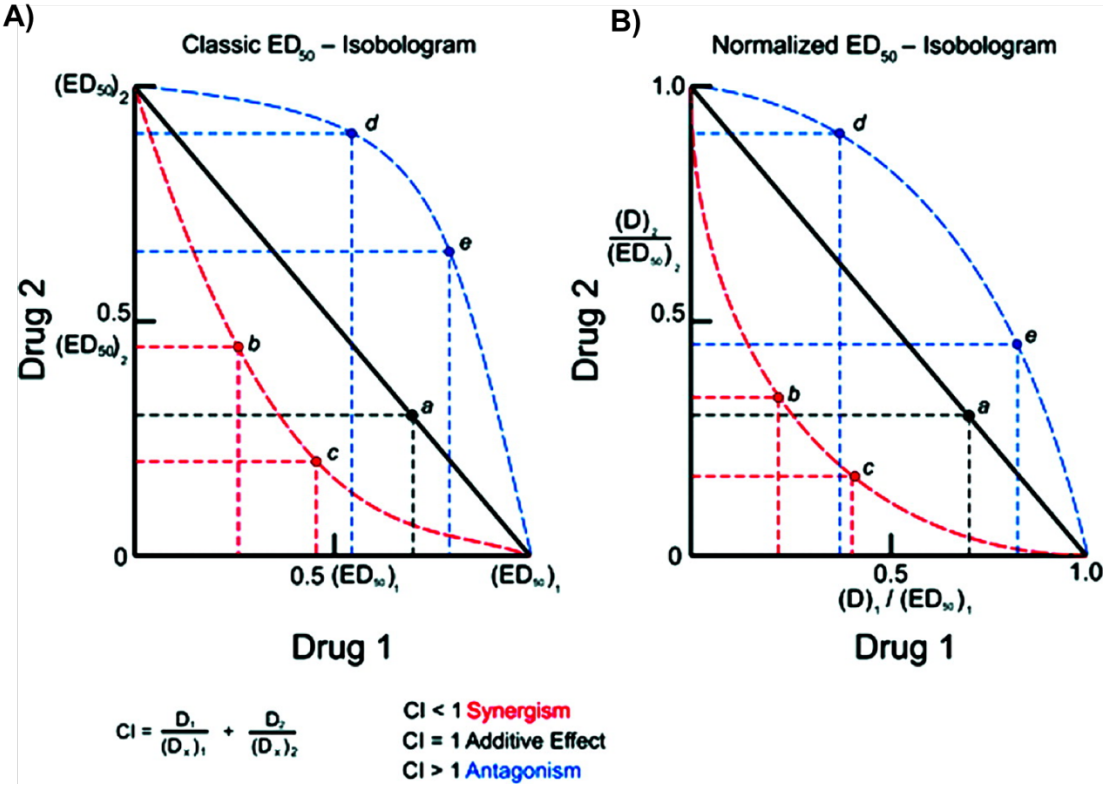

Figure 9. Isobologram generated by Compusyn. A) is a classical isobologram and B) is a normalized isobologram. Drugs 1 and 2 are theoretical examples of two drugs combined, and axis x and y represent the IC50 or the ED50 of each drug. Both ED50 and IC50 are interchangeable terms that represent a range of concentrations that result in 50% of the total effect. Figure extracted from reference (205).

9.2.2. Dose-reduction Index (DRI) table and plot

One main benefit of a synergistic drug combination is that it can enhance or maintain the effectivity of a therapy while reducing the doses of drugs used in combination. Given the effect of each drug as a monotherapy, Compusyn will generate a Dose Reduction Index (DRI) for all synergistic drug combinations. To calculate the DRI of drug combinations, it first is necessary to define the EC50 (the drug concentration that results in a half-maximum response) of each drug as a monotherapy. If the analysis is being done *in vivo*, the LD50 (the dose of each monotherapy that kills 50% of the animals) needs to be stipulated. Based

on the MEE, the Combination Index theorem, and the EC50 of each drug, Compusyn generates the DRI table **(Figure 10A),** and the DRI plot **(Figure 10B).** The DRI measures how much of a dose of each drug can be reduced in combination to still produce a synergistic combination. The DRI also provides the predicted effect of each predicted synergistic combination. The DRI plot also compares the predicted synergistic combinations calculated by Compusyn, and the actual combinations tested *in vitro* or *in vivo*.

A)

Cell lines	Panobinostat + ZOL		
	CI	DRI	
		Panobinostat	*ZOL*
LNCAP	0.48 (0.07)	8.58 (3.56)	3.2 (0.71)
PC3	0.63 (0.098)	4.15 (1.76)	2.96 (1.5)
DU145	0.31 (0.03)	5.75 (0.32)	7.28 (0.98)
RPMI8226	0.58 (0.26)	4.16 (2.5)	4.23 (1.96)
KMS12BM	0.67 (0.1)	0.13 (0.1)	1.68 (0.1)
KMS21BM	0.18 (0.2)	4.1 (0.1)	16.32 (5.42)
DU145R80	0.69 (0.14)	1.65 (0.07)	3.9 (0.84)

B)

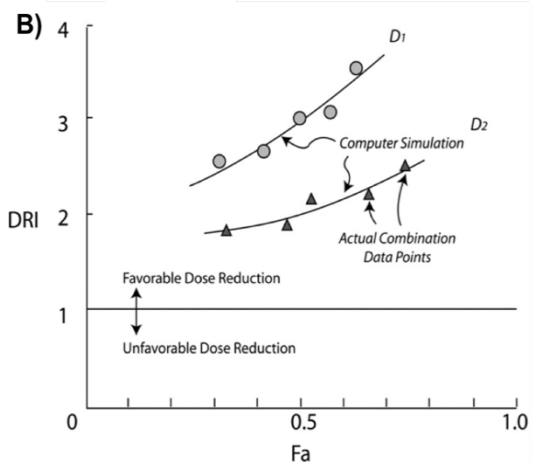

Figure 10. DRI table and plot. DRI table **(A)**, which was extracted from reference (210) as an example, represents the combination of the drugs Panobinostat and ZOL. The first column shows all the cell lines used in the experiment. The second column displays the CI, which are the Combination Indexes for each combination of Panobinostat and ZOL tested in each cell line. The number without parentheses represents the actual calculated CI for the actual drug combinations tested in the experiments, and the number inside parentheses is the CI suggested by Compusyn when the doses are reduced. The third column represents the DRI, which indicates how much the doses of Panobinostat and ZOL used in combination should be reduced to produce a more synergistic combination. The DRI plot **(B)**, which was extracted from Chou–Talalay manuscript in reference (205), gives the visual representation of the tested drug doses (points and triangles) and the dose of drugs that should be used in combination as indicated by Compusyn (line). The plot also displays the fraction of affected (Fa) for each combination plotted. D1 and D2 are two different drugs that are used in combination, which, in this plot, shows that the DRI of drug 1 (D1) in combination is higher than the DRI of drug 2 (D2).

9.2.3. Median-Effect plot

The Median-Effect plot shows the dose-effect relationship of each drug used in combination. Compusyn generates a dose-effect curve **(Figure 10A)** and the Median-Effect plot, which is the same dose response curve log transformed **(Figure 10B).** The log-transformed data clearly depicts the dose-effect relationship even when very low doses are used. This representation holds true for all dose-effect curves that follow the physicochemical principle of the mass-action law regardless of unit or mechanism of action (211). Since the Median-Effect plot yields a straight line, the theoretical minimum doses of two drugs combined allow the drawing of the full dose-effect curve, even when only a few doses were actually tested *in vitro*. That is why Compusyn can predict the dose-effect nature of these drugs combined and decide if a combination of drugs used in predicted doses will result in an effect that is greater, equal, or less than any dose of the individual drugs.

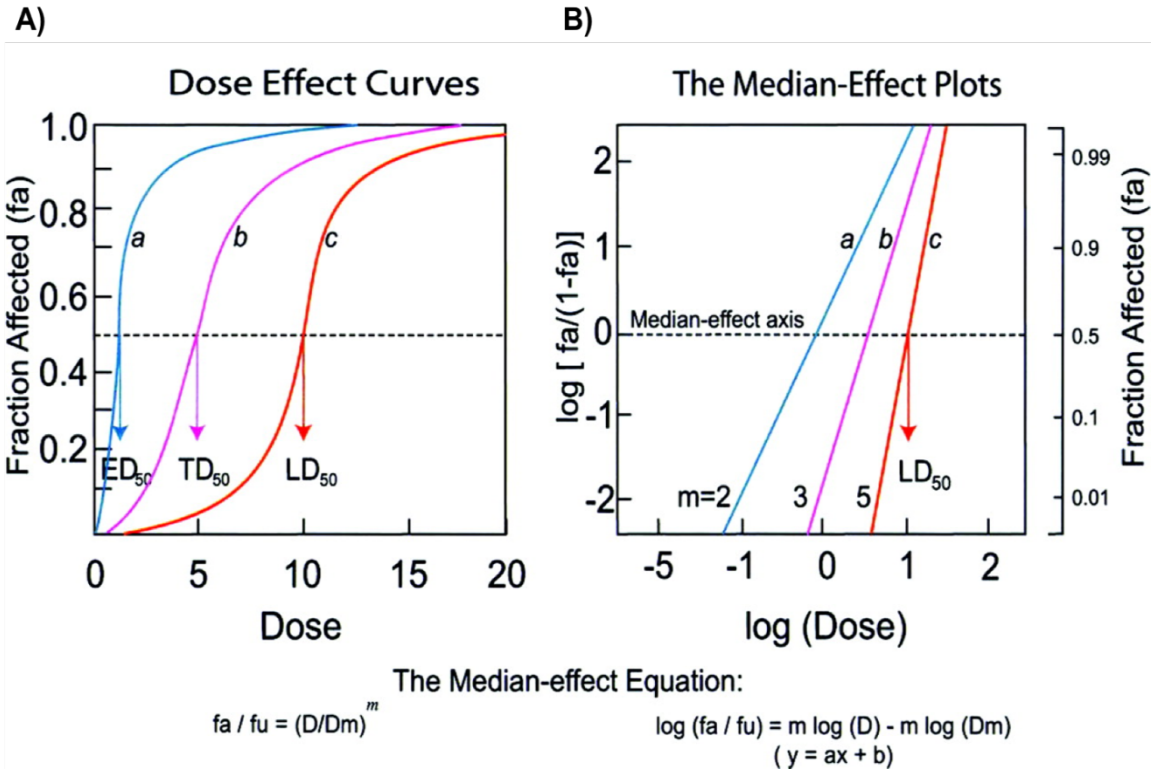

Figure 11. Compusyn representation of the drug dose-effect curve. The drug-effect curve **(A)** is predicted and represented as a sigmoid curve. In the Median-Effect plot **(B)**, there is a log-

transformed representation of this curve, which clear visualizes the effect of very low doses of the drug. In this plot, the log [(fraction of affected fa)/ (fraction of unaffected fu)] yields a straight line with slope (m) and the x-intercept of log (Dm), where Dm equals the anti-log of the x-intercept. Figure 11 is extracted from reference (205). EC50 dose of drug with causes 50% of maximum effect; TD50 is the median toxic dose of a drug or toxin and is the dose at which toxicity occurs in 50% of cases; LD50 is the dose that kills 50% of animals.

9.2.4. Combination-Index plot

The **Combination-Index plot (Fa-CI)** generated using Compusyn displays the interaction (synergism, additivity, or antagonism) of drugs used in combination with their respective predicted effects **(Figure 11A).** In theory, since both the isobologram and the Fa-CI plot generated in Compusyn are based on the Chou–Talalay Combination Index theorem, they should yield identical conclusions about the CI of drugs used in combination. The main difference between the isobologram and the Fa-CI plot is that the isobologram is dose-oriented, whereas the Fa-CI plot is effect-oriented. In addition, while the isobologram shows the CI only between two drugs, the Fa-CI plot can simultaneously show the effects (Fa = fraction of affected) of multiple drugs in any number of combinations in the same graphical representation. The Fa-CI plot considers CI < 1 as synergistic; CI=1 additive; and CI> 1 antagonistic. The log-transformed Fa-CI (the Fa-log(CI)) is also provided by Compusyn, and it is useful to show very low synergism or very strong antagonism values **(Figure 11B)**. The Fa-log(CI) plot not only reduces the out-of-scale points in the Fa-CI plot, but it also makes the presentation symmetrical with the additive effect localizing at 0 since log (CI=1) is 0. Consequently, synergism is shown as a negative value and antagonism is shown as a positive value.

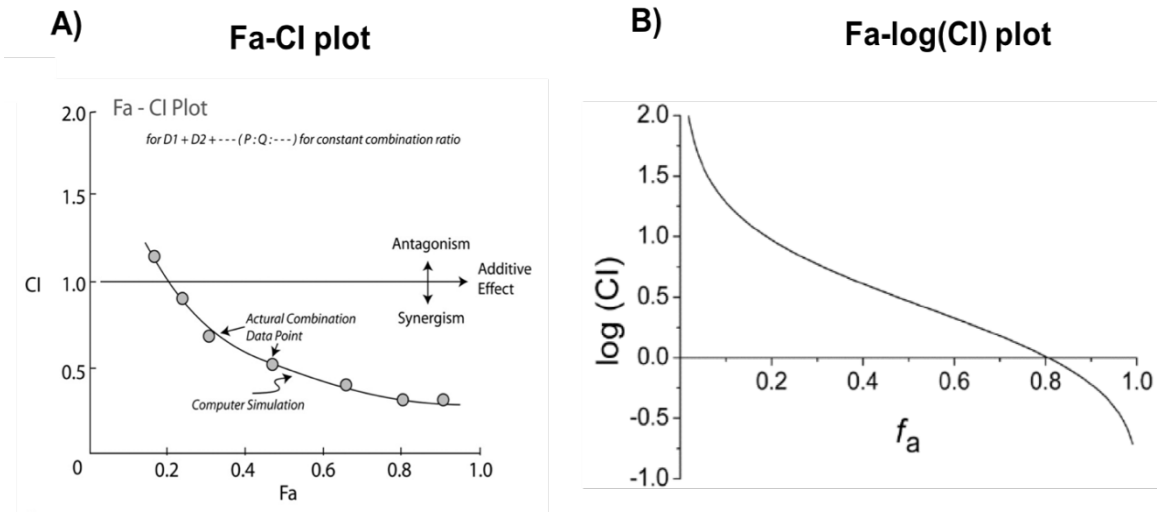

Figure 12. Combination-Index plot. The Fa-CI plot **(A)** displays the Combination Index of the drugs (y-axis) as a function of their effect, or the fraction of affected (Fa). In this graph, CI<0 indicates synergism; CI = 1 additive effect; and CI > 1 antagonism. In the Fa-log (CI) **(B),** the Fa-CI is log-transformed making the additive effect Log CI=0; synergism Log CI<0; and antagonism Log CI > 0. The line generated in the Fa-log (CI) represents drug combinations. Graph A was extracted from reference (205).

9.2.5. Polygonogram

The concept of the polygonogram does not come from mathematical derivations but from practical utility (205, 212). The polygonogram displays an easy to understand visual depiction of multiple drugs used in combination and their CI.

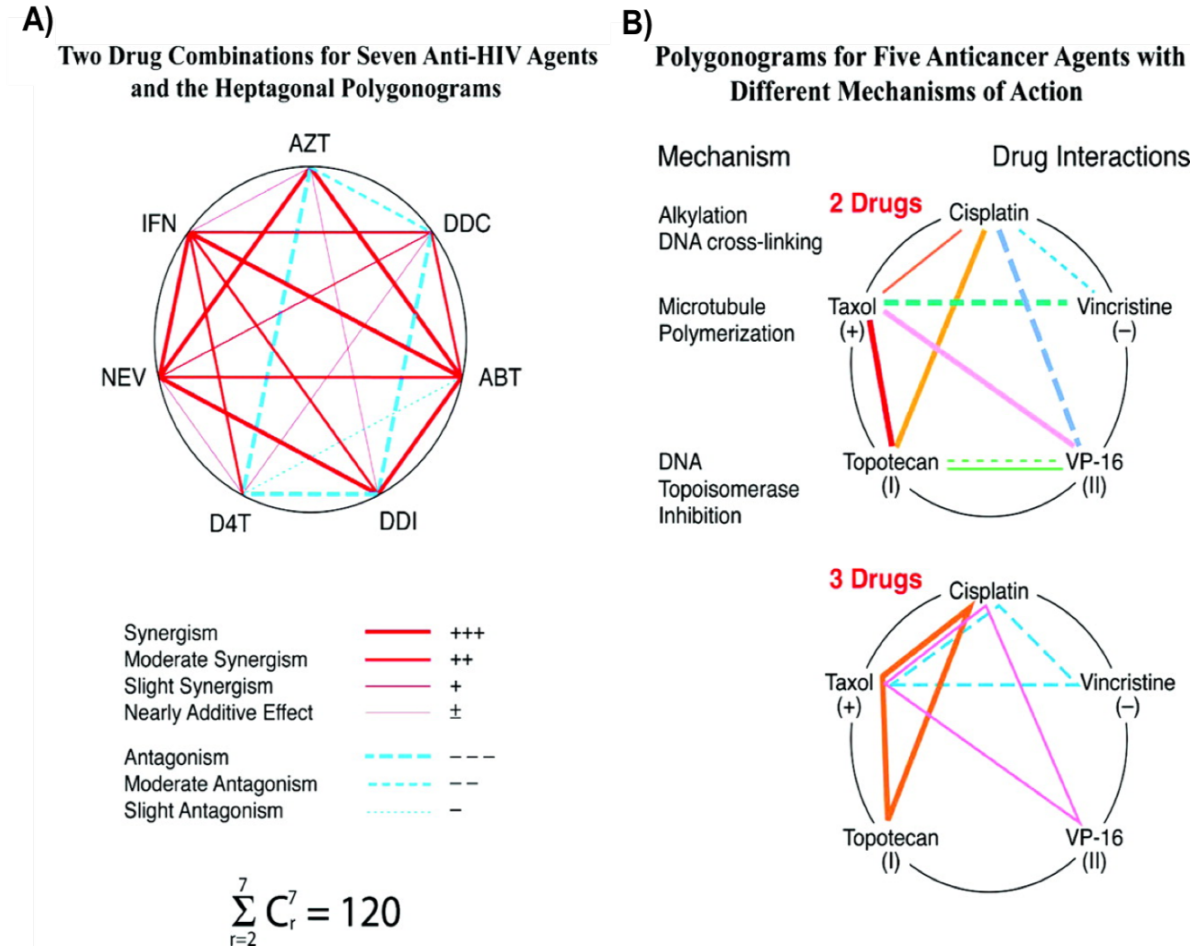

Figure 13. Polygonogram graphical representation. Figures **(A)** and **(B)** display examples of multiple drugs used in combination and their respective CIs. Figure 13 was extracted from reference (205).

10. *In vitro* assays to assess combinations among drugs

10.1. Cell viability assays

An *in vitro* quantitative cell viability assay is commonly used to test cells' viability after being treated with drugs as monotherapies (e.g., EC50) or in combinations. The assay output produces a colorimetric indication that is proportional to the number of cells that survived treatment. There are several commercially available viability assay kits (e.g., Cell Counting Kit-8 (CCK-8), MTS assay, MTT assay, and others), and most of the kits are based on enzymatic conversion of **tetrazolium chloride** to **formazan** by cellular dehydrogenases and reductases to develop the colorimetric indication. Color intensity translates to optical-density values (OD values) through a 96-well plate reader that is set to register the OD values at absorbance level of 490nm. The enzymatic conversion of tetrazolium chloride to formazan is mostly done by enzymes that are active in viable cells with intact membranes and normal physiology. Because enzymes from cells that are going through apoptosis can also contribute to the production of formazan, the assay usually shows a level of background that does not reflect the number of cells that survive the treatment. To mitigate this limitation, 96-well plates treated with drugs are assessed at different time points so that the progression of the cells over time can be accurately determined.

Viability assays, however, are not the best way to assess the efficiency of combination therapies involving radiation because when the cells are irradiated the DNA damage induces cell-cycle arrest, and cells become apoptotic a few days later. But even though irradiated cells can no longer proliferate and will not be viable after a few days, the cells can still efficiently convert tetrazolium chloride to formazan as cellular dehydrogenases are still active. Consequently, because irradiated cells can still form formazan they can give the erroneous impression that they are still viable and this is a limitation when viability assays are used to assess the cytotoxicity of combination therapies involving radiation. In this case different time points might not be sufficient to access viability of cells in later time points, as cells undergo apoptosis usually after five days of being irradiated. Most cells in culture start to die from nutrient starvation by this point, as media is not periodically

changed. Thus, when effects of radiation can be observed, cells are not dying due to irradiation but by high media acidity and nutrient starvation. In addition, later time points which would give a real representation of radiation effect cannot be accessed as viability assays have to be terminated usually by the 7th day from the start of treatment.

10.2. Colony formation assay

The colony formation assay (CFA) is an *in vitro* assay designed to assess whether cells can still proliferate, or, in case of cancer cells, still undergo unlimited replication after being treated with a therapy. The assay is based on the ability of a single cell to grow into a colony after being exposed to a given drug or combination of drugs. Before or after treatment, cells are seeded at appropriate dilutions to form colonies in two to three weeks post-treatment. After this amount of time passes, the colonies are fixed, stained, and counted. Colony numbers in untreated plates determines the plating efficiency **(Figure 12A)**, which reflects whether that untreated cell line has the potential to form colonies. After determining the plating efficiency, the colonies that form after being exposed to a particular treatment are counted to determine their survival fraction **(Figure 12B).**

Although CFA can be used to assess the potential of any drug to inhibit cell proliferation, CFA is the gold standard *in vitro* method to determine the killing effect of radiation (213, 214). The effect of radiation on cells is not immediate. After being irradiated, cells go through cell-cycle arrest and progress to apoptosis at least five days after the radiation-induced DNA damage. Because CFA's incubation time is two to three weeks, the assays properly reflect the efficacy of radiation during treatment.

A) $$\textbf{Plating efficiency} = \frac{\text{Number of colonies in untreated control}}{\text{number of plated cells in untreated control}}$$

B) $$\textbf{Cell survival fraction} = \frac{\text{Number of colonies}}{\text{Number of plated cells} \times \text{Plating efficiency}}$$

Figure 14. Colony formation assay equations to assess the potential of untreated cells to grow colonies **(A)** and to assess a therapy's effectiveness in inhibiting colony growth **(B)**.

11. Chapter I: Studying IFN-expressing oncolytic adenovirus in immunocompetent hamsters as a tool to improve IFN-therapy

11.1. Introduction

Pancreatic ductal adenocarcinoma (PDAC) may soon be the third-leading cause of cancer-related death in the United States (215). Surgery is the most effective treatment for PDAC, but since most patients are diagnosed in the advanced stage of the disease, the majority of them are not candidates for surgical resection. Existing chemotherapies cannot cure PDAC, while new chemotherapy-based regimens such as FOLFIRINOX (129) and NAB-paclitaxel plus Gemcitabine (216) have not meaningfully affected patients' long-term survival rates. The lack of effective therapies against PDAC results in a five-year overall survival rate of 6%, which means that pancreatic cancer will become the second-leading cause of cancer-related death by 2017 (95). Although effective therapies are rare, clinical trials that treat PDAC patients with adjuvant IFN-α (IFN) therapy combined with radiation, 5-FU, and Cisplatin (CDDP) have reported a 20–45% increase patients' two-year survival rate (134-136), and a 35% increase patients' five-year survival rate (134, 137, 138). Other trials, including a trial that added the drug Gemcitabine to the IFN-treatment protocol—have reported a 30% increase in patients' two-year survival rate (136). These trials were designed to combine the effectiveness of surgery with IFN's chemo-radio sensitization and immunostimulatory effects (135, 137, 142-144). Although IFN-based therapeutic approaches have shown promising results, the effectiveness of IFN-therapy was limited by high IFN systemic toxicity, which causes strong flu-like symptoms and high patient drop out from therapy, and perceived low IFN concentrations intratumorally as the result of the rapid degradation of the cytokine in the bloodstream (139-141). These limitations hampered the full potential of IFN-therapy.

The study of oncolytic viruses is a growing area in cancer research because they can be genetically modified to selectively replicate in and kill cancer cells. Examples of these types of viruses include T-VEC (Imlygic™) (217), an FDA-approved therapy against melanoma, and an adenovirus-based H101 therapy, approved in China to treat head and neck cancer (218). Our group has previously reported the use of an oncolytic adenovirus

(OAd) expressing human IFN-α (OAd-IFN) as a promising platform for selective and long-term expression of IFN (25, 56). In this vector structure, we cloned the IFN gene into the adenoviral E3 region, which resulted in high expression of the cytokine in a replication-dependent manner. We have demonstrated that OAd-IFN reduces tumor burden in human PDAC xenografts in mice. We also have showed that an OAd-expressing syngeneic hamster IFN (OAd-hamIFN) was highly effective in reducing the size of tumors and extending survival in both localized and disseminated PDAC in an immunocompetent syngeneic hamster model (25, 56, 87, 94).

Here, in an attempt to improve the effectiveness of and overcome the limitations to this promising IFN-therapy, we tested the use of OAd-hamIFN in combination with 5-FU, Gemcitabine (GEM), Cisplatin (CDDP), and radiation in treatment schemes that resemble the IFN clinical trials mentioned above. We hypothesized that the replication-dependent expression of IFN by OAd-hamIFN will concentrate high levels of IFN in PDAC tumors and potentiate the cytokine chemo-radio sensitization capacity, while reducing its systemic toxicity. To assess the potential of OAd-hamIFN combinations with chemotherapy, radiation, and chemoradiation, we used hamster pancreatic cancer cells *in vitro*, as well as our previously published immunocompetent syngeneic Syrian Hamster model of PDAC as our pre-clinical model (94). In contrast to mice, Syrian hamsters support human-adenovirus replication(87). Thus, using a syngeneic hamster model as our *in vivo* platform is the most appropriate approach to better understand the effect of an IFN-expressing OAd in combination with chemoradiation to treat PDAC (87, 94).

11.2. Materials and methods

Cell lines

The HP1, HAPT-1, PGHAM hamster pancreatic cancer cell lines were provided by Dr. Hollingsworth, University of Nebraska, NE, and Dr. Uchida, Nippon Medical School, Tokyo, Japan, respectively. Cells were cultured as previously described (94).

Adenovirus vectors

Oncolytic adenovirus expressing hamster IFN alpha (OAd-hamIFN) was generated **(Figure 1)** as previously reported (94, 219). We incorporated the interferon gene into the adenoviral E3 region because of the well documented high level of transgene expression from this location. The Adenovirus Death Protein (ADP) was maintained in the adenoviral E3 region while all other nonessential E3 genes such as 12.5 K, 6.7K, gp19K, RID-α and RID-β, and 14.7K were deleted to accommodate the IFN gene. Overexpression of ADP—an enhancer of apoptosis and cell killing—improves the ability of adenovirus to spread in pancreatic cancer cells and potentiates viral oncolytic capacity (25, 54, 56). The vector has incorporated the RGD-4C (Arginive-Glycine-Aspartic) motif in the HI loop of the adenovirus fiber and shifts viral tropism from the CAR receptor to integrins αvβ3 and αvβ5. As a non-IFN control, a counterpart vector expressing the firefly luciferase from the Ad E3 region instead of IFN was used (OAd-LUC). All viruses were propagated in the 911 cell line, purified by double cesium chloride density gradient ultracentrifugation, and dialyzed against phosphate-buffered saline (PBS) with 10% glycerol. Vector biological titers were determined using the plaque-forming unit assay (PFU), and the number of viral particles (VP) were measured using spectrophotometer OD_{260}. The VP/PFU ratio ranged from 10–20. We confirmed the viral structure through PCR using primers specific for the fiber, ADP, IFN, and the transgenes (24, 25, 56, 220).

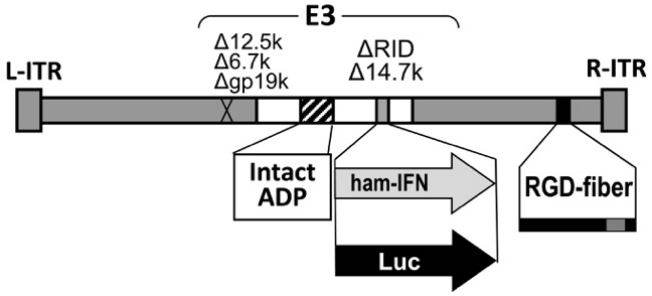

Figure 1. Structure of the oncolytic adenovirus expressing hamster IFN alpha (OAd-hamIFN) and the control vector expressing luciferase. OAd-hamIFN is a replication-competent oncolytic adenovirus that expressesing the hamster IFN-alpha gene from the adenoviral E3 region. The control vector (OAd-LUC) has the same structure as OAd-hamIFN, but has a luciferase transgene

Chemotherapy drugs

For the *in vitro* studies, we purchased Fluorouracil (5-FU), Gemcitabine (GEM), and Cisplatin (CDDP) from the University of Minnesota Boynton Pharmacy. The drugs were diluted and stored as described elsewhere (94). For *in vivo* experiments, we used diluted medical grade 5-FU in the concentration of 50mg/ml, which was also purchased from University of Minnesota Boynton Pharmacy.

Colony formation assay

We platted 1.0 x 10^6 cells in 75cm^2 cell-culture flasks and incubated them at 37^{0}C in a 5% CO_2 humidified incubator. After 24 hours, we infected the cells with OAd-hamIFN or OAd-LUC. One day after infection, we irradiated the flasks representing virus + radiation and virus + 5-FU + radiation groups using the X-RAD 320 X-ray system. The X-ray platform was positioned 50cm from the bottom of the machine and we used Filter 1 (2.0mm Aluminum/ Half Value Layer 1.0mm Cu). We then placed the radiation flasks in humidified incubator 37^{0}C/5% CO_2 for 30 minutes. After the incubation, we trypsinized the cells with 0.25% Trypsin EDTA 1X (Corning, NY) and counted them using an automated cell counter (Cellometer Auto T4, Nexcellon Biosciences, Lawrence, MA). We then serially diluted the cells using DMEM media (10% FBS and 1% Penicillin/Streptomycin) and plated them in 10cm cell-culture dishes that contained only media (OAd-hamIFN + Radiation group) or media with 5-FU (OAd-hamIFN + 5-FU + Radiation group). The cell groups representing virus + 5-FU were trypsinized, counted, serially diluted, and platted in 10cm culture dishes containing media with chemotherapy. Cells in the untreated and OAd-hamIFN treated groups were trypsinized, counted, serially diluted, and platted in 10cm culture dishes with cell-culture media. All the plates were maintained in the humidifier incubator at 37.8°C/5% CO_2, and we replaced the cell-culture media in each plate every two days. When all the plated cells in the untreated group started to show colonies, all the plates in the experiment were fixed with 4% Formalin for one hour at room temperature. We then stained the plates overnight with 1% Methylene blue, washed them with 1X PBS, and allowed them to air dry. We then counted the colonies and used the following formulas to estimate assay results:

$$\text{Plating efficiency} = \frac{Number\ of\ colonies\ in\ untreated\ control}{number\ of\ plated\ cells\ in\ untreated\ control}$$

$$\text{Cell survival fraction} = \frac{\text{Number of colonies}}{\text{Number of plated cells} \times \text{Plating efficiency}}$$

Cell Viability Assay

To perform our quantitative analyses, we plated $8x10^3$ cells/well in 96-well plates and infected them with 100 viral particles (VP)/cell of OAd-hamIFN or OAd-LUC. Four hours later, we replaced the infectious media with Dulbecco's Modified Eagle Medium (DMEM) with 5% Fetal Bovine Serum (FBS), 1% Penicillin/Streptomycin containing 5-FU; GEM, or CDDP, and further incubated the plates. We then performed a viability assay with the CellTiter-96®Aqueous One-Solution Cell Proliferation Assay MTS reagent (Promega) according to the manufacturer's instructions. For the Crystal Violet Assay, we plated $2x10^5$ cells/well in 12-well plates and infected them with 50 or 100 VP/cell. Cells were fixed and stained as previously described (94).

Combination Index analysis

Using Compusyn, we calculated the Combination Index (CI) to determine the synergism (CI<1), antagonism (CI>1), or additive effect (CI=1) between the virus, chemotherapy, and radiation (205). The EC50 of each treatment alone (OAd-hamIFN, 5-FU, and radiation) was quantitatively determined by the Colony Formation Assay (CFA) in HP1 and PGHAM cells, and the EC50 values were entered into Compusyn as monotherapies. We quantified the cytotoxicity of combination treatments using the CFA in same cell lines, and entered into Compusyn the killing effect of the combination therapies. We generated the final CI report using a non-constant ratio between the therapies. We considered strong synergism to exist when the CI<0.5 and moderate synergism when the CI=0.6–0.9.

In vivo experiment

Combinations of OAd-hamIFN with 5-FU, radiation, and 5-FU + radiation

We subcutaneously injected HP1 cells (2 x 10^6) suspended in 100 µl of PBS into both hind legs of female Golden Syrian Hamsters obtained from the Harlan Sprague Dawley facilities. The animals were divided in eight groups comprised of four animals with two tumors each. When a tumor's diameter reached 8–10 mm, we injected it with 2 x 10^{11} VP diluted in 50 µl PBS. The day of this injection was considered day 0.

On days 1, 3, 6, and 10, we gave each animal intraperitoneal injections of 20 mg/kg 5-FU and on day 3 we irradiated them with 8 Gy of radiation. The animals were then anesthetized with a mixture of 100 mg/kg Ketamine and 15 mg/kg Xylazine and placed in a customized radiation chamber where the tumors were exposed to radiation while their bodies were protected by a lead shield. We measured tumor diameter twice a week using calipers and calculated tumor volume using the formula (width^2 × length)/2. The animals were euthanized according to IACUC guidelines.

Assessment of OAd-hamIFN replication in HP1 tumors

We subcutaneously injected HP1 cells (2 x 10^6) suspended in 100 µl of PBS into both hind legs of female Golden Syrian Hamsters obtained from the Harlan Sprague Dawley facilities. The animals were divided into three groups comprised of five animals with 2 tumors each. When a tumor's diameter reached 8–10mm, we injected it with 50µL of PBS in virus in the concentration of 2 x 10^{12} VP/cell. Seven days after the initial infection, we harvested the tumors and froze them at -80°C. The frozen tumors were fixed with buffered formaldehyde and embedded in OCT cryoprotectant (15% sucrose, 0.1 mol/L phosphate buffer, pH 7.2). We then froze the tumors in liquid nitrogen, cut them into 15-µM slices, and placed them in silane-covered slides. These slices were then incubated at room temperature with the primary goat anti-hexon polyclonal antibody, washed three times, and incubated again with FITC-labeled donkey anti-goat secondary antibody. After this incubation period, we performed counterstaining with Hoechst 33342. Hexon staining was visualized using confocal microscope. Staining analysis was qualitative.

Radiation

We administered radiation *in vitro* and *in vivo* using the X-RAD 320 X-ray system (North Btanford, CT). The X-ray radiation platform was positioned 50cm from bottom of the machine and we used Filter 1 (2.0 mm Aluminum/ Half Value Layer 1.0mm Cu).

Statistical analysis

In vivo, we analyzed tumor volume over time using a linear mixed model. The outcome (tumor volume) was the square-root transformed to improve the model fit. The fixed effects included the treatment group; time (continuous); and the interaction between group and time. Random intercept and time effects were included for each animal. Twelve pairwise group tests (model contrasts) analyzed whether the slope (change over time) differed between treatment groups. We obtained p-values relative to the 5-FU + Radiation group because this was the historical control group compared to IFN-based therapies in clinical trials. For the survival study, we compared the 5-FU + Radiation and all other treatment groups using standard log-rank tests. The stepdown Bonferroni method adjusted for multiple tests in the *in vivo* and survival studies. For the *in vitro* cell viability study, we performed two-way ANOVA for each cell line and treatment condition, with a three-level treatment dose effect and a binary virus effect.

11.3. Results

Potentiation of chemotherapy by OAd-hamIFN

We assessed the cytotoxicity of OAd-hamIFN **(Figure 1)** in combination with 5-FU, GEM, and CDDP chemotherapy drugs *in vitro*. The qualitative analyses using crystal violet **(Figure 2)** and quantitative analyses using cell viability assays (**Figure 3)** showed that compared to virus or chemotherapy alone, OAd-hamIFN enhanced the cytotoxicity of all the drugs in both cell lines. We observed that the combination of OAd-hamIFN and 5-FU resulted in the strongest potentiation of cell cytotoxicity. While the cytotoxicity of treatments where OAdhamIFN was combined with CDDP or GEM varied across different cell lines, the combination of the virus and 5-FU resulted in similar cytotoxic profiles in all cell lines. Although CDDP monotherapy was not effective in killing HP1 and HAPT-1

cells, using CDDP in combination with OAd-hamIFN resulted in the greatest enhancement of cytotoxicity, which highlights the virus' role in breaking cell resistance to chemotherapy. This data indicates that an IFN-expressing OAd can significantly enhance the killing effect of chemotherapeutics used in IFN clinical trials.

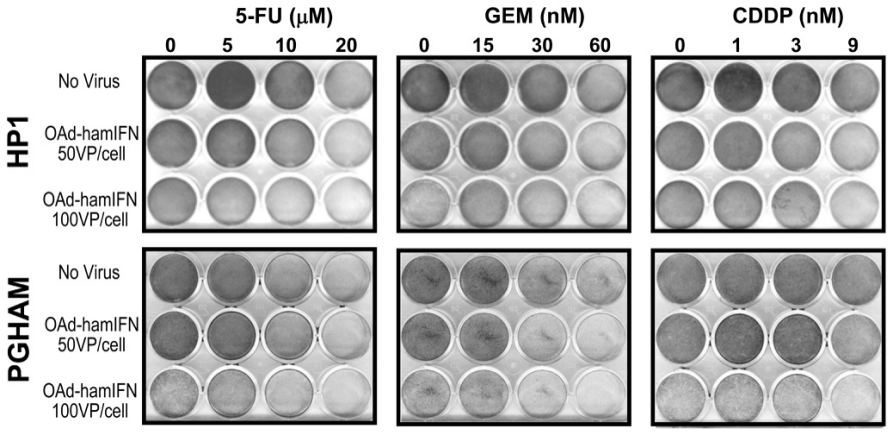

Figure 2. Qualitative analysis of the cytocidal effect of OAd-hamIFN combined with chemotherapies. Combinations of OAd-hamIFN with 5-FU, Cisplatin (CDDP), and Gemcitabine (GEM) were analyzed for their cytocidal effect in HP1 and PGHAM hamster pancreatic cancer cell lines using the crystal violet assay. In both cell lines, a combination of the virus and chemotherapy showed superior cell-killing effect compared to the virus's cytotoxicity or chemotherapy alone. By increasing of the doses of the virus and chemotherapy, the killing effect was further improved. VP: viral particle.

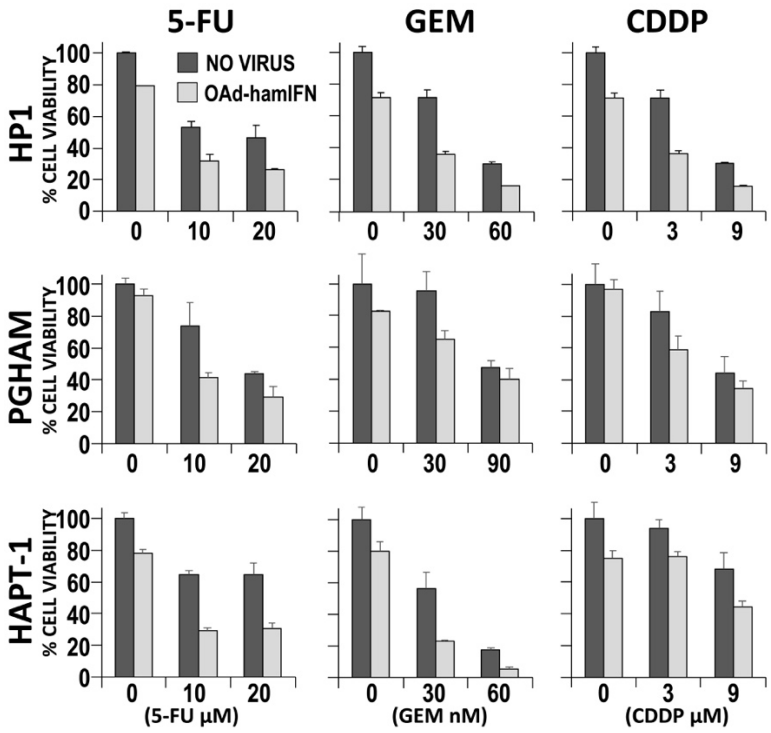

Figure 3. Quantitative analysis of the cytocidal effect of OAd-hamIFN combined with chemotherapy. We compared the cytotoxicity of 100 VP/cell of OAd-hamIFN and chemo-monotherapies to the cytocidal effect of OAd-hamIFN combination therapies with respective doses of 5-FU, GEM, and CDDP. Within each of the nine conditions, we performed a two-way ANOVA with dose and virus effects. All the effects had $p < 0.025$, which indicates that the killing effect of OAd-hamIFN + Chemotherapy was superior to the killing effect of chemotherapy or OAd-hamIFN alone. The standard deviation was used to represent the variation within individual treatments (bars on the top of histogram).

Contribution of IFN to chemotherapy cytotoxicity

We used cell viability assays to test whether IFN expressed by OAd-hamIFN could enhance cytotoxicity in combinations of OAd-hamIFN with 5-FU, GEM, and CDDP **(Figure 4)**. A comparison of OAd-hamIFN and non-IFN-expressing counterpart vector (OAd-LUC) combined with 5-FU, GEM, and CDDP showed that IFN expressed by OAd-hamIFN enhanced the killing effect of not only OAd, but also potentiated the cytotoxicity in HP1 cells of all chemotherapy drugs. The expression of IFN seemed essential to boosting the cytotoxic effect of chemotherapy. Of note, IFN exhibited a greater contribution toward accentuating cell killing with GEM and CDDP than with 5-FU.

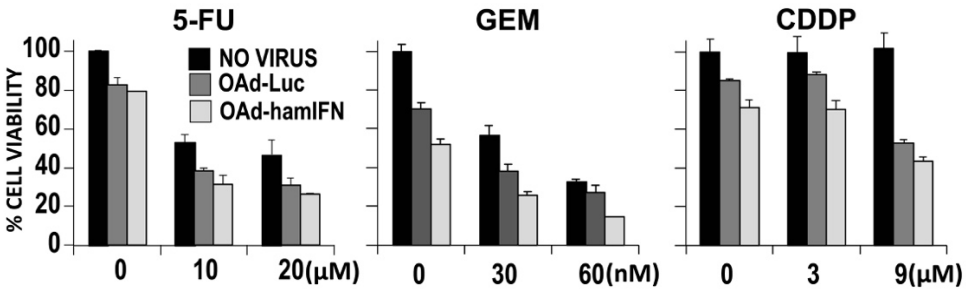

Figure 4. Contribution of IFN expressed by the adenovirus to increase the cytotoxicity of viro-chemotherapies. We used the cell viability assay to evaluate contribution of IFN expression to enhance cytoxicity of viro-chemotherapies in HP1 cells. We compared OAd-hamIFN combined with 5-FU, GEM, and CDDP to the control vector (OAd-LUC) each at the concentration of 100 VP/cell paired with the same concentrations of chemotherapeutics. Within each of the three treatment conditions, we performed a two-way ANOVA with dose and virus effects. Within each condition, the virus effect (OAd-LUC vs OAd-ham IFN) had a $p < 0.01$. The standard deviation was used to represent the variation within individual treatments (bars on the top of histogram).

Potentiation of radiation and chemoradiation by OAd-hamIFN

To further analyze the effect of radiation on the effectiveness of OAd-hamIFN treatments, we used the crystal violet assay to test combinations of OAd-hamIFN with 5-FU, radiation, and 5-FU+radiation in HP1 cells. **(Figure 5)**. We used 5-FU as the drug of choice because combinations of the virus with 5-FU showed similar cytotoxicity profiles in all the cells **(Figures 2 and 3).** 5-FU also was given to patients during all the chemotherapy cycles in IFN clinical trials. Our qualitative assessment reinforced the fact that OAd-hamIFN enhanced the killing effect of 5-FU **(Figure 5A)**, and also showed that the virus enhanced the cytotoxicity of radiation **(Figure 5B-2).** Treatments of OAd-hamIFN in combination with 5-FU+radiation—which mimicked the use of IFN + 5-FU + Radiation in IFN-clinical trials—was the most cytotoxic viral combination we tested **(Figure 5B-4).** Importantly, the treatments of OAd-hamIFN combined with higher doses of 5-FU **(Figure 5B-2)**, radiation **(Figure 5B-2)**, or 5-FU + radiation **(Figure 5B-4)** were more effective in killing cancer cells than treatments with 5-FU + Radiation **(Figure 5-3)**. The 5-FU + radiation regimen was the standard control that the clinical trials used to determine the efficacy of IFN-based therapies (134, 137, 144, 149). Overall, including IFN-expressing OAd potentiated the killing effect of all the different components used in IFN-based therapies in clinical trials,

which reinforces the view that the virus has the potential to potentiate the effectiveness of cancer therapy.

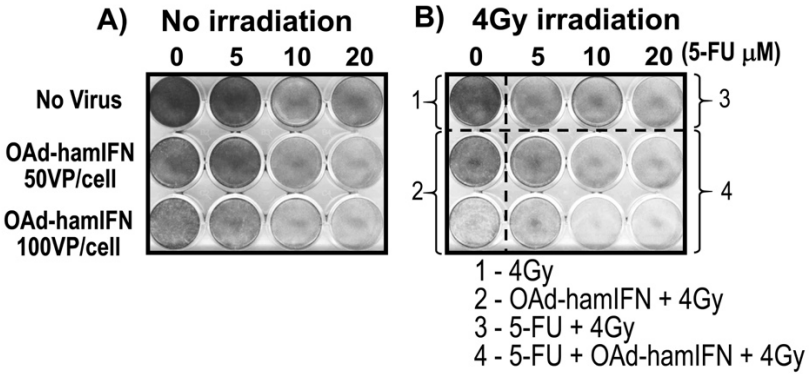

Figure 5. Addition of radiation to viro-chemotherapy resulted in superior killing effect. We analyzed the cytotoxicity of OAd-hamIFN combined with 5-FU and radiation using the crystal violet assay. We compared the cytocidal effect of combination therapy with OAd-hamIFN (50 or 100 VP/cell) and 5-FU (5, 10, and 20 μM) to cytocidal effect of combinations of OAd-hamIFN and 5-FU in the same concentrations, but with added radiation (4Gy).

OAd-hamIFN combinations with chemotherapy, radiation, and chemoradiation are highly synergistic

To characterize the interaction between the therapeutic agents combined with OAd-hamIFN, we performed the synergy analysis as described by Chou and Talalay (205). We used the colony-formation method because it is the gold-standard assay for investigating the radio-sensitivity of cancer cells **(Figure 6).** The assay output showed that treatments of OAd-hamIFN combined with 5-FU, radiation, and 5-FU+radiation were efficient and inhibited the formation of more than 50% of colonies after treatment. Because PGHAM cells were more resistant to OAd-hamIFN, 5-FU, and radiation as monotherapies, only combination treatments with higher doses of the virus, 5-FU, or radiation combined strongly inhibited colony formation. In contrast, the treatments that mimicked IFN-therapy in humans (OAd-hamIFN + 5-FU + Radiation) remarkably inhibited colony formation regardless of the doses of the chemotherapeutics. In both cell lines, an analysis of the Combination Index showed that all the treatments that included OAd-hamIFN were synergistic (CI<1), and that strong synergism (C < 0.5) occurred when OAd-hamIFN was

combined with 5-FU + radiation. Although synergism and strong cytotoxicity in HP1 cells was observed in all the OAd-hamIFN treatments, in the PGHAM cells the same happened only when the treatments included higher doses of therapeutics or when the triple therapy (OAd-hamIFN + 5-FU + Radiation) was used. Therefore, the remarkable synergy between IFN-expressing OAd and conventional PDAC therapeutics provides a great opportunity to improve the IFN-therapy's anti-tumor effects while making the therapy less toxic.

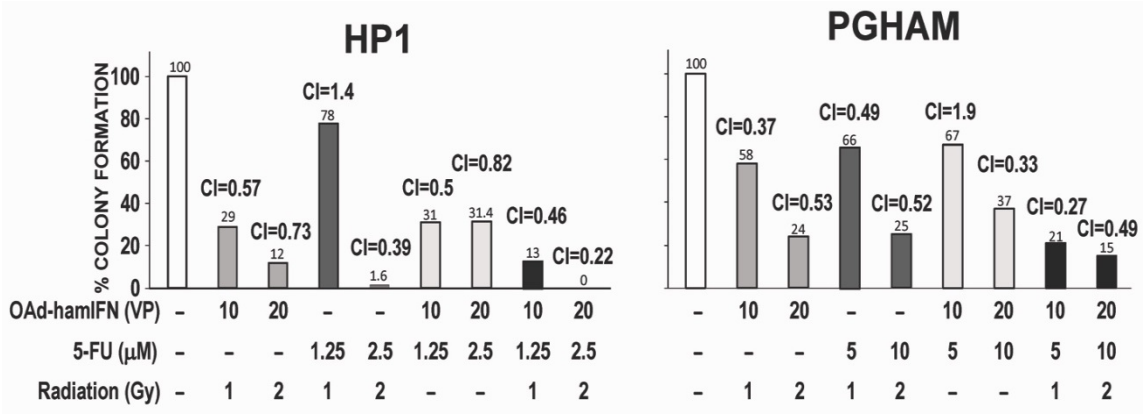

Figure 6. Quantification of cytotoxicity and synergy of OAd-hamIFN combination therapies based on the colony formation assay. Combination of OAd-hamIFN with 5-FU, radiation, and chemoradiation reduced the number of colonies formed in hamster pancreatic cancer cell lines. We identified strong synergism (CI < 1) in the groups treated with OAd-hamIFN in combination with chemotherapy, radiation, and chemoradiation. In both cell lines, combinations of OAd-hamIFN and chemoradiation in higher doses resulted in the strongest killing effect and synergistic interaction. The Chou–Talalay method was used to determine the Combination Index (CI). Synergistic effect (CI < 1); additive effect (CI = 10); antagonistic effect (CI > 1).

Inhibition of tumor growth by OAd-hamIFN combination therapies in Syrian hamsters

We also tested the effectiveness of OAd-hamIFN treatments in the syngeneic immunocompetent hamster model of pancreatic cancer **(Figure 7A)**. The treatments that included OAd-hamIFN resulted in stronger tumor growth inhibition than the treatments without the virus (**Figure 7B**). The strongest anti-tumor effect was observed in animals treated with the combination of OAd-hamIFN + 5-FU + radiation or the combination of OAd hamIFN + radiation. Compared to animals only treated with 5-FU + radiation (a

control group used in prior IFN clinical trials), which control group averaged a 358% increase in the anti-tumor effect between Day 0 and Day 25, the anti-tumor effect in the triple-therapy group increased an additional 11% ($p=0.0021$ vs controls) and the anti-tumor effect of OAD hamIFN + radiation group increased an additional 44% ($p=0.01$). One animal that was treated with the triple therapy experienced complete tumor elimination.

Although the animals that were treated with OAd-hamIFN + 5-FU had smaller tumors than the animals in the control group (5-FU + radiation), the anti-tumor effect was not statistically significant (180% average increase at day 25; $p=0.41$). Comparisons between animals treated with OAd-LUC + Radiation and OAd-hamIFN + Radiation showed that IFN expressed by OAd-hamIFN greatly contributed to stronger tumor growth inhibition. Finally, in addition to the strongest anti-tumor effect, the animals treated with viral therapies experienced the slowest regrowth of the tumors.

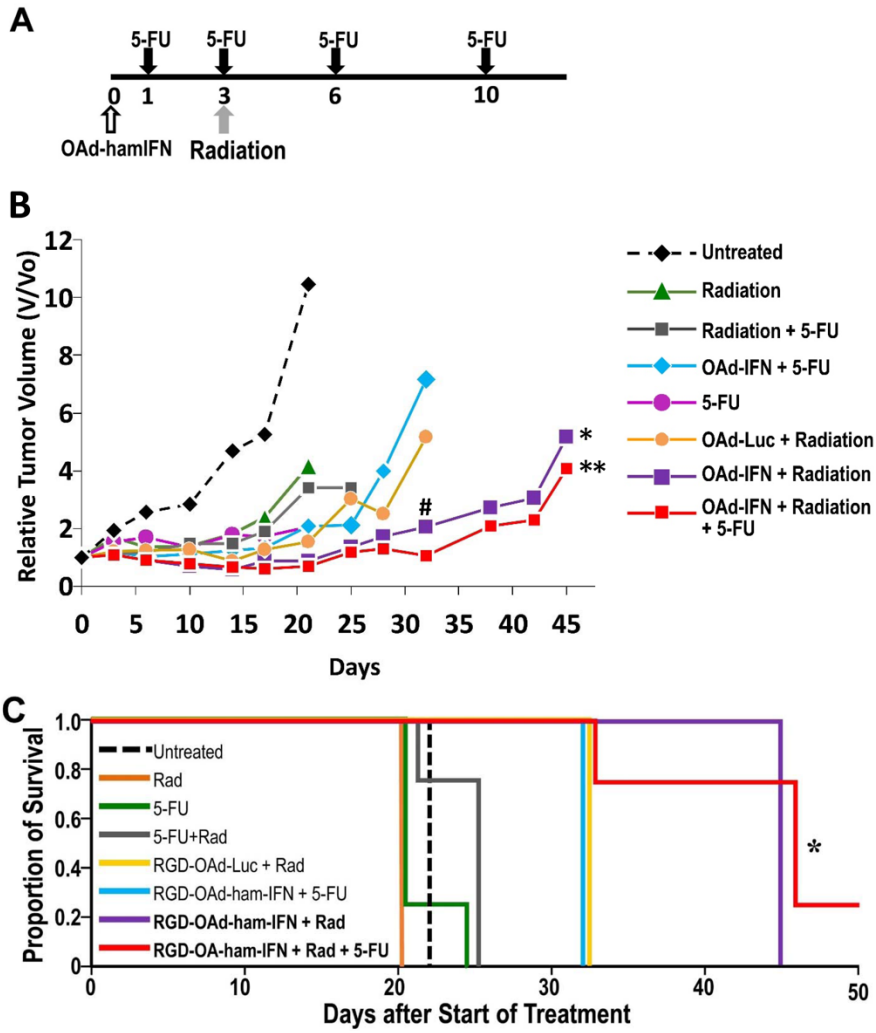

Figure 7. Improved anti-tumor effect and survival of OAd-hamIFN combination therapies *in vivo*. We compared the anti-tumor effect and survival of combination therapy groups against the chemoradiation group (5-FU + Radiation). **(A**) Treatment schedule used in hamsters. **(B)** Besides showing the strongest anti-tumor effect, the animals treated with viral therapies demonstrated the slowest tumor regrowth. **(C)** The survival rate of animals treated with OAd-hamIFN combined with 5FU and radiation was significantly improved. The animals in the untreated and chemoradiation groups were euthanized earlier because of tumor size and ascites. $p < 0.05$ vs Radiation+5-FU (*); $p < 0.005$ (**) vs Radiation+5-FU; $p<0.01$ vs OAd-Luc+radiation (#).

Survival study in Syrian hamsters

We monitored the survival of hamsters treated with OAd-hamIFN combined with 5-FU, radiation and 5-FU + radiation for 45 days after their initial treatment **(Figure 7C).** treatments with 5-FU or radiation as monotherapies were not effective—the survival rates

were similar to those of untreated animals (median 21 days). The animals that were treated with OAd-hamIFN combination treatments, however, survived longer than the monotherapy groups and the control-therapy group (5-FU + Radiation; median survival of 25 days), which represent conventional PDAC treatments. The hamster in the group that received OAd-hamIFN + Radiation and the triple-therapy (OAdhamIFN + 5-FU + Radiation) survived the longest of all the groups—a median survival period of 45 days ($p=0.06$ and 0.02 vs controls, respectively). The triple therapy was the only therapy that showed a statistically significant survival period compared to the control chemoradiation group and was the only therapy that resulted in complete tumor regression in one animal. The OAd-hamIFN + 5-FU treatment group also had a longer survival period (median 32 days) compared to the 5-FU + Radiation control group, but this result was not statistically significant. A comparison of the survival rate in the OAd-LUC + Radiation group and the group treated with OAd-hamIFN + Radiation showed that the virus's expression of IFN significantly contributed to improved survival when virotherapy is combined with radiotherapy. Our survival data correlated well with the previous therapeutic study **(Figure 7B)**, and supports our hypothesis that using IFN-expressing OAd in treatment regimens that mimic IFN-based therapy may extend human patients' survival periods.

Replication of OAd-hamIFN in immunocompetent hamsters

Because hamsters are immunocompetent, it is possible that infecting a tumor with OAd-hamIFN can stimulate an anti-viral immune response that can stop OAd-hamIFN replication in the tumor **(Figure 8).** To assess the replication of OAd-hamIFN in hamsters bearing HP1 tumors, we compared replication of non-IFN expressing OAd (OAd-LUC) with replication of OAd-hamIFN in tumors seven days post-infection of tumors. To do that comparison, we stained for the adenovirus hexon protein, which is a component of adenovirus capsid. Hexon is coded by the adenovirus's late genes, and presence of this protein indicates that the virus can complete a full replication cycle in infected cells. The data showed that both viruses could replicate in HP1 tumors, and that although OAd-hamIFN expresses a immunostimulatory cytokine, the replication of this vector was not inhibited. Therefore, using IFN-expressing OAd in immunocompetent hamsters is not only

capable of potentiating the effect of chemoradiation, but also holds the potential to stimulate anti-tumor immunity by releasing tumor-specific peptides during oncolysis.

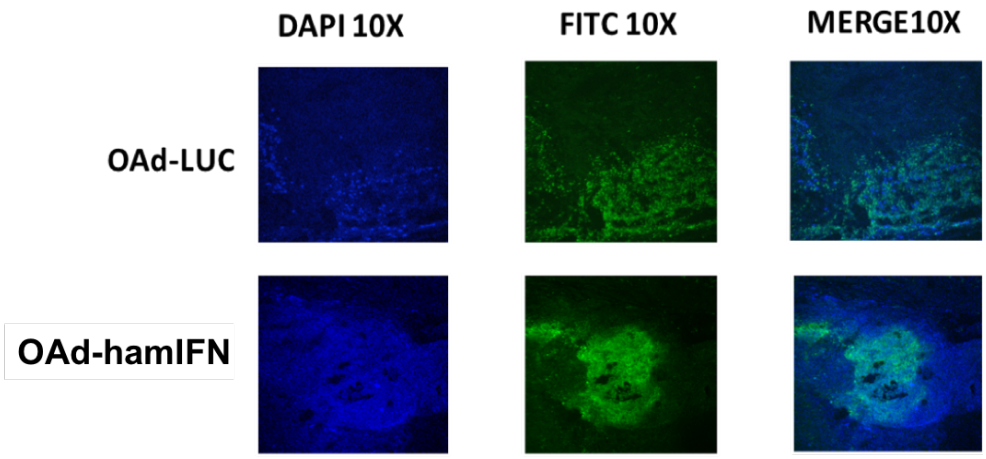

Figure 8. Replication of OAd-hamIFN in immunocompetent hamsters. We compared the replication of a non-IFN expressing OAd (OAd-LUC) and an IFN-expressing OAd (OAd-hamIFN) in HP1 tumors in immunocompetent hamsters. We stained the Hexon protein—a capsid protein coded by the adenovirus's late genes—with FITC seven days after viral infection. The data showed that both viruses could replicate in tumors and that the fact OAd-hamIFN expresses an immunostimulatory cytokine did not abolished viral replication.

11.4. Figures

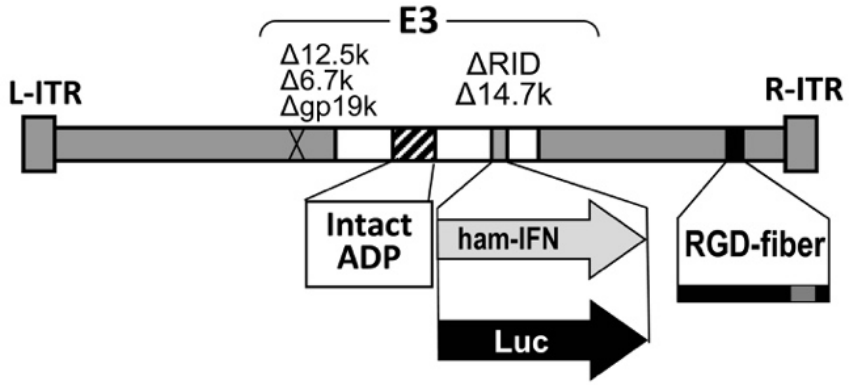

Figure 1. Structure of the oncolytic adenovirus expressing hamster IFN alpha (OAd-hamIFN) and the control vector expressing luciferase. OAd-hamIFN is a replication-competent oncolytic adenovirus that expressesing the hamster IFN-alpha gene from the adenoviral E3 region. The control vector (OAd-LUC) has the same structure as OAd-hamIFN, but has a luciferase transgene instead of hamIFN.

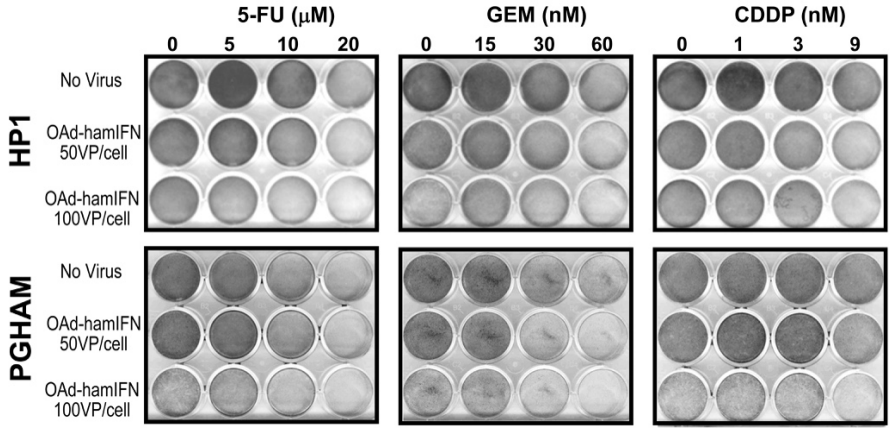

Figure 2. Qualitative analysis of the cytocidal effect of OAd-hamIFN combined with chemotherapies. Combinations of OAd-hamIFN with 5-FU, Cisplatin (CDDP), and Gemcitabine (GEM) were analyzed for their cytocidal effect in HP1 and PGHAM hamster pancreatic cancer cell lines using the crystal violet assay. In both cell lines, a combination of the virus and chemotherapy showed superior cell-killing effect compared to the virus's cytotoxicity or chemotherapy alone. By increasing of the doses of the virus and chemotherapy, the killing effect was further improved. VP: viral particle.

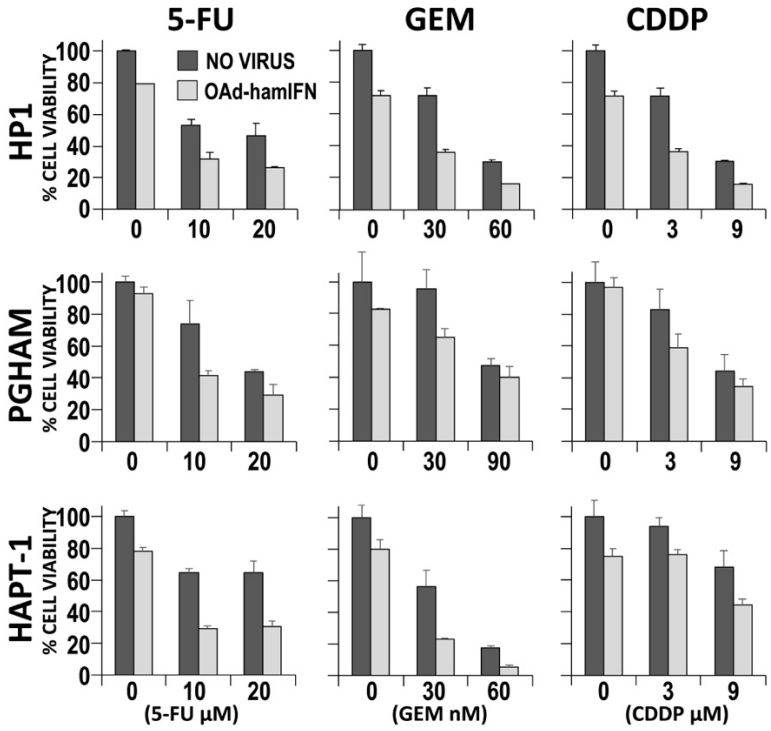

Figure 3. Quantitative analysis of the cytocidal effect of OAd-hamIFN combined with chemotherapy. We compared the cytotoxicity of 100 VP/cell of OAd-hamIFN and chemo-monotherapies to the cytocidal effect of OAd-hamIFN combination therapies with respective doses of 5-FU, GEM, and CDDP. Within each of the nine conditions, we performed a two-way ANOVA with dose and virus effects. All the effects had $p < 0.025$, which indicates that the killing effect of OAd-hamIFN + Chemotherapy was superior to the killing effect of chemotherapy or OAd-hamIFN alone. The standard deviation was used to represent the variation within individual treatments (bars on the top of histogram).

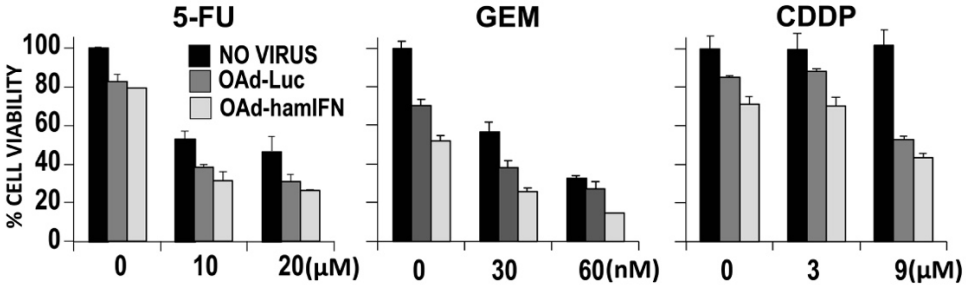

Figure 4. Contribution of IFN expressed by the adenovirus to increase the cytotoxicity of viro-chemotherapies. We used the cell viability assay to evaluate contribution of IFN expression to enhance cytoxicity of viro-chemotherapies in HP1 cells. We compared OAd-hamIFN combined with 5-FU, GEM, and CDDP to the control vector (OAd-LUC) paired with the same concentrations

of chemotherapeutics. Within each of the three treatment conditions, we performed a two-way ANOVA with dose and virus effects. Within each condition, the virus effect (OAd-LUC vs OAd-ham IFN) had a $p < 0.01$. The standard deviation was used to represent the variation within individual treatments (bars on the top of histogram).

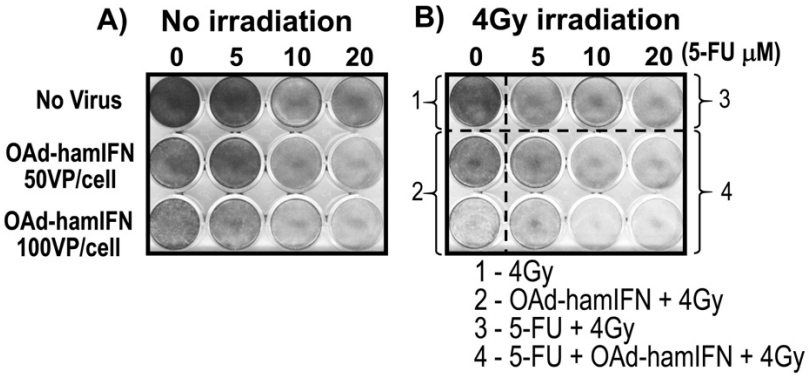

Figure 5. Addition of radiation to viro-chemotherapy resulted in superior killing effect. We analyzed the cytotoxicity of OAd-hamIFN combined with 5-FU and radiation using the crystal violet assay. We compared the cytocidal effect of combination therapy with OAd-hamIFN (50 or 100 VP/cell) and 5-FU (5, 10, and 20 μM) to cytocidal effect of combinations of OAd-hamIFN and 5-FU in the same concentrations, but with added radiation (4Gy).

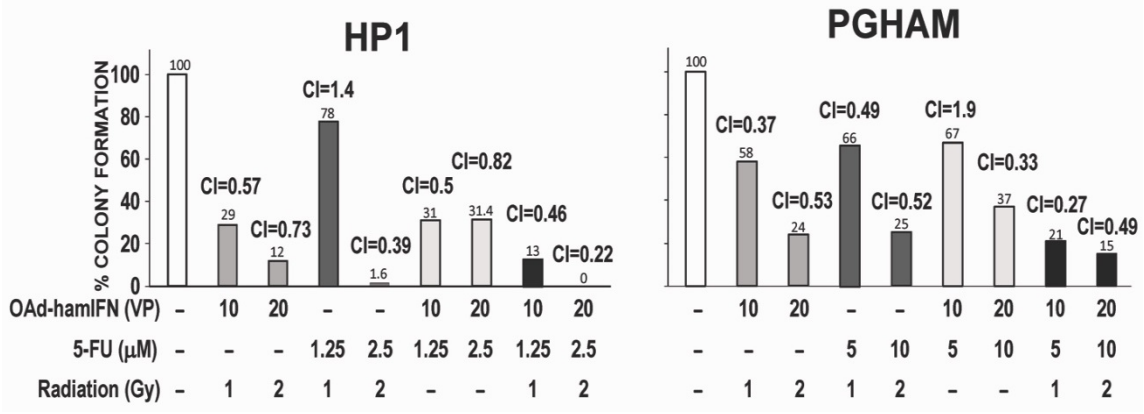

Figure 6. Quantification of cytotoxicity and synergy of OAd-hamIFN combination therapies based on the colony formation assay. Combination of OAd-hamIFN with 5-FU, radiation, and chemoradiation reduced the number of colonies formed in hamster pancreatic cancer cell lines. We identified strong synergism (CI < 1) in the groups treated with OAd-hamIFN in combination with chemotherapy, radiation, and chemoradiation. In both cell lines, combinations of OAd-hamIFN and chemoradiation in higher doses resulted in the strongest killing effect and synergistic interaction. The Chou–Talalay method was used to determine the Combination Index (CI). Synergistic effect (CI < 1); additive effect (CI = 10); antagonistic effect (CI > 1).

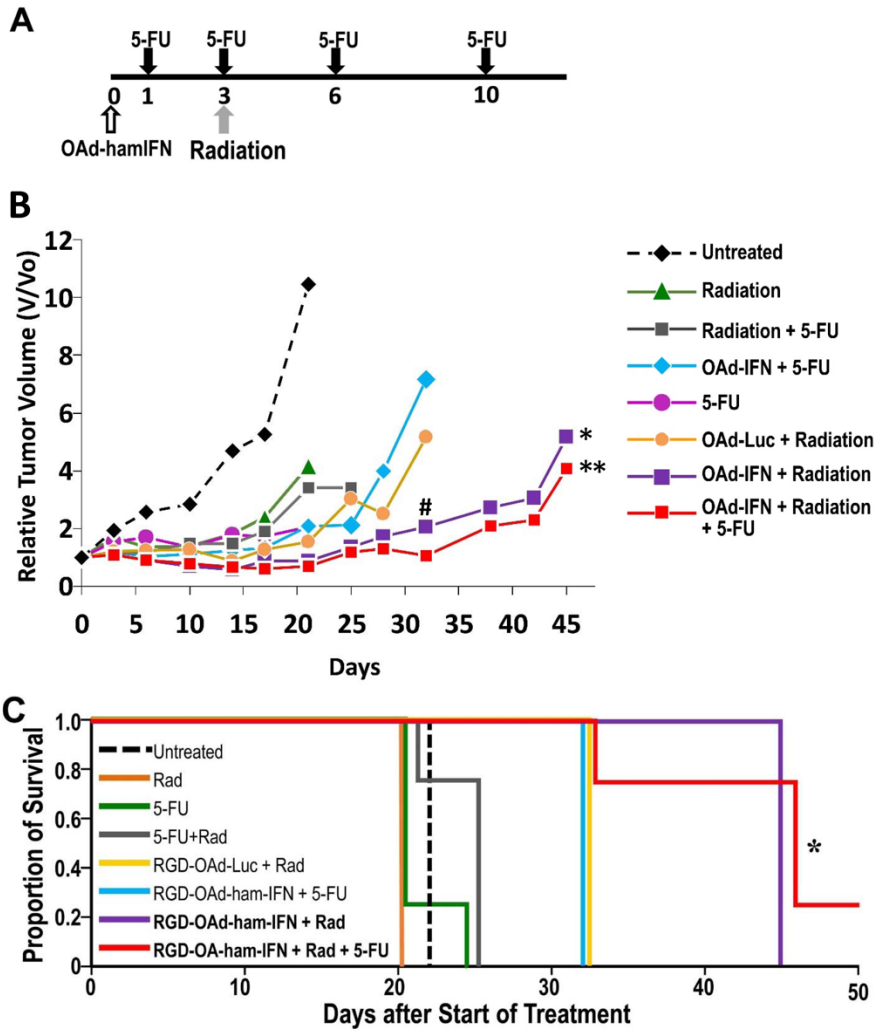

Figure 7. Improved anti-tumor effect and survival of OAd-hamIFN combination therapies *in vivo*. We compared the anti-tumor effect and survival of combination therapy groups against the chemoradiation group (5-FU + Radiation). **(A**) Treatment schedule used in hamsters. **(B)** Besides showing the strongest anti-tumor effect, the animals treated with viral therapies demonstrated the slowest tumor regrowth. **(C)** The survival rate of animals treated with OAd-hamIFN combined with 5FU and radiation was significantly improved. The animals in the untreated and chemoradiation groups were euthanized earlier because of tumor size and ascites. $p < 0.05$ vs Radiation+5-FU (*); $p < 0.005$ (**) vs Radiation+5-FU; $p<0.01$ vs OAd-Luc+radiation (#).

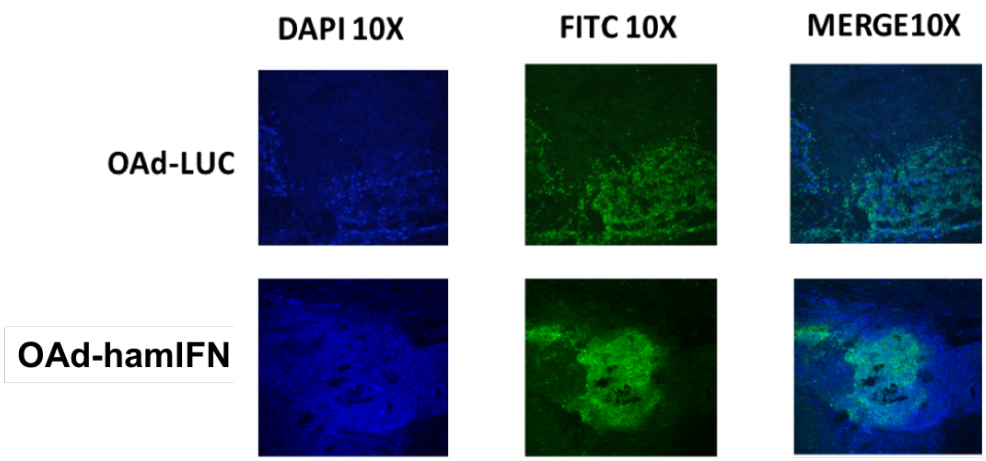

Figure 8. Replication of OAd-hamIFN in immunocompetent hamsters. We compared the replication of a non-IFN expressing OAd (OAd-LUC) and an IFN-expressing OAd (OAd-hamIFN) in HP1 tumors in immunocompetent hamsters. We stained the Hexon protein—a capsid protein coded by the adenovirus's late genes—with FITC seven days after viral infection. The data showed that both viruses could replicate in tumors and that the fact OAd-hamIFN expresses an immunostimulatory cytokine did not abolished viral replication.

11.5. Discussion

We investigated the use of a replication-competent oncolytic adenovirus expressing IFN as a tool to boost the efficacy and overcome the limitations of IFN-based chemoradiation therapy, which is one of few therapeutic protocols that has been effective in treating PDAC.

We used a Syrian hamster model to conduct our studies because Syrian hamsters are permissive to human-adenovirus replication and they provide a unique immunocompetent model to objectively analyze the effect of an adenovirus-produced immunostimulatory cytokine. Using this model, we assessed the use of OAd-expressing hamster IFN in therapeutic protocols similar to the IFN-based therapy used in prior PDAC clinical trials. We believed that using OAd—which is known to enhance the killing effect of chemotherapy and radiation (25, 56, 94, 221-224)—combined with a chemo-radio sensitizer such as IFN would significantly improve the effectiveness of chemoradiation therapy.

Our data showed that IFN expressed by OAd-hamIFN augmented the capability of OAd to sensitize cells to 5-FU, GEM, and CDDP. The potentiation effect of these drugs is extremely important because they are commonly used to treat pancreatic cancer. We also demonstrated that using OAd-hamIFN in combination with 5-FU, radiation, or 5-FU + radiation enhanced the killing of cells *in vitro*, and resulted in the most effective treatments *in vivo*. Most importantly, the treatment of OAd-hamIFN in combination with 5-FU and radiation mimicked IFN therapy in clinical trials and was consistently highly effective in eliminating cancer cells *in vitro* and *in vivo*. These data support our conclusion that adding an IFN-expressing OAd to chemotherapy, radiation, or chemoradiation is a promising approach to further improving already one of the most promising pancreatic cancer therapies.

The Combination Index (CI) analysis showed that double-therapy treatments of OAd-hamIFN with 5-FU or radiation were synergistic (CI<1), and that triple-therapy treatments (OAd-hamIFN + 5-FU + Radiation) were strongly synergistic (CI<0.5). In HP1 cells, all the viral treatments that showed synergism correlated with strong cytotoxicity, which indicates that the synergism translated to treatment efficacy. In PGHAM cells, the synergism in double-therapies groups (OAd-hamIFN + 5-FU and OAd-hamIFN + Radiation) correlated with strong cytotoxicity but only when higher doses of therapeutics were used. This result can be explained by the fact that PGHAM cells were more resistant to killing by virus, 5-FU, and radiation as single therapies. Nevertheless, using OAd-hamIFN in combination with both 5-FU and radiation resulted in highly synergistic and cytotoxic treatments regardless of the dose of therapeutics used. This result, therefore, suggests that the chemo-radio sensitization capacity of both the virus and IFN contributed to improve treatment efficacy even when cells are not susceptible to monotherapies.

Based on prior reports of other groups, we expected this synergistic interaction between OAd-hamIFN and radiation, 5-FU, and chemoradiation. Radiation predominantly causes double-strand breaks (DSB) in cell DNA, which leads to mitosis crisis and cell apoptosis (146, 225). The adenovirus E4 proteins impede DSB repair by binding and inhibiting DNA-dependent protein kinase (DNA-PK), which is one of the main components of the non-homologous end joining (NHEJ) repair pathway (224, 226). Therefore, the strong

synergism between radiation and OAd-hamIFN is supposed to be a combination of inhibition of DNA repair by OAd and the radio-sensitization effect of IFN expressed by the virus. There are no clear reports exploring the mechanism of action by which OAd sensitizes cells to chemotherapy drugs. It is known that IFN induces the double stranded RNA-activated protein kinase (PKR) in cells, and that PKR shuts down protein translation (227) . It is possible that that inhibition of protein synthesis combined with the DNA damage caused by 5-FU leads to synergism in OAd-hamIFN combinations with 5-FU. In addition, by manipulating cells to produce new viral progenies instead of cellular proteins, OAd contributes to the potentiation of cell stress and cell death when IFN and 5-FU are present. All these concepts could play a role in creating the strong synergism observed when OAd-hamIFN is combined with both 5-FU and radiotherapy.

Previous work from our group reported that OAd-hamIFN as a single therapy in the hamster model of pancreatic cancer resulted in an impressive therapeutic response (94). Current *in vivo* data using the same model showed that treatment with OAd-hamIFN in combination with 5-FU or radiation—and especially 5-FU + Radiation—resulted in superior inhibition of tumor growth, improved survival, and delayed tumor regrowth compared to the chemo-radiotherapy group, which is a conventional PDAC treatment.

Animals that were treated with triple-combination therapy (OAd-hamIFN + 5-FU + Radiation) showed the strongest anti-tumor effect in our study. In fact, one animal displayed complete tumor remission. Although no animals showed tumor remission in the group we treated with OAd-hamIFN + Radiation, the anti-tumor effect and survival in this group was similar to the triple-combination group. These data highlight the concept that OAd-hamIFN not only improves the anti-tumor effect of chemoradiation, but also greatly potentiates the efficacy of radiotherapy alone. This suggests that the calculated synergism of OAd-hamIFN + Radiation treatments *in vitro* might be translatable to a therapeutic effect *in vivo*. Comparison between the group treated with OAd-LUC + Radiation and the group treated with OAd-hamIFN + Radiation also indicates that the presence of IFN is essential for enhancing the anti-tumor effect of radiotherapy. It is well known that radiation can potentiate the systemic efficacy of immunostimulatory cytokines like IFN by activating innate and adaptive immune responses during treatment (228, 229). As OAd releases

tumor-specific peptides during oncolysis and because IFN stimulates the maturation and activation of antigen-presenting cells, the activity of T-helper cells, and enhances MHC-I expression (137, 143), it is possible that the improved therapeutic response in animals treated with OAd-hamIFN and radiation is the result of the formation of an anti-tumor immune response. The remarkable therapeutic effect shown in animals treated with OAd-hamIFN + Radiation suggests that chemotherapy could be excluded from the IFN therapy protocol for patients that who cannot tolerate its toxicity.

Although the animals treated with OAd-hamIFN in combination with 5-FU with smaller tumors survived longer compared to the chemo-radiotherapy control group, this result was not statistically significant. The decreased efficacy of 5-FU regimens *in vivo* could be explained by the short-half-life of 5-FU (approximately 30 minutes), and the long intervals between each 5-FU administration to the animals. In human clinical trials, 5-FU is continuously administered to patients to maintain a constant concentration of the drug in the blood (135-137), but in our animal model we administered the drug every 2–4 days. While the constant administration of 5-FU to animals is not feasible, it is possible that a more frequent chemotherapy injection protocol could have improved the efficacy of OAd-hamIFN combinations with 5-FU. Despite a weaker 5-FU regimen, using 5-FU in triple combinations (OAd-hamIFN + 5-FU + Radiation) resulted in the strongest therapeutic effect in the study. This observation suggests that the strong synergism (CI<0.5) found in combinations of virus and chemoradiation *in vitro* might have contributed to potentiate the anti-tumor effect of the triple combination *in vivo*.

Another important aspect of our study is that all groups that we treated with OAd-hamIFN therapies showed delayed tumor regrowth compared to the non-OAd-treated groups. Although our project did not assess it, the stimulation of an anti-tumor immune response in OAd-treated animals could be responsible for reduced tumor recurrence. A report by Aoki and colleagues supports this hypothesis. That report indicated that injecting a tumor with an IFN-expressing adenovirus reduced not only the size of the tumor, but also caused an NK-mediated anti-tumor effect in a contralateral untreated tumor (119).

Thus, because we used the immunocompetent hamster model of PDAC, we believe that the stimulation of NK cells could have contributed to delayed tumor regrowth in OAd-hamIFN treated animals. As replication of IFN-expressing OAd was not inhibited in immunocompetent hamsters, we believe that oncolysis by the virus, which exposes tumor specific peptides to the immune system, combined with immunostimulatory effect of IFN contributed to anti-tumor immune response formation during therapy. Even though the tools for immunological analyses in hamsters are currently limited, a thorough evaluation of the stimulation of anti-tumor immunity in OAd-hamIFN-treated hamsters is necessary to better understand the formation of anti-tumor immunity.

In summary, our data suggest that using IFN-expressing oncolytic adenovirus in treatment protocols involving chemotherapy, radiation, or chemoradiation can provide an effective therapy for PDAC. The synergism between IFN-expressing OAd and chemotherapy, radiation, and chemoradiation may allow physicians to reduce the therapeutic doses used in IFN-based regimens, which will contribute to development of better-tolerated clinical regimens. The remarkable anti-tumor effect of OAd-hamIFN + Radiation suggests that it might be possible to reduce or eliminate chemotherapy from treatment of patients who cannot tolerate chemotherapy, increasing the adherence of patients to IFN-based therapy.

There is a need for additional studies of IFN-expressing OAd as an improved IFN treatment modality for PDAC. IFN therapy is one of the few approaches that has been shown to improve both short- and long-term patient survival, and adding an IFN-expressing OAd to existing treatments may one day lead our field to develop an effective multimodal pancreatic cancer treatment.

12. Chapter II: Analysis of the Combination Index and therapeutic response of an IFN-expressing oncolytic adenovirus in combination with chemotherapy, radiation, and chemoradiation in human pancreatic cancer cell lines and immunodeficient mice.

12.1. Introduction

As mentioned in the introduction to Chapter I, the subcutaneous administration of IFN alpha combined with 5-FU, CDDP, and radiation in an adjuvant setting is one of the few therapeutic protocols that has been effective in improving the short- and long-term survival rates of PDAC patients (134, 135, 137, 138, 145). Compared to a two-year survival rate of 43% after surgery and chemoradiation (135), and a five-year survival rate of 20% after surgery alone, treatment with IFN therapy increased patients' two-year survival rate by 20–41%, and their five-year survival rate by 35%. Furthermore, in the long term 28% of patients who reached five-year survival following treatments with IFN therapy survived at least ten years; nine of these patients lived more than ten years; and seven of these patients remain alive and show no signs of the disease (145). Aside from IFN therapy, there is no current alternative PDAC therapy that results in such a remarkable increase in long-term survival of patients. While IFN therapy has been effective in treating PDAC, its limitations included high IFN systemic toxicity and low levels of the cytokine in tumors, both of which have hampered the therapy's full potential. Aiming to overcome these drawbacks and improve the efficacy of promising IFN therapy, we hypothesized that an oncolytic adenovirus expressing human IFN alpha (OAd-IFN) mimicking IFN therapy would improve the efficacy of current therapeutic regimens. Because cyclooxygenase 2 (cox-2) is known to be upregulated in a majority of PDAC tumors (230, 231), we included the cox-2 promoter upstream of the E1 region of adenovirus genome since this region is responsible for initiating viral replication. Previous studies from our group have proven that cox-2 controlled OAd-IFN restricted its replication to cox-2 positive PDAC cells (25, 56), and that treating mice bearing PDAC xenografts with OAd-IFN results in a superior anti-tumor effect compared to treatment with non-replicative IFN-expressing vectors both controlled or not controlled by cox-2 (56). To enhance OAd-IFN infectivity in PDAC cells, we also included a chimeric 5/3 fiber modification in the viral construct. We have shown that this fiber modification increases virus infectivity in a variety of PDAC cells as it shifts virus

tropism from the CAR receptor—which is highly deficient in PDAC cells—to desmoglein type 2, which has higher expression in PDAC cells than in normal cells (25). Finally, to potentiate OAd-IFN oncolysis and spreading in PDAC cells, and to express high levels of IFN in a replication-dependent manner, we deleted most of the genes in the adenovirus E3 region and reintroduced the adenovirus death protein (ADP) and human IFN-alpha gene (IFN). We have shown that these vector modifications resulted in overexpression of ADP, which increases vector cytotoxicity in PDAC cells, and causes time-dependent over-expression of IFN as detected by ELISA (25, 56).

We hypothesize that combining OAd-IFN with 5-FU, CDDP, and radiation in treatments mimicking IFN therapy will concentrate IFN expression in the tumor site and thereby enhance the cytotoxic effect of chemoradiation while reducing IFN-associated systemic toxicity. As discussed in Chapter I, because IFN is a chemo-radio sensitizer, concentrating IFN expression in the tumor site should significantly potentiate the cytotoxic effect of chemoradiation during therapy. Because it is well reported in the literature that using a replication-selective adenovirus to deliver a toxic transgene can reduce its systemic toxicity (232-234), we believe that expressing high concentrations of IFN focused on the tumor site will decrease the systemic toxicity of IFN and make more tolerable to patients.

Although our earlier studies using an immunocompetent hamster model of pancreatic cancer showed that combinations of IFN-expressing oncolytic adenovirus with 5-FU, radiation, and 5-FU with radiation resulted in a superior anti-tumor effect and survival compared to group treated with chemoradiation, a more detailed understanding of how oncolytic adenoviruses work with chemoradiation is needed.

Our hamster model was immunocompetent and oncolytic adenoviruses (OAd) are highly immunogenic. Thus, although IFN-expressing OAd combined with chemotherapy, radiation, and chemoradiation was synergistic *in vitro*, it is possible that the stimulation of an anti-tumor immune response contributed to an improved therapeutic effect *in vivo*. Therefore, to better assess how combinations of an IFN-expressing OAd performs *in vivo*, and exclude the interference of the immune system in the effectiveness of the therapy, we conducted our studies using immunodeficient mice bearing xenografts of human PDAC.

Because OAds do not replicate in mice and the animals were immunodeficient, treating the PDAC xenografts with OAd-IFN can assess how the virus actually interacts with chemotherapy and radiation.

In vitro testing of OAd-IFN combined with 5-FU, radiation, and 5-FU + radiation showed that the combinations were moderately to highly synergistic in human PDAC cells. Addition of CDDP to the chemotherapy regimen (5-FU + CDDP) was shown to inhibit OAd-IFN, but inclusion of radiation to OAd-IFN combined with 5-FU + CDDP (OAd-IFN + (5-FU+CDDP) + Radiation) abolish chemotherapy inhibition to virus, turning treatments highly synergistic and extremely cytotoxic *in vitro* and *in vivo*. Use of virus with the describe chemotherapy protocol and radiation is a close representation of IFN-therapy performed in clinical trials, and this treatment was the most efficacious treatment *in vivo*. As radiation was shown to override chemotherapy inhibition to the virus *in vitro* and *in vivo*, we tested different radiation regimens combined with OAd-IFN. We showed that treating tumors with radiation before infecting them with OAd-IFN enhanced the therapy's anti-tumor effect. Thus, to potentiate even further the effectiveness of OAd-IFN in treatments that mimic IFN therapy, we suggest testing this new radiation regimen in therapeutic combinations that include OAd-IFN.

Finally, because IFN induces an anti-virus effect in infected cells, we tested whether IFN expressed by OAd-IFN would inhibit virus replication. We showed that the expression of IFN by the vector (or the injection of IFN concomitantly with OAd) does not eliminate viral replication in PDAC tumors. Therefore, using an IFN-expressing OAd in therapies representing the IFN-therapy should contribute to therapy efficacy by stimulating anti-tumor immune response through oncolysis.

In summary, because IFN-therapy is one of the few therapeutic regimens that is effective in treating PDAC, developing an OAd-based IFN-therapy could result in an effective treatment for the disease.

12.2. Material and methods

Cell lines

The human pancreatic ductal adenocarcinoma cells Mia-Paca-2 and S2013 were obtained from the American Type Culture Collection (Manassas, VA). The cells were maintained in DMEM media supplemented with 5% Fetal Bovine Serum (FBS) and 1% Penicillin/Streptomycin. The cells were stored as adherent monolayers in a humidifier incubator at 37.8°C and 5% CO_2.

Vector structure

Vectors used in OAd-IFN in vitro and in vivo combination therapies

We generated a replication-competent IFN-expressing oncolytic adenovirus (OAd-IFN) **(Figure 1)** as described previously (25, 220, 235). To enhance the vector's infectivity in PDAC cells, which are deficient in the CAR receptor, which is the natural receptor for an adenovirus (Ad) Type 5 infection, we included a chimeric 5/3 fiber. The chimeric fiber contains the knob of an Ad Type 3 added to the shaft of an Ad type 5 fiber. This modification shifts the tropism of OAd-IFN to Desmoglein-2, which is highly expressed in PDAC cells (24, 236). To enhance the cytotoxicity and spreading of OAd-IFN in PDAC cells, and to achieve replication-dependent expression of IFN-α, we deleted most of the nonessential genes from Ad E3 region and added the Adenovirus Death Protein (ADP) and human IFN-α (IFN) genes to this region (235, 237). To restrict OAd-IFN from infecting the PDAC cells (which have been reported to overexpress Cox-2) the Cox-2 promoter was added upstream of Ad E1 region because this region is responsible for initiating viral replication (25). We also generated Cox-2 controlled counterpart vector expressing luciferase (OAd-LUC) instead of IFN **(Figure 1).** We performed virus propagation, purification, storage, titration, and structure confirmation as described in previous publications (24, 25).

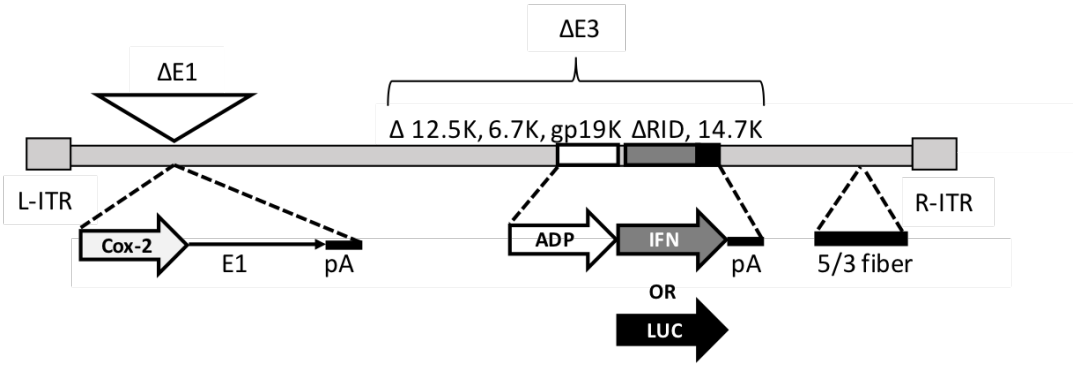

Figure 1. Vector structure. Structures of IFN-expressing oncolytic adenovirus (OAd-IFN), and counterpart vector expressing luciferase (OAd-LUC) are displayed. To restrict replicating vectors to PDAC cells, the Cox-2 promoter was included upstream of Adenovirus (Ad) E1 region, which is the region that initiates virus replication. In both vectors, we deleted most non-essential genes from Ad E3 region and included the Adenovirus Death Protein (ADP). In the OAd-IFN vector, we added human IFN-α (IFN) gene to the Ad E3 region, whereas for the OAd-LUC vector, we added the Luciferase gene (LUC) in place of the IFN gene.

Vectors used to access replication of IFN-expressing OAd in PDAC tumors

OAdIFN-α and OAd-Luciferase contain 5/3 fiber modification and inclusion of human IFN alpha or luciferase genes in Ad E3 region as described for OAd-IFN and OAd-LUC **(Figure 1).** ADP was also included in Ad E3 region as in OAd-IFN and OAd-LUC vectors. Adenovirus wild type promoter was kept upstream of Ad E1 region. Vectors were used to infect PANC-1 tumors for visualization of viral replication using confocal microscopy **(Figure 7)**. Viral propagation, purification, storage, titration, and structure confirmation were performed as described in previous publications (24, 25).

Combination Index analysis

Calculation of the Combination Index (CI) to determine synergism (CI < 1), antagonism (CI > 1), or additive effect (CI = 1) between virus, chemotherapy, and radiation was performed using Compusyn software(205). The EC50 of each treatment alone (OAd-IFN, OAd-LUC, 5-FU, (5-FU + CDDP), and radiation) was quantitatively determined by the Colony Formation Assay (CFA) in S2013 and MIA-PACA-2 cells, and ED50 values were entered as monotherapies in Compusyn. Quantification of cytotoxicity of combination

treatments was determined by CFA in same cell lines, and killing effect was entered as the combination therapies in Compusyn. Final report with CI was generated using non-constant ratio between therapies. Strong synergism was considered when CI < 0.5 and moderate synergism when CI = 0.6 to 0.9.

In vivo experiments

Combinations of OAd-IFN with (5-FU+ CDDP), radiation, and (5-FU+ CDDP) + radiation

MIA-PACA-2 cells (2 x 10^6) suspended in 100 µl of PBS were subcutaneously injected into both hind legs of 6-8 weeks old female athymic nude mice obtained from Charles River Laboratories. Animals were divided in 8 groups with 7 tumors per group. When one of tumor's diameters reached 8 - 10 mm, they were injected with 1 x 10^{10} VP OAd-IFN diluted in 50 µl PBS. The day of virus injection was considered as Day 0. Intraperitoneal injections of 20 mg/kg 5-FU were given on days 2, 4, 5, 6, and CDDP was given on day 2 only. Radiation groups had tumors irradiated on day 2 at the same shortly after administration of the first dose of 5-FU and CDDP **(Figure 6)**. Previous to 4Gy irradiation, animals were anesthetized with 100 mg/kg Ketamine and 15 mg/kg Xylazine and placed in customized radiation chamber where tumors were exposed to radiation while the animal's bodies were protected with lead shield. Tumor diameter was measured two times per week using calipers. Tumor volume was calculated considering tumor volume = (width^2 × length)/2. The animals were euthanized according to IACUC guidelines when one of the tumor's diameters was bigger than 20mm.

Assessment of OAd-IFN replication in PDAC tumors

PANC-1 cells (5 x 10^6) suspended in 100 µl of PBS, and were subcutaneously injected into both hind legs of 6-8 weeks old female athymic nude mice obtained from Charles River Laboratories. Animals were divided in 4 groups with 8 tumors per group. When one of tumor's diameters reached 6-8 mm, they were injected with 1 x 10^{10} VP of OAdIFN-α or OAd-Luciferase diluted in 50 µl PBS **(Figure 7)**. Groups treated with OAd-Luciferase + Type I IFN had 60 Units/g of body weight of IFN injected intratumorally one day after

injection with OAd-Luciferase. After seven days, animals were euthanized according to IACUC guidelines and tumors were harvested and stored at -80°C. Tumors were stained with anti-hexon FITC labelled antibodies, and presence of hexon protein was visualized using confocal microscopy.

Statistical analysis

We used the SAS proc mixed program to generate a fit linear mixed model to analyze tumor growth/time. The log of absolute tumor volume was considered as the outcome variable, and the treatment group, time (continuous), and their interaction were considered as the predictor variables. The analysis included random effects to account for the correlation among repeated measurements in each tumor. The primary hypothesis we tested was whether the time trend, or slopes of each trend line differed among the groups. When the tumor volume was 0, its log volume was defined as "1" during the analysis. Because the chemoradiation group was the reference group used in the IFN-therapy clinical trials, the group we treated with (5-FU + CDDP) + radiation was the internal control group in the experiments **(Figure 6A)**. In **Figure 6B,** combination of OAd-IFN with 5-FU+CDDP was the comparison group**.**

12.3. Results

Establishing monotherapy EC50

To assess the Combination Index (CI) between OAd-IFN and the therapeutic used in IFN-therapy using Compusyn, and to choose the doses of combined therapeutics in later experiments, we established the ED50 of OAd-IFN, 5-FU, and radiation as monotherapies using the Colony Formation Assay in the S2013 and MIA-PACA-2 PDAC cell lines **(Figure 2).** I used CFA because it is the gold standard assay to evaluate the effectiveness of radiation *in vitro*. We included a non-IFN expressing counterpart vector (OAd-LUC) in the assessment because we wanted to evaluate how much IFN contributed to the CI analysis and the cytotoxicity of the therapy in experiments that compared combinations of OAd-IFN and OAd-LUC with monotherapies. When comparing the two PDAC cell lines, S3013 was more sensitive to all the tested monotherapies. After determining the ED50 of each

drug, we chose to use the lowest and least effective doses of each monotherapy in combination studies in later experiments.

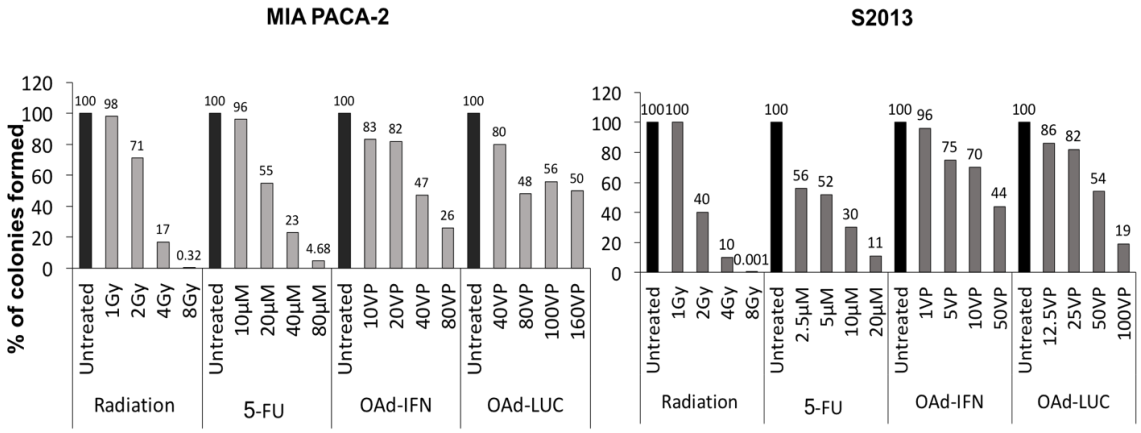

Figure 2. Establishing monotherapy ED50 in Colony Formation Assay. We tested a range of doses of OAd-IFN, OAd-LUC, 5-FU, and radiation in MIA-PACA-2 and S2013 PDAC cells. The data shows that S2013 is slightly more sensitive to monotherapies than MIA-PACA-2. The numbers on top of the histogram bars reflect the percentage of colonies that formed after each monotherapy treatment.

IFN expressed by OAd-IFN contributes to stronger cytotoxicity and synergism in OAd-IFN combinations with chemotherapy, radiation, and chemoradiation

By using ED50s values for S2013, and the killing effect of OAd-IFN combined with 5-FU, radiation, and 5-FU + radiation in CFA, we used Compusyn to calculate the Combination Index (CI) of the OAd-IFN treatments **(Figure 3).** I focused on S2013 to more thoroughly evaluate the CI because this cell line is more sensitive monotherapies, having the potential to clearly reflect the interaction between the therapy components. Comparisons of colony-formation inhibition in combinations of OAd-LUC—a counterpart vector not expressing IFN—and OAd-IFN combined with radiation showed that IFN expressed by OAd-IFN induced a higher level of cytotoxicity or colony-formation inhibition in the treatments **(Figure 3A and B).** The synergism (CI<1) between OAd-IFN and lower doses of radiation was stronger than the synergism in combinations of OAd-LUC with same radiation dose. Although an increase in the dose of radiation in combination with both OAd-IFN and OAd-LUC resulted in more cytotoxic treatments, the combination index was driven towards a

more additive (CI=1) or antagonistic interaction (CI>1) between the virus and the radiation, showing increase of radiation dose during therapy have the potential to decrease therapy efficacy. Treatments of OAd-LUC or OAd-IFN combined with 5-FU **(Figure 3C and D)** showed that, while combinations including OAd-LUC were antagonistic and less cytotoxic, combinations with OAd-IFN were highly synergistic and strongly cytotoxic. This data highlight that IFN expressed by the vector greatly contributed to improved cytotoxicity and enhanced the synergism between the virus and the chemotherapy. Because the historic comparison control used in IFN-therapy was 5-FU + radiation, we analyzed the CI and cytotoxicity of 5-FU combined with radiation **(Figure 3G).** These combinations were moderately synergistic and highly cytotoxic, especially when we used higher doses of chemoradiation. Finally, comparisons between OAd-LUC and OAd-IFN in treatment that mimicked IFN-therapy (OAd-IFN + 5-FU + radiation) **(Figure 3. E and F)** showed that IFN expressed by the virus contributed to more synergistic and cytotoxic combinations, especially when very low doses of OAd-IFN (0.5 VP/cell) and radiation (2Gy) were combined.

In summary, this data highlight that the synergistic interaction between OAd-IFN and the drugs used in IFN-therapy show that the virus has great potential to reduce therapy toxicity because it allows doctors to reduce the doses of the therapeutics used together while maintaining or enhancing their efficacy.

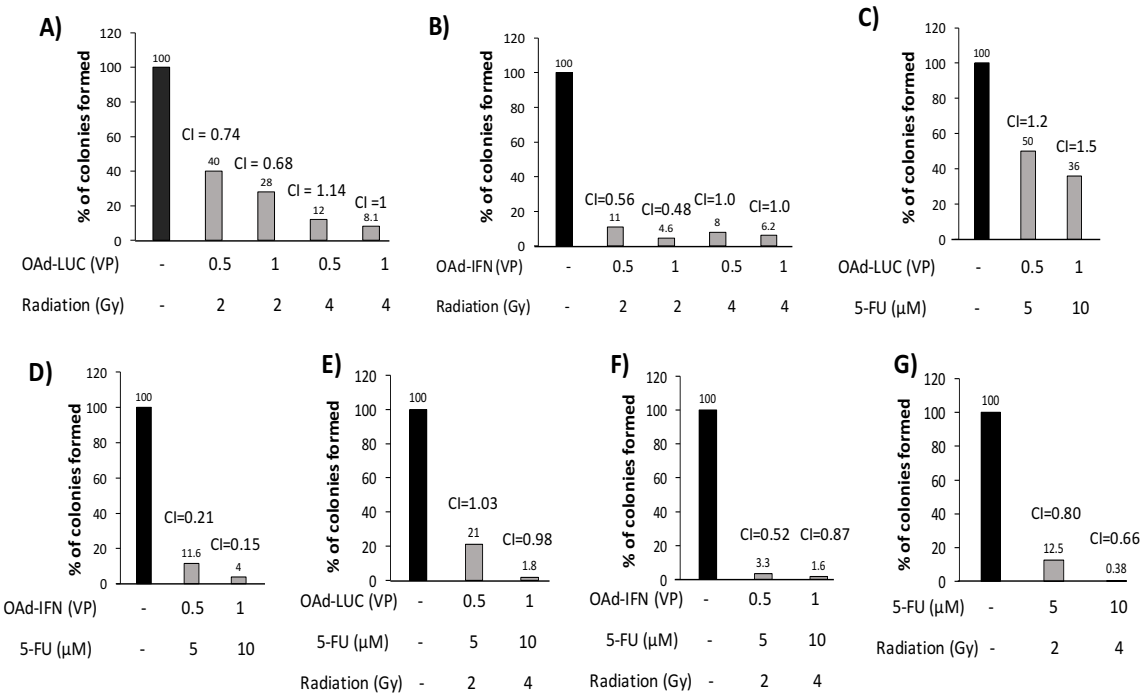

Figure 3. IFN contribution to cytotoxicity and synergistic interaction between OAd-IFN and chemotherapy, radiation, and chemoradiation. Displayed is an analysis of Combination Index (CI) of OAd-IFN combination in S2013 using colony formation assay. Combinations of OAd-LUC **(A)** or OAd-IFN **(B)** and radiation shows that IFN expressed by OAd-IFN potentiates synergism when low dose of radiation is used. Combinations of OAd-LUC with chemotherapy results in antagonism **(C)**, while combinations of OAd-IFN with same chemotherapy doses were highly synergistic **(D)**. **(E)** Use of OAd-LUC in treatments that mimic IFN-therapy (virus combined with chemoradiation) were additive (CI=1) or moderately synergistic (CI=0.98), while use of OAd-IFN in same therapeutic set-up resulted in synergism with any of the radiation and chemotherapy doses tested **(F)**. As 5-FU in combination with radiation was the reference therapy used to compare effectiveness of IFN-therapy in clinical trials, we decided to test this therapeutic regimen. Data showed that combinations of 5-FU and radiation were highly cytotoxic and synergistic **(G)**. (CI<1) synergism, (CI=1) additive effect, and (CI>1) antagonism. The numbers on top of the histogram bars reflect the percentage of colonies that formed after each monotherapy treatment.

Effect of radiation in OAd-IFN combinations tested in PDAC cell line used in pre-clinical model

Because an increase in the dose of radiation in OAd-IFN combinations resulted in less synergistic Combination Indexes (CI) in the S2013 PDAC cell line **(Figure 3B)**, we used CFA to assess whether the same was true for MIA-PACA-2, the PDAC cell line we used to establish xenografts in our pre-clinical model. Comparisons between combinations of OAd-LUC and OAd-IFN with radiation showed that, although an increase in the dose of radiation in OAd-LUC combinations resulted in a less cytotoxic and a more antagonistic (CI=0.66 versus CI = 1.31) treatments **(Figure 4A),** the OAd-IFN combinations became more cytotoxic and synergistic (CI=0.5 versus CI=0.35) when the dose of radiation increased. **(Figure 4B)**. This data confirmed that, in the case of the MIA-PACA-2 cell line (which was less susceptible to radiation and OAd-IFN when each were used as monotherapies **(Figure 2)**), IFN expressed by OAd-IFN could potentiate effect of radiation. Our analysis of the CI in treatments using combinations of 5-FU and radiation showed that an increase in the dose of radiation resulted in a more antagonistic CI (CI=0.95 versus CI=1.25), which diminished the cytotoxic effect **(Figure 4C)**. Comparisons of OAd-LUC and OAd-IFN in treatments that mimicked IFN-therapy (IFN + 5-FU + Radiation) showed that, although an increase in the dose radiation makes combinations of 5-FU + radiation antagonistic, the IFN expressed by the virus overcame this antagonistic interaction and made combinations of OAd-IFN + 5-FU + Radiation highly synergistic and cytotoxic **(Figure 4D)**. These data support including an IFN-expressing OAd in treatments that mimic IFN-therapy. Using OAd-IFN consistently potentiates the effect of chemoradiation and improved the efficacy of therapy. If an IFN-expressing OAd is included in IFN-therapy protocols, the synergistic interaction between the virus and therapeutic components can reduce the amounts of chemoradiation dose and contribute to a less toxic treatment.

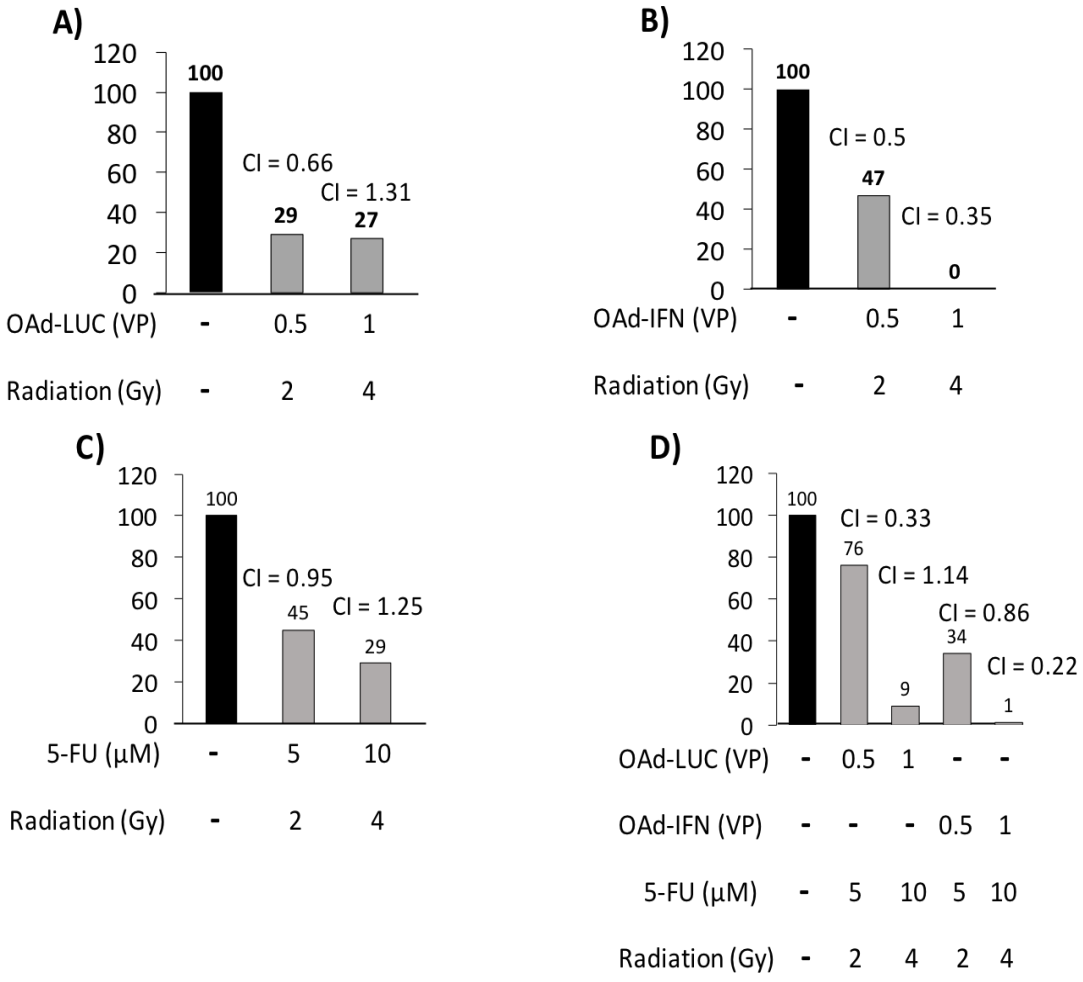

Figure 4. Effect of radiation on OAd-IFN combinations tested in cell lines used in the pre-clinical model of PDAC. Displayed is the effect of radiation in combination with OAd-IFN using colony formation in the MIA-PACA-2 PDAC cell line. This cell line is used to form human PDAC xenografts in nude mice. CFA output shows that while combinations of OAd-LUC with low doses of radiation were synergistic (CI=0.66), increase of dose of radiation in combination with virus abolished synergistic interaction (CI=1.31) **(B)**. On the other hand, use of OAd-IFN with either low or high doses of radiation were both highly synergistic (CI=0.5 and CI=0.35) **(C)**. **(D)** Combinations of either OAd-LUC or OAd-IFN in treatment protocol mimicking IFN-therapy (IFN + 5-FU + Radiation) were highly synergistic when low doses of therapeutics were used, but only combinations of OAd-IFN with higher doses of chemotherapy or radiation were highly synergistic. The numbers on top of the histogram bars reflect the percentage of colonies formed after treatment. (CI<1) synergism, (CI=1) additive effect, and (CI>1) antagonism.

Use of radiation with combinations of OAd-IFN and 5-FU + CDDP results in highly cytocidal and synergistic combinations

In the first stage of IFN-therapy, patients are exposed to one bolus dose of CDDP, continuous administration of 5-FU, and fractionated radiation **(Figure 5A).** After we confirmed that OAd-IFN can synergistically potentiate the killing effect of 5-FU and radiation, we decided to assess if the same effect occurred when OAd-IFN was combined with CDDP + 5-FU or with CDDP + 5-FU and radiation **(Figure 5).**

We performed the CFA in MIA-PACA-2 PDAC cells and calculated the CI. Because earlier experiments showed that combinations of OAd-IFN with 2 and 4Gy of radiation were synergistic **(Figures 3 and 4),** we decided to lower the radiation doses to 1 and 2GY in this assay **(Figure 5)**. Because we want to use OAd-IFN to reduce the toxicity of therapy, it was necessary to study the efficacy of combinations of very low doses of therapeutics.

We first assessed the killing effect of 5-FU combined with CDDP, and later evaluated the cytotoxic effect and CI of CDDP + 5-FU combined with radiation**.** The data showed that combinations of chemotherapy drugs and low doses of radiation were moderately cytotoxic, and that the cytotoxicity increased when we used higher doses of therapeutics **(Figure 5B)**. Nevertheless, the CI for both treatments were antagonistic, and we observed higher antagonism when we combined higher doses of chemotherapy and radiation. Treatments of OAd-LUC and 5-FU + CDDP were antagonistic, and we observed extreme antagonism when we used low doses of the virus and chemotherapy. This antagonism translates to a diminished killing effect in OAd-LUC combined with lower or higher doses of therapeutics **(Figure 5C)**. OAd-IFN in combination with CDDP + 5-FU also was antagonistic. Although combinations with OAd-IFN were less antagonistic and more cytotoxic compared to combinations with OAd-LUC, the killing effect was also effected by treatment with 5-FU + CDDP **(Figure 5D)**. Despite this result, using either OAd-LUC or OAd-IFN in combination with 5-FU + CDDP and radiation were highly cytotoxic and synergistic **(Figure 5E)**. This data demonstrated that addition of radiation to treatment regimen overruled viral antagonism, turning the treatment regimen highly effective in killing PDAC cells.

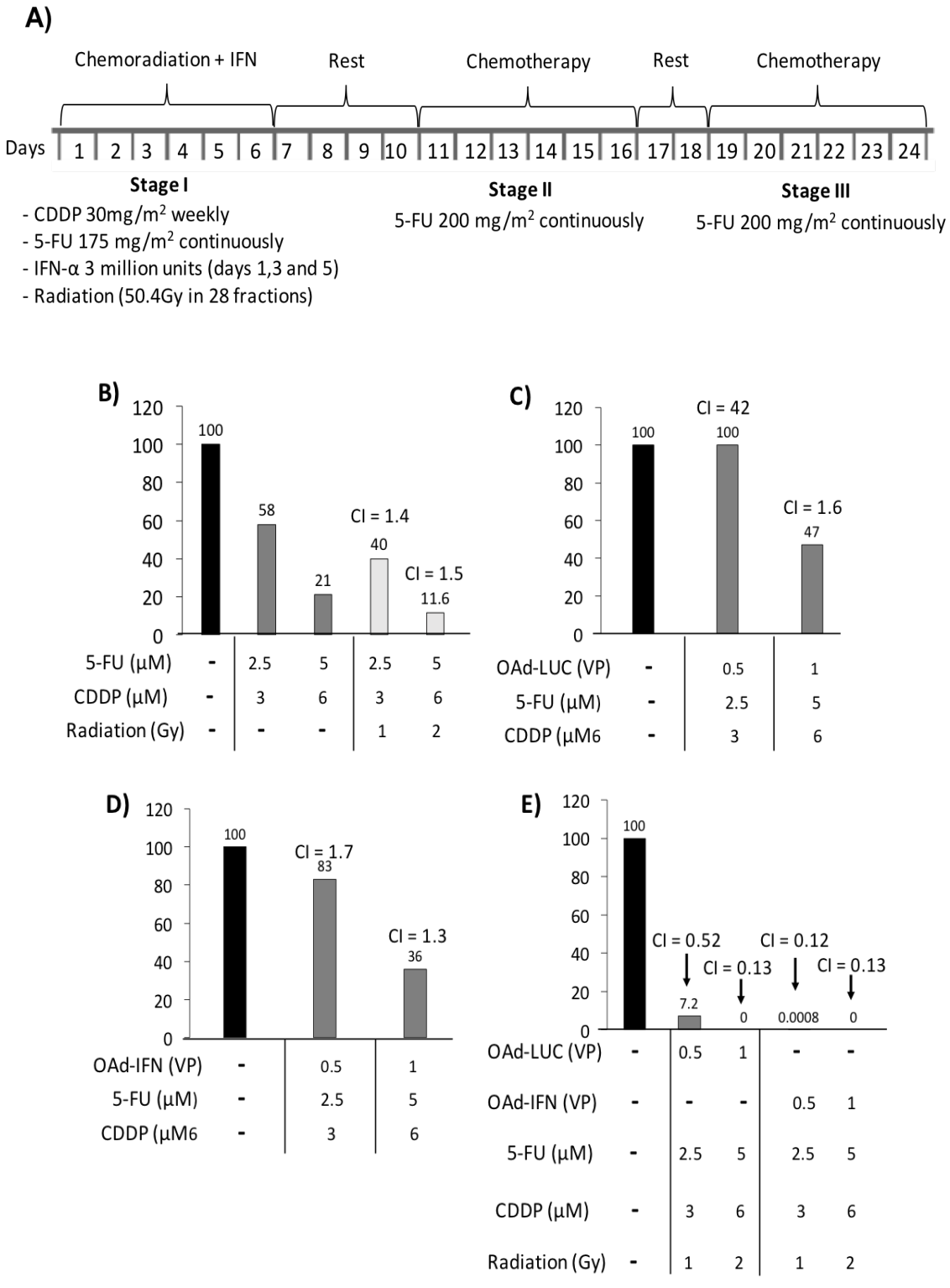
A)
Chemoradiation + IFN
Rest
Chemotherapy
Rest
Chemotherapy
Days
1 2 3 4 5 6 7 8 9 10 11 12 13 14 15 16 17 18 19 20 21 22 23 24
Stage I
- CDDP 30mg/m2 weekly
- 5-FU 175 mg/m2 continuously
- IFN-α 3 million units (days 1,3 and 5)
- Radiation (50.4Gy in 28 fractions)
Stage II
5-FU 200 mg/m2 continuously
Stage III
5-FU 200 mg/m2 continuously
B)
120
100
80
60
40
20
0
100
58
21
CI = 1.4
40
CI = 1.5
11.6
5-FU (μM) - 2.5 5 2.5 5
CDDP (μM) - 3 6 3 6
Radiation (Gy) - - - 1 2
C)
120
100
80
60
40
20
0
100
CI = 42
100
CI = 1.6
47
OAd-LUC (VP) - 0.5 1
5-FU (μM) - 2.5 5
CDDP (μM6 - 3 6
D)
120
100
80
60
40
20
0
100
CI = 1.7
83
CI = 1.3
36
OAd-IFN (VP) - 0.5 1
5-FU (μM) - 2.5 5
CDDP (μM6 - 3 6
E)
120
100
80
60
40
20
0
100
CI = 0.52
CI = 0.13
CI = 0.12
CI = 0.13
7.2
0
0.0008
0
OAd-LUC (VP) - 0.5 1 - -
OAd-IFN (VP) - - - 0.5 1
5-FU (μM) - 2.5 5 2.5 5
CDDP (μM) - 3 6 3 6
Radiation (Gy) - 1 2 1 2

Figure 5. Using radiation with combinations of OAd-IFN with 5-FU + CDDP results in highly cytotoxic and synergistic combinations. To better replicate the IFN-therapy used to treat PDAC patients in clinical trials (A), we used CFA in MIA-PACA-2 to assess the CI and cytotoxicity of OAd-IFN combined with (5-FU + CDDP), and radiation. (B) Combinations of CDDP + 5-FU with radiation show that although two chemotherapy doses are used in combination with radiation, these combinations are antagonistic (CI>1). Combinations of either OAd-LUC (C) or OAd-IFN (D) with (5-FU + CDDP) were all shown to be antagonistic (CI>1), but very strong antagonism was only shown when low doses of non-IFN expressing OAd (OAd-LUC) was combined with

Treating mice with OAd-IFN in combinations that mimic IFN therapy results in reduced tumor growth

To test the efficacy of OAd-IFN in combinations that mimic IFN therapy, and to assess the interaction between OAd-IFN and therapeutics used in this therapy, we treated nude mice bearing MIA-PACA-2 xenografts with OAd-IFN combinations representing IFN-therapy **(Figure 6)**. To better replicate IFN-therapy in clinical trials **(Figure 5A)**, we chose 5-FU + CDDP as our chemotherapy regimen, and treatment with 5-FU + CDDP combined with radiation (chemoradiation) as our control group. Experimental results showed that compared to the control chemoradiation group, the groups treated with OAd-IFN combined with radiation, or OAd-IFN combined with 5-FU + CDDP and radiation showed the strongest anti-tumor effect, while combination of OAd-IFn with 5-FU + CDDP were less efffective **(Figure 6A)**. After Day 9 of the treatment, the tumors treated with OAd-IFN in combination with 5-FU + CDDP presented exponential growth, and this treatment was weaker than treatment with OAd-IFN alone. This result suggests that the antagonism we observed in combinations of OAd-IFN and 5-FU + CDDP *in vitro* **(Figure 5C)** had translated to a diminished therapeutic effect *in vivo*. The tumor-growth rate (TGR), or percent of tumor growth/day, of the tumors in the chemoradiation group and the groups treated with OAd-IFN combined with chemotherapy, radiation, or chemoradiation were respectively 3.6%, 9%, 6.9%, and 0.6%. The TGR data showed that, although the treatments with OAd-IFN combinations did not reduce the tumor growth compared with the chemoradiation group, combinations of the virus with radiation or with 5-FU + CDDP

and radiation increased tumor debulking, resulting in smaller tumors throughout the treatment. However, despite the fact tumor volumes in the group treated with OAd-IFN + Radiation were smaller, the TGR in this group was 6.9%, which was higher than the TGR in control chemoradiation group (TGR=3.6%). This might have happened because the average tumor volume in the group treated with OAd-IFN + Radiation was smaller in the beginning of the experiment. The average tumor volume consisted of the average of all tumor volumes presented that group, and this was the value used to plot each time point in the graph represented in **Figure 6A.** Thus, although tumors in the OAd-IFN + Radiation group randomly included a variety of tumors (larger and smaller) just as the other treatment groups, tumors that were smaller might have responded better to the therapy.

Although the efficacy of OAd-IFN in combination chemoradiation was high throughout most of the experiment, some tumors in this group showed exponential growth by Day 18, and this growth largely contributed to the accentuated increase in the average tumor volume value for this group by the end of the experiment **(Figure 6A).** While this exponential tumor growth looked detrimental to therapy efficacy, two tumors in this group (OAd-IFN + (5-FU + CDDP) + Radiation) showed complete remission. This observation shows that there was variability in the therapeutic effect of this therapy. Nevertheless, the accelerated tumor growth of some tumors does not invalidate the effectiveness of this therapy as use of OAd-IFN combined with chemoradiation (OAd-IFN + (5-FU + CDDP) + Radiation) was the only treatment regimen capable of considerably decrease the tumor growth rate of tumors (TGR=0.6%). I speculate that because this treatment includes OAd-IFN combined with 5-FU + CDDP, and this chemotherapy regimen was shown to antagonize OAd-IFN, antagonism to the virus contributed to accelerated tumors growth of some tumors. It is also possible that repeated administration of the virus during therapy would have abolished this variable therapeutic effect. It is widely known that virotherapies usually employ repeated administration of viruses in the treatment of cancer(11).

The least effective therapy in this study were OAd-IFN (TGR= 6.1%), 5-FU + CDDP (TGR=8.7), and OAd-IFN + (5-FU + CDDP) (TGR=9%). As viral only treated group showed a TGR of 6.1%, this data reinforced that use of 5-FU + CDDP in combination with OAd-IFN (TGR=9%) severely impacted OAd-IFN effectivity.

To determine whether we could reproduce this result, and to rule out the fact that the variation in the average tumor volume in the beginning of the experiment contributed to therapeutic effect, we conducted another experiment to test the efficacy of all the viral combinations **(Figure 6B).** Experiment output showed that combination of OAd-IFN with 5-FU + CDDP was the worst viral combination therapy in the study (TGR=6%), confirming this chemotherapy regimen might hamper effectiveness of therapy. Data also showed that treatments with OAd-IFN in combination with radiation or chemoradiation were effective in keeping tumor volume low (respective TGR of 2% and 0.4%). Consistent with our previous study, treatment with OAd-IFN + (5-FU + CDDP) + radiation was the most effective therapy (TGR=0.4%) in the study. Therefore, we concluded that although variation in initial tumor volume might have played a role in variability of therapeutic effect in the first experiment **(Figure 6A)**, combinations of OAd-IFN with radiation or chemoradiation were still highly effective therapies when initial tumor volume was uniform **(Figure 6B)**.

In summary, our data support including an IFN-expressing OAd in combination with chemoradiation regiments that mimic IFN therapy. Although we observed antagonism between the virus and the chemotherapies used, adding radiation to the therapy regimen appeared to surmount the antagonism and make the therapy effective.

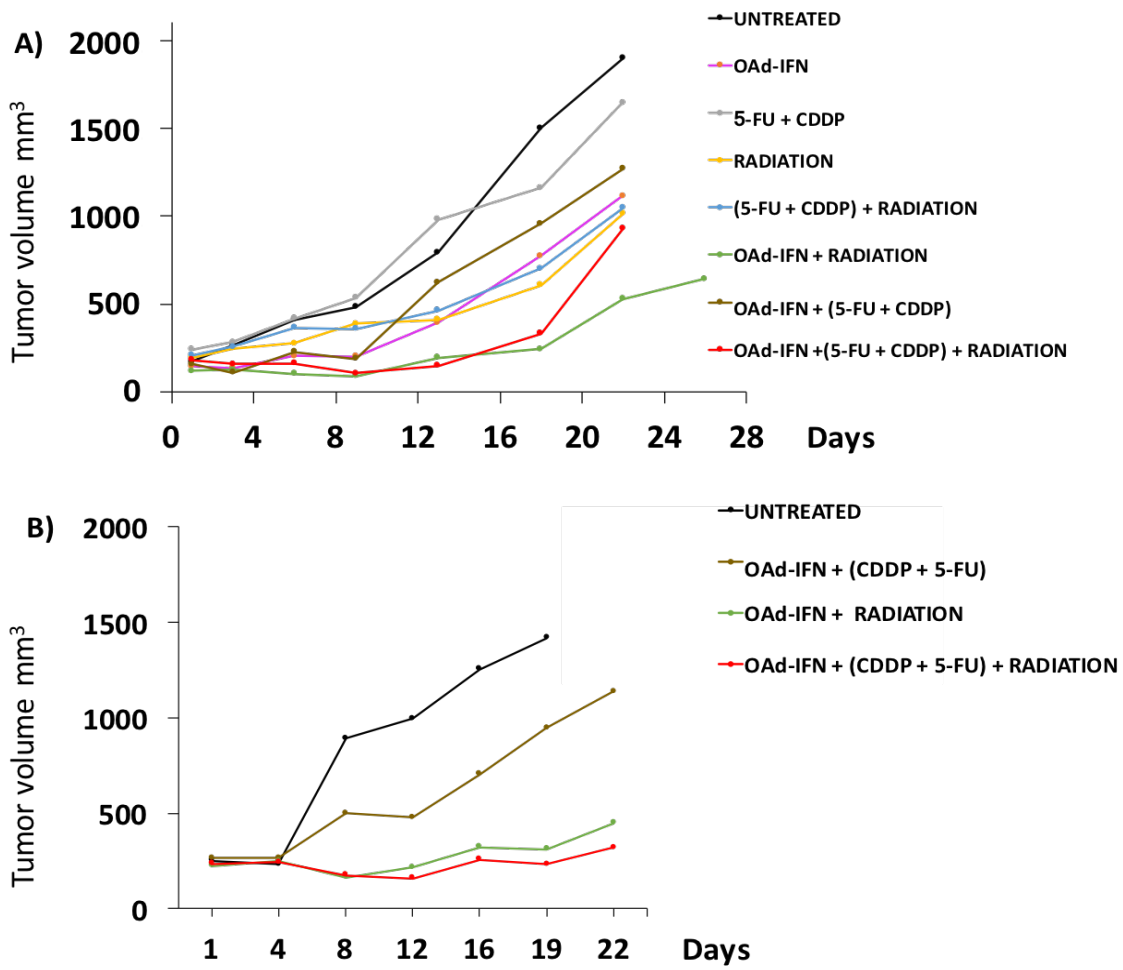

Figure 6. Therapeutic effect of OAd-IFN combinations in nude mice. Nude mice bearing MIA-PACA-2 PDAC cell xenografts were treated with OAd-IFN combinations. To better replicate IFN-therapy in clinical trials, the chemotherapy regimen consisted of 5-FU + CDDP. Tumor Growth Rate (TGR), or the amount (%) of tumor volume increase/day was used to compare therapy groups. **(A)** Compared to the control-therapy group (5-FU + CDDP) + radiation (TGR = 3.6%), treating animals with OAd-IFN + radiation (TGR=6.9) or OAd-IFN + (5-FU + CDDP) + Radiation (TGR=0.6%) resulted in the most effective therapies to decrease tumor volume over time. Compared to group treated with OAd-IFN (TGR=6.1%), group treated with OAd-IFN + (5-FU + CDDP) (TGR=9%) had the anti-tumor effect suppressed. However, inclusion of radiation to treatment regimen (OAd-IFN + (5-FU + CDDP) + Radiation) abolished virus antagonism by chemotherapy, resulting in the most effective therapy in the study (TGR=0.6%) **(B)** To confirm if adding 5-FU + CDDP to OAd-IFN treatments affected treatment efficacy, and if variation in initial tumor volume impacted therapeutic effect of therapies, we repeated the experiment testing OAd-IFN combinations with 5-FU + CDDP, radiation, and (5-FU + CDDP) + Radiation. Data confirmed that using 5-FU + CDDP with OAd-IFN strongly inhibited the virus (TGR=6.6%), and that combinations of OAd-IFN with radiation

(TGR=2%) and chemoradiation (TGR=0.4%) showed the strongest anti-tumor effect. Again, use of virus in combinations closely resembling IFN-Therapy in clinical trials (OAd-IFN + (5-FU + CDDP) + Radiation) resulted in the best therapy to inhibit tumor growth. The graph shows the absolute tumor volume over time.

IFN expression by OAd or combination of OAd with universal IFN does not affect viral replication

IFN is known to induce an antiviral state in cells that will limit viral infection. To assess whether IFN expression by an OAd can restrict its own replication, we compared the replication of an IFN-expressing OAd (OAdIFN-α) with the replication of a non-IFN expressing OAd (OAd-Luciferase) in PANC-1 xenografts **(Figure 7A and B)**. We assessed OAd replication by using confocal microscopy and FITC staining of the adenovirus hexon protein, which is a structural protein encoded during OAd late gene expression. The data showed that, just like an OAd that does not express IFN **(Figure 7A),** IFN-expressing OAd could replicate in PDAC xenografts **(Figure 7B)**.

To replicate IFN-therapy, we injected 60U/g body weight of Universal type I IFN (type I IFN) into the tumor after infecting it with OAd-Luciferase **(Figure 7C)**. We used universal type I IFN because the action of IFN is species-specific (119) and universal type I IFN is effective in multiple animal species. The Type I IFN dose we used was equivalent to the IFN dose used to treat patients in IFN-therapy. Our assessment of OAd-Luciferase replication showed that the virus could replicate even when IFN was present intratumorally.

Thus, these data corroborated our conclusion that although IFN has the potential to inhibit viral replication in infected cells, expression of IFN by OAd does not inhibit OAd replication in tumors. Therefore, using IFN-expressing OAd to treat PDAC should combine the vector's oncolytic potential with the anti-tumor effect of IFN during therapy.

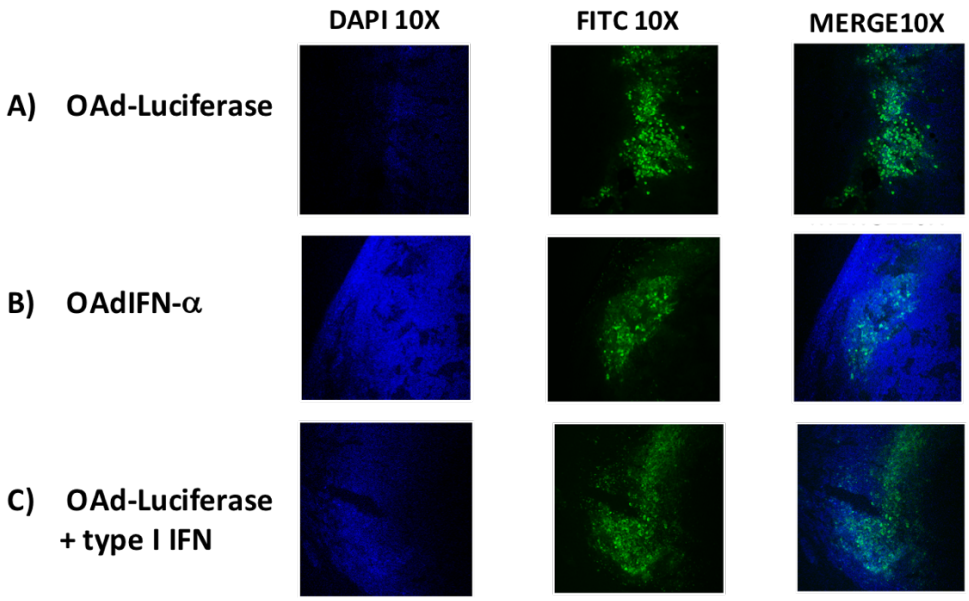

Figure 7. Effect of IFN expressed by OAd in viral replication. We assessed OAd replication in nude mice bearing xenografts of PANC-1 PDAC cells. Confocal images of viral replication show the FITC staining of the adenoviral hexon capsid protein. Comparisons of viral replication between a non-IFN expressing OAd (OAd-Luciferase) **(A)**, and an IFN-expressing OAd (OAdIFN-α) **(B)** show that both viruses are able to replicate in tumors, and although OAdIFN-α expresses an antiviral cytokine, the virus can still replicate in tumors. Combining type I IFN with OAd-Luciferase **(C)** confirms that IFN does not inhibit viral replication. Tumors were stained seven days post infection with the virus.

Effect of radiation timing on OAd-IFN combinations *in vivo*

Our analysis of the *in vitro* and *in vivo* data clearly shows that adding radiation to combinations of OAd-IFN + (5-FU + CDDP) overrules chemotherapy's antagonistic effect on the virus and improves the virus' efficacy when used in triple combination (OAd-IFN + (5-FU + CDDP) + radiation). To determine if changing the timing of the radiation can enhance the efficacy of OAd-IFN combinations with radiation, and to potentially improve the therapeutic effect of the triple combination, we tested different radiation schedules in combination with OAd-IFN. We performed the study in mice bearing MIA-PACA-2 tumors and assessed the relative growth of the tumors **(Figure 8)**. We used the group treated with OAd-IFN + 4GY as our reference group because this was the treatment protocol used in our earlier *in vivo* experiments **(Figure 6)**. Because IFN is a radiosensitizer, in this group

we attempted to concentrate the virus' IFN expression in tumors before administering the radiation (4GY). This strategy not only reflects the treatment protocol in IFN therapy, but also potentiates the radiation effect in tumor cells. The data show that administering unfractionated (4Gy) or fractionated (2GY + 2GY) radiation before infecting the tumor with the virus resulted in the study's most effective treatment protocols.

Compared to the tumor-growth rate (TGR) in the reference therapy (TGR=9.6%), using unfractionated radiation (4Gy + OAd-IFN) or fractionated radiation ((2Gy + 2Gy) + OAd-IFN) before infecting the tumor with the virus resulted in the greatest tumor growth inhibition (TGR=2%, $p < 0.01$; and TGR=6%, $p=0.08$, respectively). Between these two radiation regimens, administering a full radiation dose (4Gy) before treatment with OAd-IFN was more efficacious because it induced complete remission in two tumors and markedly hampered tumor growth in early stages of the therapy. The least effective radiation schedule was the administration of fractionated radiation after infecting the tumor with OAd-IFN (OAd-IFN + (2Gy + 2Gy)) (TGR= 7.9%, $p=0.4$). These data demonstrated that the effectiveness of therapy is significantly diminished if radiation insult after virus infection is weaker. This observation is consistent with our *in vitro* CFA data **(Figure 5),** which showed that an increase in the dose of radiation after OAd-IFN infection enhances the synergistic and cytotoxic effect of treatments in MIA-PACA-2 cells. In summary, we suggest that to enhance the anti-tumor effect therapies mimicking IFN therapy (OAd-IFN + (5-FU + CDDP) + Radiation), a radiation schedule where the radiation is administered before the OAd-IFN infection should be explored. This new therapeutic approach might enhance the effectiveness of OAd-IFN in combination with chemoradiation and diminish the variability of efficacy when tumors are treated with OAd-IFN in combination with 5-FU + CDDP and radiation.

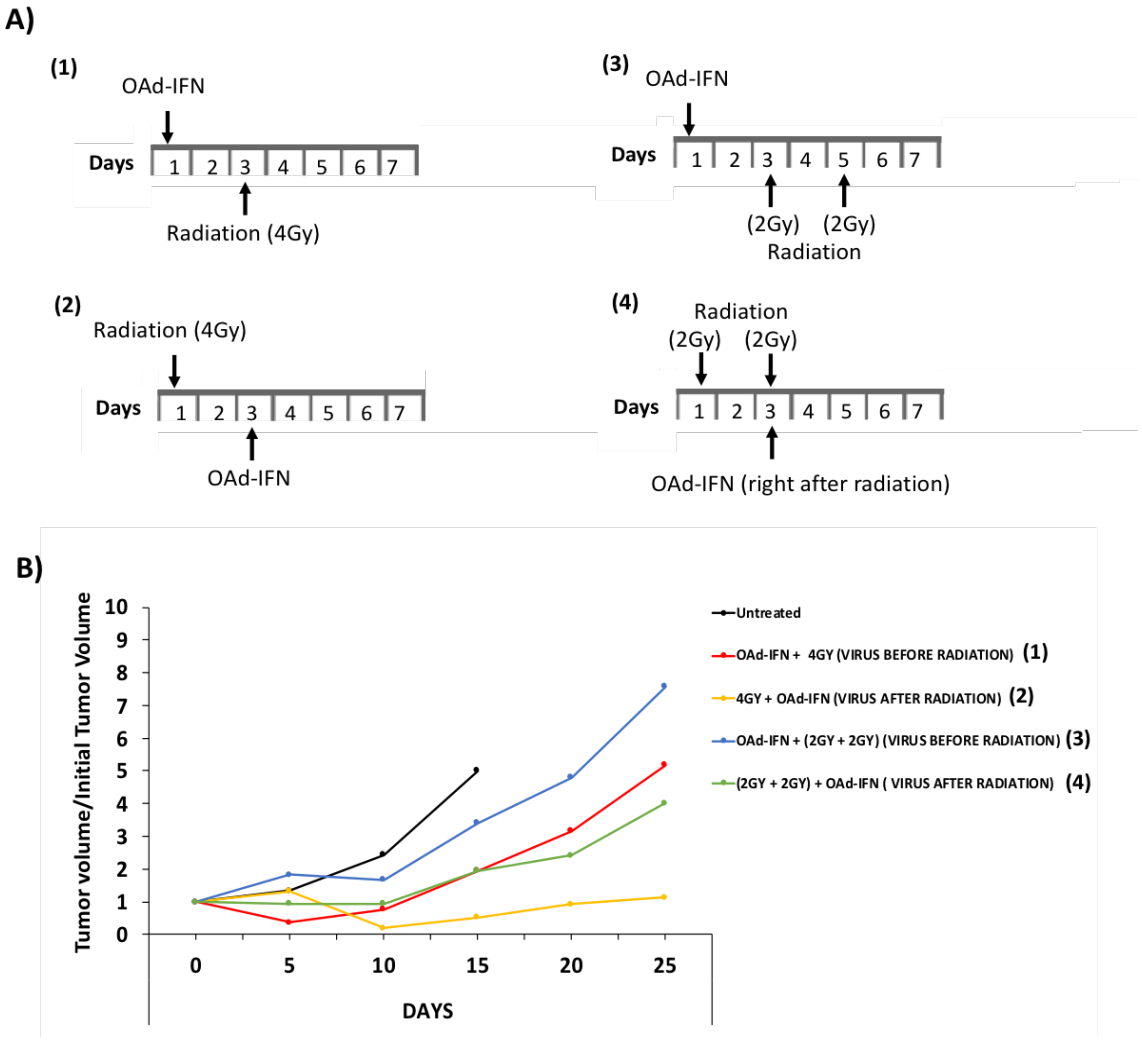

Figure 8. Effect of radiation timing on OAd-IFN combinations. To assess if modifying radiation timing can enhance the efficacy of combinations of OAd-IFN with radiation, we tested different radiation schedules in combination with OAd-IFN in mice bearing Mia-Paca-2 tumors. The experiment's control group was OAd-IFN + 4Gy (1), which consisted of infecting the tumors with OAd-IFN before radiation. This was the same radiation protocol we used in earlier *in vivo* experiments (Figure 6). Tumor Growth Rate (TGR), or the amount (%) of tumor volume increase/day was used to compare therapy groups. **(A)** Radiation schedule in OAd-IFN treatments. **(B)** Data showed that using full radiation dose (4GY + OAd-IFN (2); TGR=0.2%) or fractionated radiation ((2Gy + 2GY) + OAd-IFN (4); TGR=6.6%) before infecting the tumors with OAd-IFN resulted in the study's most effective therapies with the strongest anti-tumor effects. Compared to the reference therapy (OAd-IFN + 4Gy (1), TGR=9.6%), use of fractionated radiation after virus infection (OAd-IFN +2Gy + 2Gy (3); TGR=7.9%) was the least effective treatment regimen. This showed that in case radiation is administered after viral infection, higher dose of radiation should

be considered. The graph displays the relative volume of the tumors, which reflects the tumor-growth rate over time. Graph was plotted using geometric mean of the average relative tumor volume.

12.4. Figures

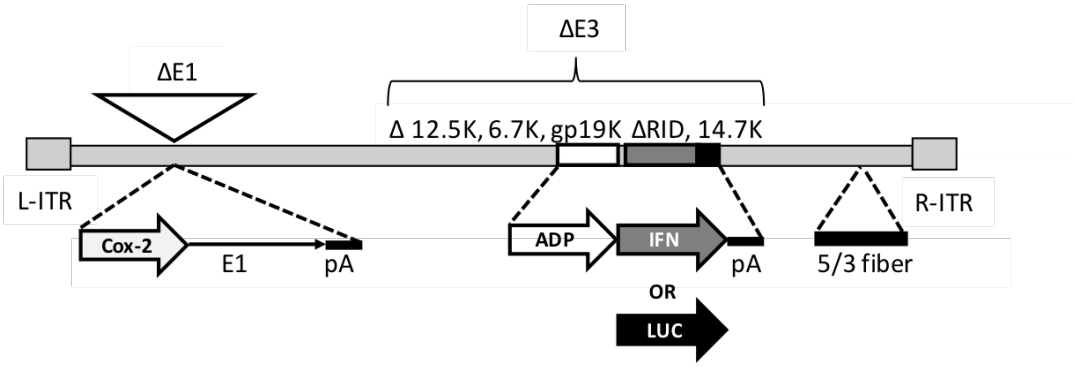

Figure 1. Vector structure. Structures of IFN-expressing oncolytic adenovirus (OAd-IFN), and counterpart vector expressing luciferase (OAd-LUC) are displayed. To restrict replicating vectors to PDAC cells, the Cox-2 promoter was included upstream of Adenovirus (Ad) E1 region, which is the region that initiates virus replication. In both vectors, we deleted most non-essential genes from Ad E3 region and included the Adenovirus Death Protein (ADP). In the OAd-IFN vector, we added human IFN-α (IFN) gene to the Ad E3 region, whereas for the OAd-LUC vector, we added the Luciferase gene (LUC) in place of the IFN gene.

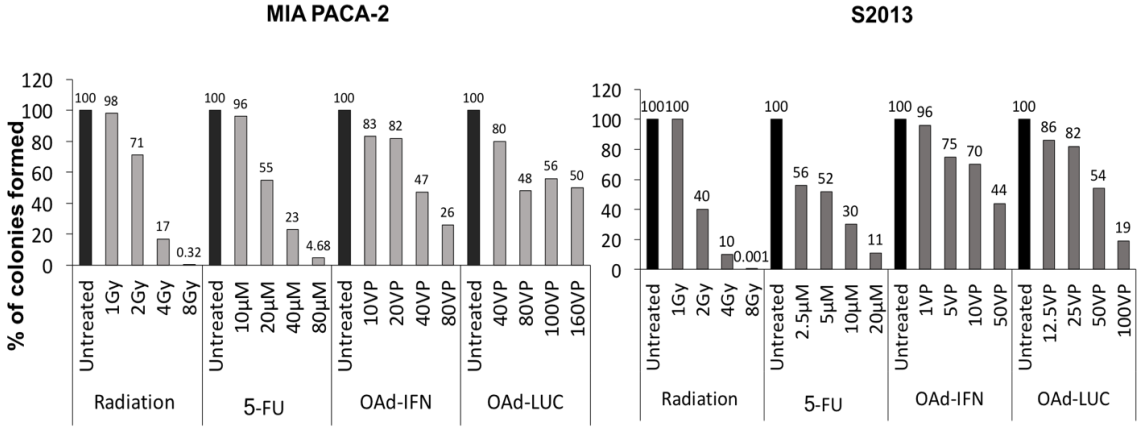

Figure 2. Establishing monotherapy ED50 in Colony Formation Assay. We tested a range of doses of OAd-IFN, OAd-LUC, 5-FU, and radiation in MIA-PACA-2 and S2013 PDAC cells. The data shows that S2013 is slightly more sensitive to monotherapies than MIA-PACA-2. The numbers on top of the histogram bars reflect the percentage of colonies that formed after each monotherapy treatment.

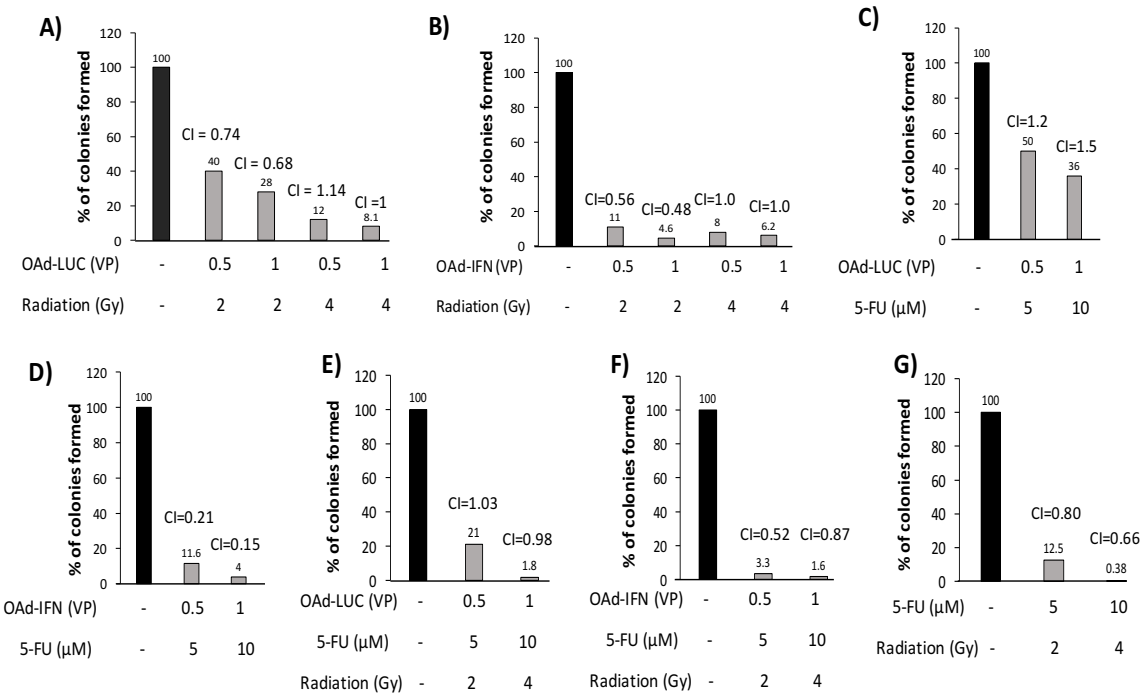

Figure 3. IFN contribution to cytotoxicity and synergistic interaction between OAd-IFN and chemotherapy, radiation, and chemoradiation. Displayed is an analysis of Combination Index (CI) of OAd-IFN combination in S2013 using colony formation assay. Combinations of OAd-LUC **(A)** or OAd-IFN **(B)** and radiation shows that IFN expressed by OAd-IFN potentiates synergism when low dose of radiation is used. Combinations of OAd-LUC with chemotherapy results in antagonism **(C)**, while combinations of OAd-IFN with same chemotherapy doses were highly synergistic **(D)**. **(E)** Use of OAd-LUC in treatments that mimic IFN-therapy (virus combined with chemoradiation) were additive (CI=1) or moderately synergistic (CI=0.98), while use of OAd-IFN in same therapeutic set-up resulted in synergism with any of the radiation and chemotherapy doses tested **(F)**. As 5-FU in combination with radiation was the reference therapy used to compare effectiveness of IFN-therapy in clinical trials, we decided to test this therapeutic regimen. Data showed that combinations of 5-FU and radiation were highly cytotoxic and synergistic **(G)**. (CI<1) synergism, (CI=1) additive effect, and (CI>1) antagonism. The numbers on top of the histogram bars reflect the percentage of colonies that formed after each monotherapy treatment.

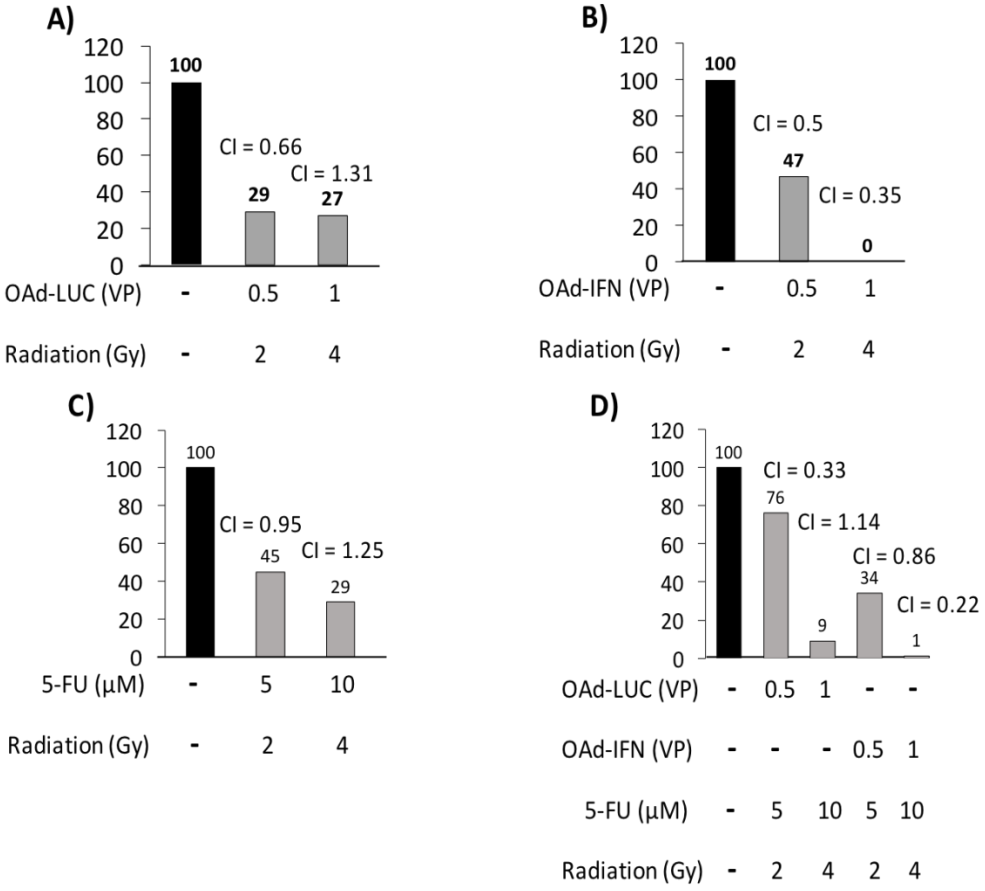

Figure 4. Effect of radiation on OAd-IFN combinations tested in cell lines used in the pre-clinical model of PDAC. Displayed is the effect of radiation in combination with OAd-IFN using colony formation in the MIA-PACA-2 PDAC cell line. This cell line is used to form human PDAC xenografts in nude mice. CFA output shows that while combinations of OAd-LUC with low doses of radiation were synergistic (CI=0.66), increase of dose of radiation in combination with virus abolished synergistic interaction (CI=1.31) **(B)**. On the other hand, use of OAd-IFN with either low or high doses of radiation were both highly synergistic (CI=0.5 and CI=0.35) **(C)**. **(D)** Combinations of either OAd-LUC or OAd-IFN in treatment protocol mimicking IFN-therapy (IFN + 5-FU + Radiation) were highly synergistic when low doses of therapeutics were used, but only combinations of OAd-IFN with higher doses of chemotherapy or radiation were highly synergistic. The numbers on top of the histogram bars reflect the percentage of colonies formed after treatment. (CI<1) synergism, (CI=1) additive effect, and (CI>1) antagonism.

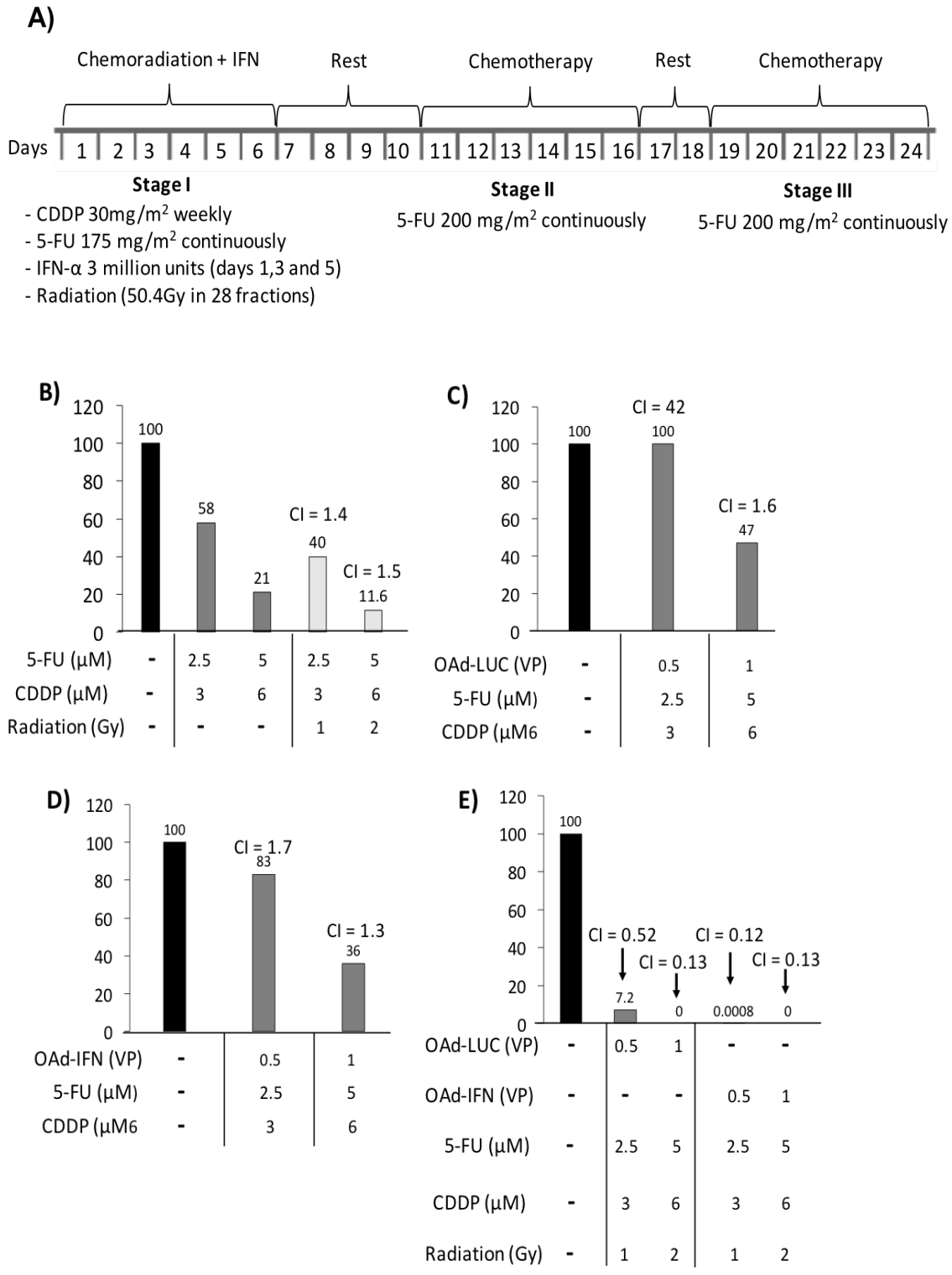

Figure 5. Using radiation with combinations of OAd-IFN with 5-FU + CDDP results in highly cytotoxic and synergistic combinations. To better replicate the IFN-therapy used to treat PDAC

patients in clinical trials **(A)**, we used CFA in MIA-PACA-2 to assess the CI and cytotoxicity of OAd-IFN combined with (5-FU + CDDP), and radiation. **(B)** Combinations of CDDP + 5-FU with radiation show that although two chemotherapy doses are used in combination with radiation, these combinations are antagonistic (CI>1). Combinations of either OAd-LUC **(C)** or OAd-IFN **(D)** with (5-FU + CDDP) were all shown to be antagonistic (CI>1), but very strong antagonism was only shown when low doses of non-IFN expressing OAd (OAd-LUC) was combined with chemotherapies (CI=42) **(C)**. Despite antagonism between chemotherapies and OAds, and between chemotherapies and radiation, inclusion of radiation to OAd treatment (OAd-IFN + (5-FU + CDDP) + Radiation) or (OAd-LUC + (5-FU + CDDP) + Radiation) resulted in highly synergistic and cytotoxic treatments. Very stronger synergism (CI<0.3) was specially observed in combinations including OAd-IFN **(E)**. (CI<1) synergism, (CI=1) additive effect, and (CI>1) antagonism. Numbers on top of the histogram bars reflect the percentage of colonies formed after treatment.

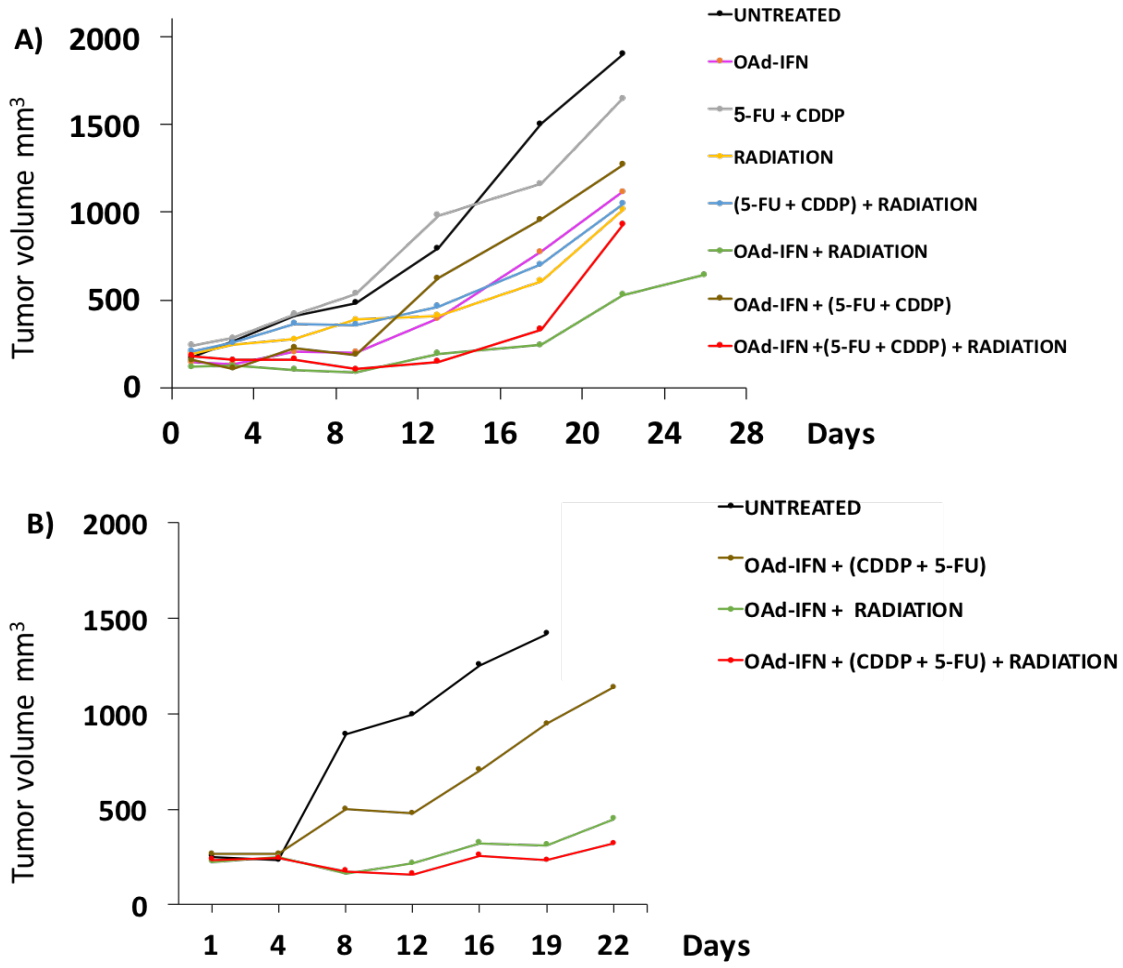

Figure 6. Therapeutic effect of OAd-IFN combinations in nude mice. Nude mice bearing MIA-PACA-2 PDAC cell xenografts were treated with OAd-IFN combinations. To better replicate IFN-therapy in clinical trials, the chemotherapy regimen consisted of 5-FU + CDDP. Tumor Growth Rate

(TGR), or the amount (%) of tumor volume increase/day was used to compare therapy groups. **(A)** Compared to the control-therapy group (5-FU + CDDP) + radiation (TGR = 3.6%), treating animals with OAd-IFN + radiation (TGR=6.9) or OAd-IFN + (5-FU + CDDP) + Radiation (TGR=0.6%) resulted in the most effective therapies to decrease tumor volume over time. Compared to group treated with OAd-IFN (TGR=6.1%), group treated with OAd-IFN + (5-FU + CDDP) (TGR=9%) had the anti-tumor effect suppressed. However, inclusion of radiation to treatment regimen (OAd-IFN + (5-FU + CDDP) + Radiation) abolished virus antagonism by chemotherapy, resulting in the most effective therapy in the study (TGR=0.6%) **(B)** To confirm if adding 5-FU + CDDP to OAd-IFN treatments affected treatment efficacy, and if variation in initial tumor volume impacted therapeutic effect of therapies, we repeated the experiment testing OAd-IFN combinations with 5-FU + CDDP, radiation, and (5-FU + CDDP) + Radiation. Data confirmed that using 5-FU + CDDP with OAd-IFN strongly inhibited the virus (TGR=6.6%), and that combinations of OAd-IFN with radiation (TGR=2%) and chemoradiation (TGR=0.4%) showed the strongest anti-tumor effect. Again, use of virus in combinations closely resembling IFN-Therapy in clinical trials (OAd-IFN + (5-FU + CDDP) + Radiation) resulted in the best therapy to inhibit tumor growth. The graph shows the absolute tumor volume over time.

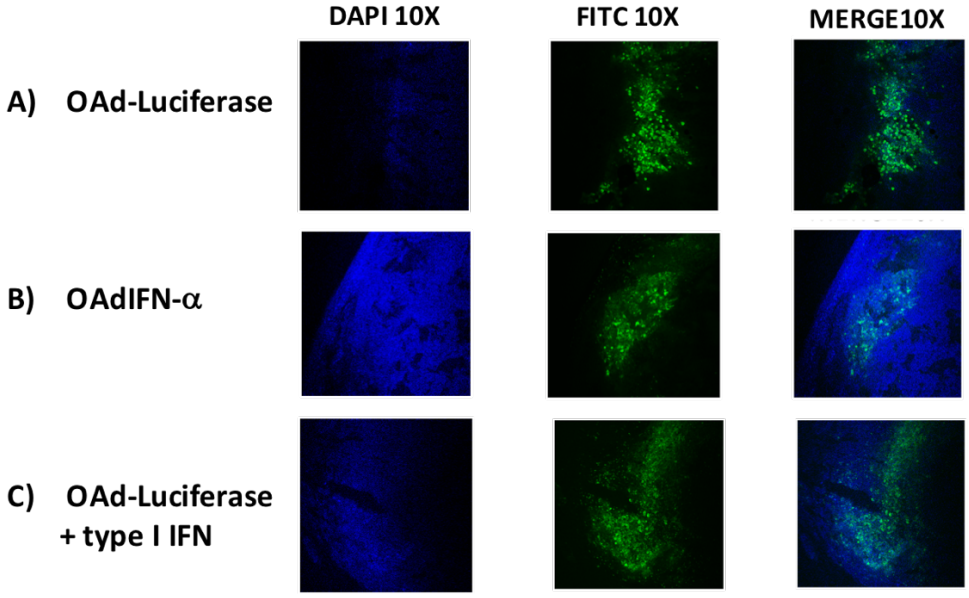

Figure 7. Effect of IFN expressed by OAd in viral replication. We assessed OAd replication in nude mice bearing xenografts of PANC-1 PDAC cells. Confocal images of viral replication show the FITC staining of the adenoviral hexon capsid protein. Comparisons of viral replication between a non-IFN expressing OAd (OAd-Luciferase) **(A)**, and an IFN-expressing OAd (OAdIFN-α) **(B)** show that both viruses are able to replicate in tumors, and although OAdIFN-α expresses an antiviral cytokine, the virus can still replicate in tumors. Combining type I IFN with OAd-Luciferase

(C) confirms that IFN does not inhibit viral replication. Tumors were stained seven days post infection with the virus.

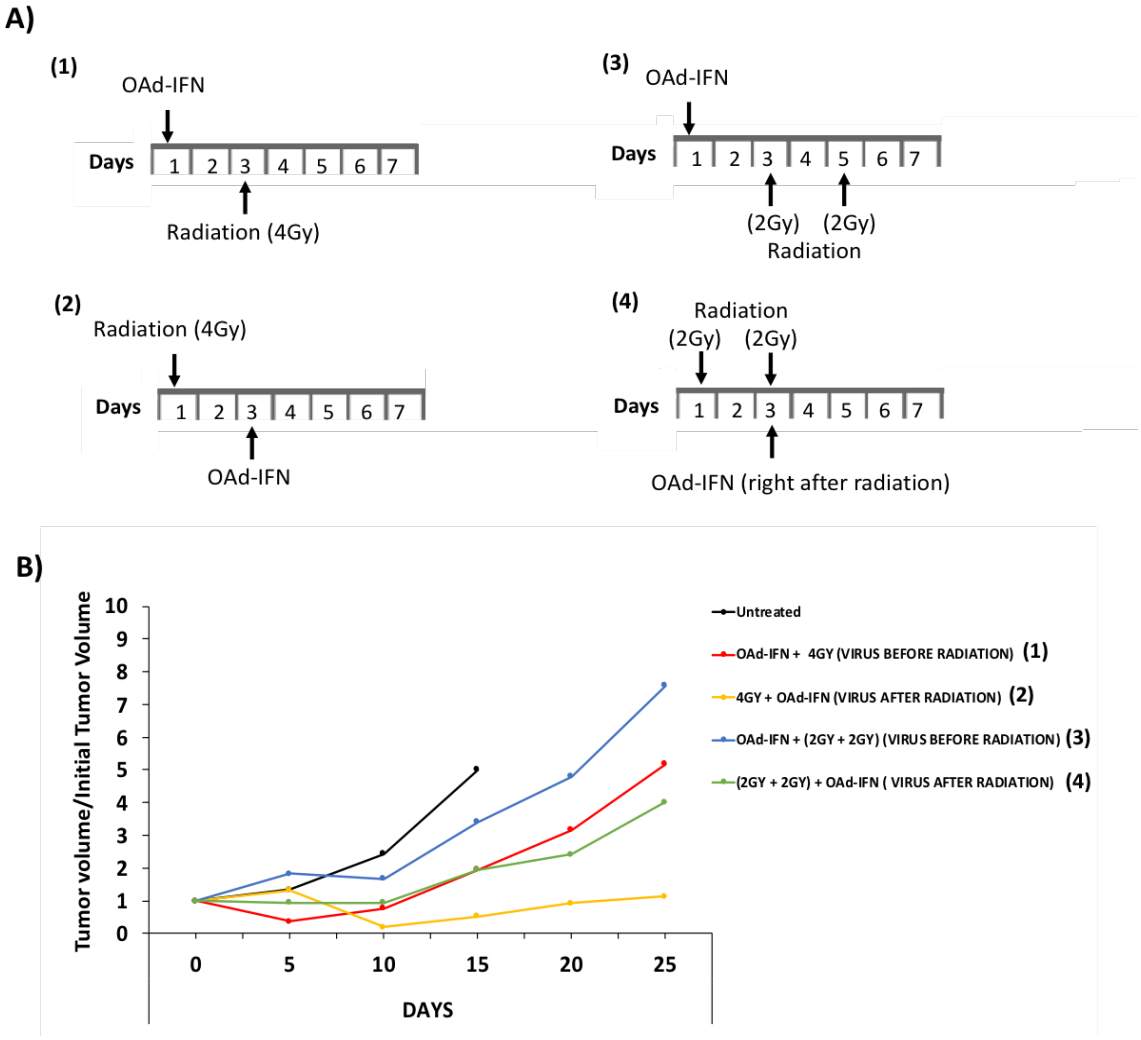

Figure 8. Effect of radiation timing on OAd-IFN combinations. To assess if modifying radiation timing can enhance the efficacy of combinations of OAd-IFN with radiation, we tested different radiation schedules in combination with OAd-IFN in mice bearing Mia-Paca-2 tumors. The experiment's control group was OAd-IFN + 4Gy (1), which consisted of infecting the tumors with OAd-IFN before radiation. This was the same radiation protocol we used in earlier *in vivo* experiments (Figure 6). Tumor Growth Rate (TGR), or the amount (%) of tumor volume increase/day was used to compare therapy groups. **(A)** Radiation schedule in OAd-IFN treatments. **(B)** Data showed that using full radiation dose (4GY + OAd-IFN (2); TGR=0.2%) or fractionated radiation ((2Gy + 2GY) + OAd-IFN (4); TGR=6.6%) before infecting the tumors with OAd-IFN resulted in the study's most effective therapies with the strongest anti-tumor effects. Compared to the reference therapy (OAd-IFN + 4Gy (1), TGR=9.6%), use of fractionated radiation after virus

infection (OAd-IFN +2Gy + 2Gy (3); TGR=7.9%) was the least effective treatment regimen. This showed that in case radiation is administered after viral infection, higher dose of radiation should be considered. The graph displays the relative volume of the tumors, which reflects the tumor-growth rate over time. Graph was plotted using geometric mean of the average relative tumor volume.

12.5. Discussion

Using IFN-α in combination with 5-FU, CDDP, and radiation in an adjuvant setting has been highly effective in improving the short- and long-term survival of PDAC patients (134, 135, 145, 149). Although efficacious, the potential of this therapy is negatively affected by IFN-associated systemic toxicity and low intratumoral levels of IFN. To improve one of the few known effective therapeutic regimens for treating PDAC, we tested the use of IFN-expressing oncolytic adenovirus (OAd-IFN) in combination with chemoradiation in regimens that mimic IFN therapy in clinical trials.

The data showed that combinations of OAd-IFN with 5-FU, radiation, and 5-FU + radiation were synergistic and highly effective in killing PDAC cells *in vitro* **(Figures 3 and 4)**. Testing CDDP and 5-FU combination chemotherapy (5-FU + CDDP) with OAd-IFN demonstrated that chemotherapies are antagonistic to the virus **(Figure 5).** Despite that, we demonstrated that inclusion of radiation to combinations with OAd-IFN and (5-FU + CDDP) eliminated the antagonism created by the chemotherapies resulting in highly cytotoxic and synergistic treatments *in vitro* **(Figure 5).** We also showed that 5-FU + CDDP antagonism to OAd-IFN was also observed *in vivo*, but addition of radiation to therapy eradicated chemotherapy antagonism to OAd-IFN (OAd-IFN + (5-FU + CDDP) + Radiation) improving therapy efficacy **(Figure 7).** In summary, our data consistently showed that including OAd-IFN in combination with the therapeutics used in IFN-therapy is highly effective, especially when the virus is used in treatments that mimic the IFN-therapy (OAd-IFN + 5-FU + radiation) **Figure 4,** or (OAd-IFN + (5-FU + CDDP) + Radiation) **Figures 5 and 6**.

Despite the effectiveness of triple-combination therapies (OAd-IFN + (5-FU + CDDP) + Radiation) *in vitro*, it is possible that the inhibition of OAd-IFN by (5-FU + CDDP) impacted triple-combination therapy effect *in vivo* **(Figure 6 A and B).** It is clear that the

antagonism between OAd-IFN and (5-FU + CDDP) predicted in our *in vitro* experiment **(Figure 5)** translated to a diminished therapeutic effect of the virus in combination with chemotherapies *in vivo* **(Figure 6).** Our *in vivo* experiment showed that, although it is highly effective, the therapeutic effect of triple combinations varied when tested in two different experiments **(Figure 6 A and B).** Since tumors have irregular vascularization, which can affect the dose of chemotherapy delivered to tumors (238-240), the variability of the therapeutic effect in triple combinations in these two experiments could possibly be explained by the uneven delivery of chemotherapy to tumors treated with OAd-IFN + (5-FU + CDDP) + radiation. In the triple-therapy group **(Figure 6A)**, given that the chemotherapy was inhibitory to OAd-IFN, tumors that responded poorly to triple combinations by the end of the experiment could have received more chemotherapy doses than tumors that showed higher growth inhibition **(Figure 6A).** But although some tumors grew exponentially at the end of therapy in the first *in vivo* experiment **(Figure 6A),** other tumors in the same group showed complete remission. On the other hand, repetition of the *in vivo* experiment testing OAd-IFN combinations with (5-FU + CDDP), radiation, and (5-FU + CDDP) with radiation **(Figure 6B)** did not show variability in therapeutic effect in the triple combination therapy. It is possible that in the second experiment all the tumors received similar concentrations of chemotherapy. While we did not observe any tumor remissions in the second *in vivo* experiment, tumors were consistently smaller compared to groups treated with OAd-IFN combined with chemotherapy or with radiation. Variability of therapeutic effect in the triple combination therapy in these two *in vivo* experiments could also indicate that the repeated injection of the virus during therapy is a variable that needs to be explored.

It is clear that adding radiation to antagonistic combinations of the virus and 5-FU + CDDP surmounts chemotherapy's inhibition of the virus *in vitro* and *in vivo* **(Figures 5 and 6)**. Therefore, we propose that new radiation schedules be created in combination with OAd-IFN **(Figure 8).** We showed that using radiation before infecting the tumor with the virus (4GY + OAd-IFN) or ((2Gy + 2Gy) + OAd-IFN) resulted in superior tumor growth inhibition compared to the radiation schedule that we used in our first *in vivo* experiments **(Figure 8, OAd + 4Gy (1))**. Although we did not test the new radiation protocol in combination of OAd-IFN with 5-FU + CDDP, we expect that enhancing the effectiveness

of the virus in combination with radiation will result in an improved triple combination anti-tumor effect regardless of the amount of chemotherapy regimen used. We predict that using radiation before viral infection will eliminate the variability of the therapeutic effect in triple combination, and has the potential to make this therapeutic regimen even more effective.

We do not recommend, however, reducing the amount of chemotherapies used in triple combination because in patients PDAC is a highly heterogeneous tumor (241, 242). Using 5-FU (a DNA-damaging base analog that further inhibits DNA and RNA synthesis) in conjunction with CDDP (an DNA-damaging agent) will increase the likelihood that more cells are affected by the treatment, whether or not they are resistant to any of the therapeutics used in IFN therapy (radiation, chemotherapy, and IFN). The goal of combination therapy is to cause cell distress and cell death through different pathways so that as many cancer cells as possible can be eliminated during treatment. Combining two DNA-damaging chemotherapy drugs with radiation (which potentiates double-strand break) and IFN (which enhances the effectiveness of chemoradiation) as in the IFN therapy protocol increases the chances that most tumor cells will be affected.

Although chemotherapy is used consistently with OAds and has been shown to improve the anti-tumor effect during treatment (243-245), our preliminary studies suggested that 5-FU inhibits OAd-IFN replication (200). The data showed that administering 5-FU before or after OAd-IFN infection reduces the viral DNA copy number compared to OAd-IFN treatment alone. Although we observed that effect, *in vitro* data testing combination of OAd-IFN with 5-FU clearly shows therapy is highly synergistic and cytotoxic **(Figure 3D)**. We also show that IFN expressed by OAd-IFN enhances 5-FU cytotoxicity in PDAC cells **(Figure 3C)**. On the other hand, using 5-FU + CDDP as the chemotherapy regimen combined with OAd-IFN eliminates the chemosensitization produced by IFN to 5-FU, and therapy becomes antagonistic and weakly cytotoxic. To better understand the effect of 5-FU + CDDP in OAd-IFN, further studies accessing impact of these chemotherapies in viral replication need to be performed.

The reason why addition of radiation to OAd-IFN combination with 5-FU + CDDP abolishes antagonism is unclear. Treatment of cancer cells with radiation and chemotherapies induces cellular stress, which, in turn, upregulates expression of NF-κB expression in treated cells (246-249). One of the activators of Cox-2—which is included upstream of the OAd-IFN's E1 region and controls its replication—is NF-κB (250). It is possible that higher expression of NF--κB in cells treated with OAd-IFN + (5-FU + CDDP) + radiation compared to the cells treated with OAd-IFN + (5-FU + CDDP) enhanced viral replication which contributed to triple therapy higher efficacy **(Figures 5 and 6).** Although a possible explanation, up-regulation of the NF--κB pathway must be assessed in tumor cells after radiation and chemotherapy treatments, and these levels should be correlated with virus replication.

When cells are infected with a virus, they produce IFN which acts in an autocrine and paracrine manner to induce an anti-viral state in cells and shut down virus replication. We showed that IFN expression by OAd-IFN does not eliminate viral replication in tumors **(Figure 7).** This phenomenon can be explained by the adenovirus' expression of VA-RNA, which inhibits RNA-activated protein kinase (PKR)—one of the main components of the IFN pathway that induces an anti-viral state in infected cell, and shuts down protein translation (60). IFN not only protects the cells during infection, but also acts as an immunomodulatory cytokine that can induce the activation and maturation of NK, T-helper cells, and dendritic cells, and increase MHC-1 expression in the cell surface. Therefore, as IFN was proven not to inhibit viral replication, using IFN-expressing OAd in IFN therapy can potentially stimulate an anti-tumor immune response by exposing tumor-specific peptides to the immune system during oncolysis. Because patients who develop an anti-tumor immune response show higher survival rates and decreased rates of tumor recurrence (252-254), we believe that using an IFN-expressing OAd in IFN therapy can not only enhance therapy efficacy by potentiating the effect of chemotherapy and radiation by IFN, but it also can stimulate the formation of a robust anti-tumor response in patients and significantly contribute to their long-term survival after therapy.

In summary, we conclude that using an IFN-expressing Cox-2 controlled OAd in combination with chemoradiation can significantly improve IFN therapy and overcome its

limitations. PDAC localized oncolysis and IFN expression by OAd-IFN combined with the highly synergistic interaction between the virus and chemoradiation indicates that the virus can reduce therapy toxicity while improving its efficacy. Because IFN therapy is one of the few therapeutic regimens shown to improve patients short- and long-term survival rates, developing an OAd-IFN based IFN-therapy could result in an effective PDAC treatment therapy.

13. Summary

Pancreatic cancer may soon be the third-leading cause of cancer-related death in the United States. Because the disease is usually diagnosed in its late stage, greater than 80% of patients cannot undergo surgery, which is the most effective treatment for the disease. Only 6% of patients with PDAC who do not undergo surgery survive for five years or more and their post-diagnosis survival period is usually only three to four months. Despite these discouraging statistics, adjuvant therapy with IFN-α combined with 5-FU, CDDP, and radiation has produced a remarkable 35% increase in patients' five-year survival rates. Not only has this therapy improved patients' long-term survival rates, it also has improved their short-term survival rates by 20–41%. While this therapy is effective, its limitations include high IFN-associated systemic toxicity and low levels of IFN in tumors. These limitations prompt many patients to drop out of the therapy, diminish the beneficial effects of IFN during therapy, and compromise the full efficacy of the therapy.

To overcome these limitations, we studied an IFN-expressing oncolytic adenovirus expressing human IFN (OAd-IFN) or hamster IFN (OAd-hamIFN) in therapeutic regimens that mimicked IFN therapy.

We tested the combinations with OAd-IFN vector in an immunodeficient mice model bearing PDAC xenografts, and the combinations with OAd-hamIFN in a syngeneic immunocompetent hamster model of PDAC. Although studies in mice can display the interaction between therapeutic components during therapy, the hamster model demonstrates how the immune system can potentiate the effectiveness of conventional treatments.

Tests of IFN-expressing OAd in human or hamsters PDAC cells consistently demonstrated that combinations of IFN-expressing OAds with chemotherapy, radiation, and chemoradiation resulted in highly synergistic and effective therapies *in vitro* and *in vivo*. Although use of stronger chemotherapy regimen (5-FU + CDDP) with IFN-expressing OAd in human PDAC cells was shown to be antagonistic to virus, inclusion of radiation to this combination (OAd + (5-FU + CDDP) + Radiation) resulted in the most efficacious therapy *in vitro* and in immunodeficient mice bearing human PDAC xenografts. Knowing that radiation abolished chemotherapy antagonism to virus, we suggested to improve radiation protocol administered with IFN-expressing OAd. *In vivo* testing of new radiation protocols in combination with IFN-expressing OAd showed that use of radiation before virus infection enhanced treatment efficacy. Thus, we recommend that this new radiation protocol be further explored in treatments mimicking IFN therapy.

Our studies using the immunocompetent hamster PDAC model suggested that stimulating an anti-tumor immune response during treatment contribute to improved therapy efficacy. The data also demonstrated that the IFN expressed by the vector potentiated the effects of radiation and chemoradiation *in vivo*. These observations suggest that including an IFN-expressing OAd in therapies that resemble IFN therapy could not only potentiate the therapy's efficacy by stimulating an anti-tumor response, but it could also increase efficacy by potentiating IFN chemoradiosensitizaton in tumors. In addition to contributing to patients' long-term survival (252-254), the stimulation of an anti-tumor immune response can also strengthen tumor debulking in neo-adjuvant therapies in conjunction with chemoradiation's elimination of cancer cells. Because IFN is an immunostimulant, it is possible that using OAd—whose oncolysis exposes tumor antigens to the host's immune system— combined with chemoradiation can reduce tumor burden and make more patients eligible for surgery. If this effect is fully realized, OAd-based IFN-therapy could be a breakthrough in PDAC treatment since more than 80% of patients are excluded from adjuvant therapy protocols because the local PDAC is highly advanced at the time of diagnosis.

In summary, our studies in hamsters and mice support including an IFN-expressing OAd in therapeutic protocols that mimic clinical IFN-based chemoradiation regimens. The data

we compiled in these two distinct models complement each other and show that mechanistically all the therapeutic components work well together to synergistically eliminate PDAC cells. The data also indicate that using IFN-expressing OAds can potentially stimulate tumor-specific immunity that enhances therapeutic efficacy. The strong synergism between IFN-expressing OAd and chemoradiation emphasizes that adding virus to IFN therapy could reduce associated toxicities by allowing the physician to reduce drug doses used in combination. Furthermore, including a Cox-2 promoter to control virus replication might mitigate IFN systemic toxicity by restricting and concentrating the production of this cytokine in PDAC tumors. These findings show that adding IFN-expressing OAd to IFN therapy can overcome IFN therapy's two main limitations: high IFN-associated systemic toxicity and low intratumoral levels of IFN. Thus, we support and recommend further studies in immunocompetent hamsters to prove if using a replication-controlled IFN-expressing OAd in combination with 5-FU, CDDP, and radiation will result in a potent therapy that mimics the IFN-based chemoradiation regimen that was successful in PDAC clinical trials. Because this treatment protocol is one of the few—if not the only— protocols shown to remarkably improve the short- and long-term survival rates of PDAC patients, developing an OAd-IFN-based IFN therapy might finally result in a highly effective therapy to treat this devastating disease.

REFERENCES

1. Kelly E, Russell SJ. History of oncolytic viruses: genesis to genetic engineering. Mol Ther. 2007;15(4):651-9.
2. Weatherall D, Greenwood B, Chee HL, Wasi P. Science and Technology for Disease Control: Past, Present, and Future. In: Jamison DT, Breman JG, Measham AR, Alleyne G, Claeson M, Evans DB, et al., editors. Disease Control Priorities in Developing Countries. 2nd ed. Washington (DC)2006.
3. Hoppe-Seyler F, Butz K. Molecular mechanisms of virus-induced carcinogenesis: the interaction of viral factors with cellular tumor suppressor proteins. J Mol Med (Berl). 1995;73(11):529-38.
4. Chen Y, Williams V, Filippova M, Filippov V, Duerksen-Hughes P. Viral carcinogenesis: factors inducing DNA damage and virus integration. Cancers (Basel). 2014;6(4):2155-86.
5. Pelner L, Fowler GA, Nauts HC. Effects of concurrent infections and their toxins on the course of leukemia. Acta Med Scand Suppl. 1958;338:1-47.
6. Pasquinucci G. Possible effect of measles on leukaemia. Lancet. 1971;1(7690):136.
7. Zygiert Z. Hodgkin's disease: remissions after measles. Lancet. 1971;1(7699):593.
8. Taqi AM, Abdurrahman MB, Yakubu AM, Fleming AF. Regression of Hodgkin's disease after measles. Lancet. 1981;1(8229):1112.
9. Bluming AZ, Ziegler JL. Regression of Burkitt's lymphoma in association with measles infection. Lancet. 1971;2(7715):105-6.
10. Andtbacka HIR CF, Harrington K, et al. Long-term follow-up (LTFU) of overall survival (OS) data from the phase 3 OPTiM study of talimogene laherparepvec (T-VEC) for metastatic melanoma. June 29-30, 2017.
11. Bucco D. Long-Term T-VEC Results in Melanoma Provide Reassurance for Clinicians and Patients http://www.targetedonc.com/news/longterm-tvec-results-in-melanoma-provide-reassurance-for-clinicians-and-patients-expert-says2018 [
12. Rehman H, Silk AW, Kane MP, Kaufman HL. Into the clinic: Talimogene laherparepvec (T-VEC), a first-in-class intratumoral oncolytic viral therapy. J Immunother Cancer. 2016;4:53.
13. Administration USFaD. FDA approves first-of-its-kind product for the treatment of melanoma https://www.fda.gov/NewsEvents/Newsroom/PressAnnouncements/ucm469571.htm: U.S. Food and Drug Administration; 2015 [updated 10/27/2015.
14. Huebner RJ, Bell JA, Rowe WP, Ward TG, Suskind RG, Hartley JW, et al. Studies of adenoidal-pharyngeal-conjunctival vaccines in volunteers. J Am Med Assoc. 1955;159(10):986-9.
15. Huebner RJ, Rowe WP, Schatten WE, Smith RR, Thomas LB. Studies on the use of viruses in the treatment of carcinoma of the cervix. Cancer. 1956;9(6):1211-8.
16. Zielinski T, Jordan E. [Remote results of clinical observation of the oncolytic action of adenoviruses on cervix cancer]. Nowotwory. 1969;19(3):217-21.

17. Georgiades J, Zielinski T, Cicholska A, Jordan E. Research on the oncolytic effect of APC viruses in cancer of the cervix uteri; preliminary report. Biul Inst Med Morsk Gdansk. 1959;10:49-57.
18. Chang SY, Lee CN, Lin PH, Huang HH, Chang LY, Ko W, et al. A community-derived outbreak of adenovirus type 3 in children in Taiwan between 2004 and 2005. J Med Virol. 2008;80(1):102-12.
19. Maranhao AG, Soares CC, Albuquerque MC, Santos N. Molecular epidemiology of adenovirus conjunctivitis in Rio de Janeiro, Brazil, between 2004 and 2007. Rev Inst Med Trop Sao Paulo. 2009;51(4):227-9.
20. Ghebremedhin B. Human adenovirus: Viral pathogen with increasing importance. Eur J Microbiol Immunol (Bp). 2014;4(1):26-33.
21. Yamamoto M, Curiel DT. Current issues and future directions of oncolytic adenoviruses. Mol Ther. 2010;18(2):243-50.
22. Krasnykh V, Dmitriev I, Mikheeva G, Miller CR, Belousova N, Curiel DT. Characterization of an adenovirus vector containing a heterologous peptide epitope in the HI loop of the fiber knob. J Virol. 1998;72(3):1844-52.
23. Gaggar A, Shayakhmetov DM, Liszewski MK, Atkinson JP, Lieber A. Localization of regions in CD46 that interact with adenovirus. J Virol. 2005;79(12):7503-13.
24. Yamamoto M, Davydova J, Wang M, Siegal GP, Krasnykh V, Vickers SM, et al. Infectivity enhanced, cyclooxygenase-2 promoter-based conditionally replicative adenovirus for pancreatic cancer. Gastroenterology. 2003;125(4):1203-18.
25. Armstrong L, Arrington A, Han J, Gavrikova T, Brown E, Yamamoto M, et al. Generation of a novel, cyclooxygenase-2-targeted, interferon-expressing, conditionally replicative adenovirus for pancreatic cancer therapy. Am J Surg. 2012;204(5):741-50.
26. Ono HA, Davydova JG, Adachi Y, Takayama K, Barker SD, Reynolds PN, et al. Promoter-controlled infectivity-enhanced conditionally replicative adenoviral vectors for the treatment of gastric cancer. J Gastroenterol. 2005;40(1):31-42.
27. Trujillo MA, Oneal MJ, Davydova J, Bergert E, Yamamoto M, Morris JC, 3rd. Construction of an MUC-1 promoter driven, conditionally replicating adenovirus that expresses the sodium iodide symporter for gene therapy of breast cancer. Breast Cancer Res. 2009;11(4):R53.
28. Hallenbeck PL, Chang YN, Hay C, Golightly D, Stewart D, Lin J, et al. A novel tumor-specific replication-restricted adenoviral vector for gene therapy of hepatocellular carcinoma. Hum Gene Ther. 1999;10(10):1721-33.
29. Alvarez RD, Curiel DT. A phase I study of recombinant adenovirus vector-mediated intraperitoneal delivery of herpes simplex virus thymidine kinase (HSV-TK) gene and intravenous ganciclovir for previously treated ovarian and extraovarian cancer patients. Hum Gene Ther. 1997;8(5):597-613.
30. Ganly I, Kirn D, Eckhardt G, Rodriguez GI, Soutar DS, Otto R, et al. A phase I study of Onyx-015, an E1B attenuated adenovirus, administered intratumorally to patients with recurrent head and neck cancer. Clin Cancer Res. 2000;6(3):798-806.
31. Nemunaitis J, Khuri F, Ganly I, Arseneau J, Posner M, Vokes E, et al. Phase II trial of intratumoral administration of ONYX-015, a replication-selective adenovirus, in patients with refractory head and neck cancer. J Clin Oncol. 2001;19(2):289-98.

32. Hecht JR, Bedford R, Abbruzzese JL, Lahoti S, Reid TR, Soetikno RM, et al. A phase I/II trial of intratumoral endoscopic ultrasound injection of ONYX-015 with intravenous gemcitabine in unresectable pancreatic carcinoma. Clin Cancer Res. 2003;9(2):555-61.
33. Yu W, Fang H. Clinical trials with oncolytic adenovirus in China. Curr Cancer Drug Targets. 2007;7(2):141-8.
34. Marshall E. Gene therapy death prompts review of adenovirus vector. Science. 1999;286(5448):2244-5.
35. Sibbald B. Death but one unintended consequence of gene-therapy trial. CMAJ. 2001;164(11):1612.
36. SoRelle R. Human gene therapy: science under fire. Circulation. 2000;101(12):E9023-4.
37. Nemerow GR, Pache L, Reddy V, Stewart PL. Insights into adenovirus host cell interactions from structural studies. Virology. 2009;384(2):380-8.
38. Sato-Dahlman M, Miura Y, Huang JL, Hajeri P, Jacobsen K, Davydova J, et al. CD133-targeted oncolytic adenovirus demonstrates anti-tumor effect in colorectal cancer. Oncotarget. 2017;8(44):76044-56.
39. Kirby I, Davison E, Beavil AJ, Soh CP, Wickham TJ, Roelvink PW, et al. Identification of contact residues and definition of the CAR-binding site of adenovirus type 5 fiber protein. J Virol. 2000;74(6):2804-13.
40. Devaux C, Adrian M, Berthet-Colominas C, Cusack S, Jacrot B. Structure of adenovirus fibre. I. Analysis of crystals of fibre from adenovirus serotypes 2 and 5 by electron microscopy and X-ray crystallography. J Mol Biol. 1990;215(4):567-88.
41. Hunt DM. VIROLOGY - CHAPTER ONE. BASIC VIROLOGY: DEFINITIONS, CLASSIFICATION, MORPHOLOGY AND CHEMISTRY 2017 [updated Monday, July 21, 2003 Available from: http://www.microbiologybook.org/mhunt/intro-vir.htm.
42. Gaggar A, Shayakhmetov DM, Lieber A. CD46 is a cellular receptor for group B adenoviruses. Nat Med. 2003;9(11):1408-12.
43. Loustalot F, Kremer EJ, Salinas S. Membrane Dynamics and Signaling of the Coxsackievirus and Adenovirus Receptor. Int Rev Cell Mol Biol. 2016;322:331-62.
44. Ruoslahti E. RGD and other recognition sequences for integrins. Annu Rev Cell Dev Biol. 1996;12:697-715.
45. Trotman LC, Mosberger N, Fornerod M, Stidwill RP, Greber UF. Import of adenovirus DNA involves the nuclear pore complex receptor CAN/Nup214 and histone H1. Nat Cell Biol. 2001;3(12):1092-100.
46. Saphire AC, Guan T, Schirmer EC, Nemerow GR, Gerace L. Nuclear import of adenovirus DNA in vitro involves the nuclear protein import pathway and hsc70. J Biol Chem. 2000;275(6):4298-304.
47. David M. Knipe PH. Fields virology: Lippincott Williams & Wilkins 2013 06/17/2013.
48. Hoeben RC, Uil TG. Adenovirus DNA replication. Cold Spring Harb Perspect Biol. 2013;5(3):a013003.
49. Wodrich H, Guan T, Cingolani G, Von Seggern D, Nemerow G, Gerace L. Switch from capsid protein import to adenovirus assembly by cleavage of nuclear transport signals. EMBO J. 2003;22(23):6245-55.

50. Dimova DK, Dyson NJ. The E2F transcriptional network: old acquaintances with new faces. Oncogene. 2005;24(17):2810-26.
51. Moran E. Interaction of adenoviral proteins with pRB and p53. FASEB J. 1993;7(10):880-5.
52. Debbas M, White E. Wild-type p53 mediates apoptosis by E1A, which is inhibited by E1B. Genes Dev. 1993;7(4):546-54.
53. Efrat S, Serreze D, Svetlanov A, Post CM, Johnson EA, Herold K, et al. Adenovirus early region 3(E3) immunomodulatory genes decrease the incidence of autoimmune diabetes in NOD mice. Diabetes. 2001;50(5):980-4.
54. Doronin K, Toth K, Kuppuswamy M, Krajcsi P, Tollefson AE, Wold WS. Overexpression of the ADP (E3-11.6K) protein increases cell lysis and spread of adenovirus. Virology. 2003;305(2):378-87.
55. Weitzman MD. Functions of the adenovirus E4 proteins and their impact on viral vectors. Front Biosci. 2005;10:1106-17.
56. Armstrong L, Davydova J, Brown E, Han J, Yamamoto M, Vickers SM. Delivery of interferon alpha using a novel Cox2-controlled adenovirus for pancreatic cancer therapy. Surgery. 2012;152(1):114-22.
57. Fessler SP, Young CS. Control of adenovirus early gene expression during the late phase of infection. J Virol. 1998;72(5):4049-56.
58. Ramke M, Lee JY, Dyer DW, Seto D, Rajaiya J, Chodosh J. The 5'UTR in human adenoviruses: leader diversity in late gene expression. Sci Rep. 2017;7(1):618.
59. U. P. Structural and Nonstructural Adenovirus Proteins. In: Ginsberg HS (eds) The Adenoviruses The Viruses. Boston, MA: Springer; 1984.
60. Vachon VK, Conn GL. Adenovirus VA RNA: An essential pro-viral non-coding RNA. Virus Res. 2016;212:39-52.
61. Samuel CE. Antiviral actions of interferons. Clin Microbiol Rev. 2001;14(4):778-809, table of contents.
62. Bach EA, Aguet M, Schreiber RD. The IFN gamma receptor: a paradigm for cytokine receptor signaling. Annu Rev Immunol. 1997;15:563-91.
63. Pathak VK, Schindler D, Hershey JW. Generation of a mutant form of protein synthesis initiation factor eIF-2 lacking the site of phosphorylation by eIF-2 kinases. Mol Cell Biol. 1988;8(2):993-5.
64. de Gruijl TD, van de Ven R. Chapter six--Adenovirus-based immunotherapy of cancer: promises to keep. Adv Cancer Res. 2012;115:147-220.
65. Wennier S, Li S, McFadden G. Oncolytic virotherapy for pancreatic cancer. Expert Rev Mol Med. 2011;13:e18.
66. Heise C, Hermiston T, Johnson L, Brooks G, Sampson-Johannes A, Williams A, et al. An adenovirus E1A mutant that demonstrates potent and selective systemic anti-tumoral efficacy. Nat Med. 2000;6(10):1134-9.
67. Fueyo J, Gomez-Manzano C, Alemany R, Lee PS, McDonnell TJ, Mitlianga P, et al. A mutant oncolytic adenovirus targeting the Rb pathway produces anti-glioma effect in vivo. Oncogene. 2000;19(1):2-12.

68. Worgall S, Wolff G, Falck-Pedersen E, Crystal RG. Innate immune mechanisms dominate elimination of adenoviral vectors following in vivo administration. Hum Gene Ther. 1997;8(1):37-44.
69. DeWeese TL, van der Poel H, Li S, Mikhak B, Drew R, Goemann M, et al. A phase I trial of CV706, a replication-competent, PSA selective oncolytic adenovirus, for the treatment of locally recurrent prostate cancer following radiation therapy. Cancer Res. 2001;61(20):7464-72.
70. Garcia-Carbonero R, Salazar R, Duran I, Osman-Garcia I, Paz-Ares L, Bozada JM, et al. Phase 1 study of intravenous administration of the chimeric adenovirus enadenotucirev in patients undergoing primary tumor resection. J Immunother Cancer. 2017;5(1):71.
71. Thaci B, Ulasov IV, Wainwright DA, Lesniak MS. The challenge for gene therapy: innate immune response to adenoviruses. Oncotarget. 2011;2(3):113-21.
72. Liu Q, Muruve DA. Molecular basis of the inflammatory response to adenovirus vectors. Gene Ther. 2003;10(11):935-40.
73. Muruve DA, Barnes MJ, Stillman IE, Libermann TA. Adenoviral gene therapy leads to rapid induction of multiple chemokines and acute neutrophil-dependent hepatic injury in vivo. Hum Gene Ther. 1999;10(6):965-76.
74. Munhoz RR, Postow MA. Recent advances in understanding antitumor immunity. F1000Res. 2016;5:2545.
75. Woller N, Gurlevik E, Fleischmann-Mundt B, Schumacher A, Knocke S, Kloos AM, et al. Viral Infection of Tumors Overcomes Resistance to PD-1-immunotherapy by Broadening Neoantigenome-directed T-cell Responses. Mol Ther. 2015;23(10):1630-40.
76. Bell J, McFadden G. Viruses for tumor therapy. Cell Host Microbe. 2014;15(3):260-5.
77. Ahi YS, Bangari DS, Mittal SK. Adenoviral vector immunity: its implications and circumvention strategies. Curr Gene Ther. 2011;11(4):307-20.
78. Lowenstein PR, Castro MG. Inflammation and adaptive immune responses to adenoviral vectors injected into the brain: peculiarities, mechanisms, and consequences. Gene Ther. 2003;10(11):946-54.
79. Kreppel F, Kochanek S. Modification of adenovirus gene transfer vectors with synthetic polymers: a scientific review and technical guide. Mol Ther. 2008;16(1):16-29.
80. Chillon M, Lee JH, Fasbender A, Welsh MJ. Adenovirus complexed with polyethylene glycol and cationic lipid is shielded from neutralizing antibodies in vitro. Gene Ther. 1998;5(7):995-1002.
81. Beer SJ, Matthews CB, Stein CS, Ross BD, Hilfinger JM, Davidson BL. Poly (lactic-glycolic) acid copolymer encapsulation of recombinant adenovirus reduces immunogenicity in vivo. Gene Ther. 1998;5(6):740-6.
82. Seregin SS, Appledorn DM, McBride AJ, Schuldt NJ, Aldhamen YA, Voss T, et al. Transient pretreatment with glucocorticoid ablates innate toxicity of systemically delivered adenoviral vectors without reducing efficacy. Mol Ther. 2009;17(4):685-96.
83. Thomas MA, Spencer JF, Toth K, Sagartz JE, Phillips NJ, Wold WS. Immunosuppression enhances oncolytic adenovirus replication and antitumor efficacy in the Syrian hamster model. Mol Ther. 2008;16(10):1665-73.

84. Smith TA, White BD, Gardner JM, Kaleko M, McClelland A. Transient immunosuppression permits successful repetitive intravenous administration of an adenovirus vector. Gene Ther. 1996;3(6):496-502.
85. Kaplan JM, Smith AE. Transient immunosuppression with deoxyspergualin improves longevity of transgene expression and ability to readminister adenoviral vector to the mouse lung. Hum Gene Ther. 1997;8(9):1095-104.
86. Ilan Y, Jona VK, Sengupta K, Davidson A, Horwitz MS, Roy-Chowdhury N, et al. Transient immunosuppression with FK506 permits long-term expression of therapeutic genes introduced into the liver using recombinant adenoviruses in the rat. Hepatology. 1997;26(4):949-56.
87. Thomas MA, Spencer JF, La Regina MC, Dhar D, Tollefson AE, Toth K, et al. Syrian hamster as a permissive immunocompetent animal model for the study of oncolytic adenovirus vectors. Cancer Res. 2006;66(3):1270-6.
88. Blair GE, Dixon SC, Griffiths SA, Zajdel ME. Restricted replication of human adenovirus type 5 in mouse cell lines. Virus Res. 1989;14(4):339-46.
89. Jogler C, Hoffmann D, Theegarten D, Grunwald T, Uberla K, Wildner O. Replication properties of human adenovirus in vivo and in cultures of primary cells from different animal species. J Virol. 2006;80(7):3549-58.
90. Cerullo V, Koski A, Vaha-Koskela M, Hemminki A. Chapter eight--Oncolytic adenoviruses for cancer immunotherapy: data from mice, hamsters, and humans. Adv Cancer Res. 2012;115:265-318.
91. Hjorth RN, Bonde GM, Pierzchala WA, Vernon SK, Wiener FP, Levner MH, et al. A new hamster model for adenoviral vaccination. Arch Virol. 1988;100(3-4):279-83.
92. Reimann J, Miller RG. Polymorphism and MHC gene function. Dev Comp Immunol. 1983;7(3):403-12.
93. Siurala M, Vaha-Koskela M, Havunen R, Tahtinen S, Bramante S, Parviainen S, et al. Syngeneic syrian hamster tumors feature tumor-infiltrating lymphocytes allowing adoptive cell therapy enhanced by oncolytic adenovirus in a replication permissive setting. Oncoimmunology. 2016;5(5):e1136046.
94. LaRocca CJ, Han J, Gavrikova T, Armstrong L, Oliveira AR, Shanley R, et al. Oncolytic adenovirus expressing interferon alpha in a syngeneic Syrian hamster model for the treatment of pancreatic cancer. Surgery. 2015;157(5):888-98.
95. Siegel RL, Miller KD, Jemal A. Cancer Statistics, 2017. CA Cancer J Clin. 2017;67(1):7-30.
96. society Ac. Pancreatic Cancer 2017 [Available from: https://www.cancer.org/cancer/pancreatic-cancer.html.
97. Krejs GJ. Pancreatic cancer: epidemiology and risk factors. Dig Dis. 2010;28(2):355-8.
98. Uson Junior PLS, Callegaro-Filho D, Bugano DDG, Moura F, Maluf FC. Predictive Value of Serum Carbohydrate Antigen 19-9 (CA19-9) for Early Mortality in Advanced Pancreatic Cancer. J Gastrointest Cancer. 2017.
99. Network PCA. Pancreatic cancer exocrine tumors 2017 [Available from: https://www.pancan.org/facing-pancreatic-cancer/learn/types-of-pancreatic-cancer/exocrine/.

100. Bilimoria KY, Bentrem DJ, Ko CY, Ritchey J, Stewart AK, Winchester DP, et al. Validation of the 6th edition AJCC Pancreatic Cancer Staging System: report from the National Cancer Database. Cancer. 2007;110(4):738-44.
101. Oncology C. Comparative Oncology. Chapter 18, CANCER DIAGNOSIS: Bucharest: The Publishing House of the Romanian Academy; 2007.
102. research Hffpc. Pancreatic cancer prognosis 2017 [Available from: http://pancreatic.org/pancreatic-cancer/about-the-pancreas/prognosis/.
103. Andea A, Sarkar F, Adsay VN. Clinicopathological correlates of pancreatic intraepithelial neoplasia: a comparative analysis of 82 cases with and 152 cases without pancreatic ductal adenocarcinoma. Mod Pathol. 2003;16(10):996-1006.
104. Brune K, Abe T, Canto M, O'Malley L, Klein AP, Maitra A, et al. Multifocal neoplastic precursor lesions associated with lobular atrophy of the pancreas in patients having a strong family history of pancreatic cancer. Am J Surg Pathol. 2006;30(9):1067-76.
105. Distler M, Aust D, Weitz J, Pilarsky C, Grutzmann R. Precursor lesions for sporadic pancreatic cancer: PanIN, IPMN, and MCN. Biomed Res Int. 2014;2014:474905.
106. Eser S, Schnieke A, Schneider G, Saur D. Oncogenic KRAS signalling in pancreatic cancer. Br J Cancer. 2014;111(5):817-22.
107. Smit VT, Boot AJ, Smits AM, Fleuren GJ, Cornelisse CJ, Bos JL. KRAS codon 12 mutations occur very frequently in pancreatic adenocarcinomas. Nucleic Acids Res. 1988;16(16):7773-82.
108. Hruban RH, van Mansfeld AD, Offerhaus GJ, van Weering DH, Allison DC, Goodman SN, et al. K-ras oncogene activation in adenocarcinoma of the human pancreas. A study of 82 carcinomas using a combination of mutant-enriched polymerase chain reaction analysis and allele-specific oligonucleotide hybridization. Am J Pathol. 1993;143(2):545-54.
109. Almoguera C, Shibata D, Forrester K, Martin J, Arnheim N, Perucho M. Most human carcinomas of the exocrine pancreas contain mutant c-K-ras genes. Cell. 1988;53(4):549-54.
110. Cicenas J, Kvederaviciute K, Meskinyte I, Meskinyte-Kausiliene E, Skeberdyte A, Cicenas J. KRAS, TP53, CDKN2A, SMAD4, BRCA1, and BRCA2 Mutations in Pancreatic Cancer. Cancers (Basel). 2017;9(5).
111. Caldas C, Hahn SA, da Costa LT, Redston MS, Schutte M, Seymour AB, et al. Frequent somatic mutations and homozygous deletions of the p16 (MTS1) gene in pancreatic adenocarcinoma. Nat Genet. 1994;8(1):27-32.
112. Redston MS, Caldas C, Seymour AB, Hruban RH, da Costa L, Yeo CJ, et al. p53 mutations in pancreatic carcinoma and evidence of common involvement of homocopolymer tracts in DNA microdeletions. Cancer Res. 1994;54(11):3025-33.
113. Maurice D, Pierreux CE, Howell M, Wilentz RE, Owen MJ, Hill CS. Loss of Smad4 function in pancreatic tumors: C-terminal truncation leads to decreased stability. J Biol Chem. 2001;276(46):43175-81.
114. Carnevale J, Ashworth A. Assessing the Significance of BRCA1 and BRCA2 Mutations in Pancreatic Cancer. J Clin Oncol. 2015;33(28):3080-1.
115. Schoggins JW. Interferon-stimulated genes: roles in viral pathogenesis. Curr Opin Virol. 2014;6:40-6.

116. Barber GN. VSV-tumor selective replication and protein translation. Oncogene. 2005;24(52):7710-9.
117. Moerdyk-Schauwecker M, Shah NR, Murphy AM, Hastie E, Mukherjee P, Grdzelishvili VZ. Resistance of pancreatic cancer cells to oncolytic vesicular stomatitis virus: role of type I interferon signaling. Virology. 2013;436(1):221-34.
118. Hastie E, Cataldi M, Moerdyk-Schauwecker MJ, Felt SA, Steuerwald N, Grdzelishvili VZ. Novel biomarkers of resistance of pancreatic cancer cells to oncolytic vesicular stomatitis virus. Oncotarget. 2016;7(38):61601-18.
119. Ohashi M, Yoshida K, Kushida M, Miura Y, Ohnami S, Ikarashi Y, et al. Adenovirus-mediated interferon alpha gene transfer induces regional direct cytotoxicity and possible systemic immunity against pancreatic cancer. Br J Cancer. 2005;93(4):441-9.
120. Yamamoto Y, Nagasato M, Rin Y, Henmi M, Ino Y, Yachida S, et al. Strong antitumor efficacy of a pancreatic tumor-targeting oncolytic adenovirus for neuroendocrine tumors. Cancer Med. 2017;6(10):2385-97.
121. Sparer TE, Tripp RA, Dillehay DL, Hermiston TW, Wold WS, Gooding LR. The role of human adenovirus early region 3 proteins (gp19K, 10.4K, 14.5K, and 14.7K) in a murine pneumonia model. J Virol. 1996;70(4):2431-9.
122. Sester M, Ruszics Z, Mackley E, Burgert HG. The transmembrane domain of the adenovirus E3/19K protein acts as an endoplasmic reticulum retention signal and contributes to intracellular sequestration of major histocompatibility complex class I molecules. J Virol. 2013;87(11):6104-17.
123. Jonjic S, Babic M, Polic B, Krmpotic A. Immune evasion of natural killer cells by viruses. Curr Opin Immunol. 2008;20(1):30-8.
124. Bischoff JR, Kirn DH, Williams A, Heise C, Horn S, Muna M, et al. An adenovirus mutant that replicates selectively in p53-deficient human tumor cells. Science. 1996;274(5286):373-6.
125. Heise C, Sampson-Johannes A, Williams A, McCormick F, Von Hoff DD, Kirn DH. ONYX-015, an E1B gene-attenuated adenovirus, causes tumor-specific cytolysis and antitumoral efficacy that can be augmented by standard chemotherapeutic agents. Nat Med. 1997;3(6):639-45.
126. Mulvihill S, Warren R, Venook A, Adler A, Randlev B, Heise C, et al. Safety and feasibility of injection with an E1B-55 kDa gene-deleted, replication-selective adenovirus (ONYX-015) into primary carcinomas of the pancreas: a phase I trial. Gene Ther. 2001;8(4):308-15.
127. Berlin J, Benson AB, 3rd. Chemotherapy: Gemcitabine remains the standard of care for pancreatic cancer. Nat Rev Clin Oncol. 2010;7(3):135-7.
128. Neoptolemos JP, Palmer DH, Ghaneh P, Psarelli EE, Valle JW, Halloran CM, et al. Comparison of adjuvant gemcitabine and capecitabine with gemcitabine monotherapy in patients with resected pancreatic cancer (ESPAC-4): a multicentre, open-label, randomised, phase 3 trial. Lancet. 2017;389(10073):1011-24.
129. Marsh Rde W, Talamonti MS, Katz MH, Herman JM. Pancreatic cancer and FOLFIRINOX: a new era and new questions. Cancer medicine. 2015;4(6):853-63.

130. Conroy T, Desseigne F, Ychou M, Bouche O, Guimbaud R, Becouarn Y, et al. FOLFIRINOX versus gemcitabine for metastatic pancreatic cancer. N Engl J Med. 2011;364(19):1817-25.
131. Thota R, Pauff JM, Berlin JD. Treatment of metastatic pancreatic adenocarcinoma: a review. Oncology (Williston Park). 2014;28(1):70-4.
132. Yamamoto T, Yagi S, Kinoshita H, Sakamoto Y, Okada K, Uryuhara K, et al. Long-term survival after resection of pancreatic cancer: a single-center retrospective analysis. World journal of gastroenterology : WJG. 2015;21(1):262-8.
133. Bilici A. Prognostic factors related with survival in patients with pancreatic adenocarcinoma. World J Gastroenterol. 2014;20(31):10802-12.
134. Picozzi VJ, Abrams RA, Decker PA, Traverso W, O'Reilly EM, Greeno E, et al. Multicenter phase II trial of adjuvant therapy for resected pancreatic cancer using cisplatin, 5-fluorouracil, and interferon-alfa-2b-based chemoradiation: ACOSOG Trial Z05031. Ann Oncol. 2011;22(2):348-54.
135. Nukui Y, Picozzi VJ, Traverso LW. Interferon-based adjuvant chemoradiation therapy improves survival after pancreaticoduodenectomy for pancreatic adenocarcinoma. Am J Surg. 2000;179(5):367-71.
136. Linehan DC, Tan MC, Strasberg SM, Drebin JA, Hawkins WG, Picus J, et al. Adjuvant interferon-based chemoradiation followed by gemcitabine for resected pancreatic adenocarcinoma: a single-institution phase II study. Ann Surg. 2008;248(2):145-51.
137. Knaebel HP, Marten A, Schmidt J, Hoffmann K, Seiler C, Lindel K, et al. Phase III trial of postoperative cisplatin, interferon alpha-2b, and 5-FU combined with external radiation treatment versus 5-FU alone for patients with resected pancreatic adenocarcinoma -- CapRI: study protocol [ISRCTN62866759]. BMC Cancer. 2005;5:37.
138. Picozzi VJ, Kozarek RA, Traverso LW. Interferon-based adjuvant chemoradiation therapy after pancreaticoduodenectomy for pancreatic adenocarcinoma. Am J Surg. 2003;185(5):476-80.
139. Tagliaferri P, Caraglia M, Budillon A, Marra M, Vitale G, Viscomi C, et al. New pharmacokinetic and pharmacodynamic tools for interferon-alpha (IFN-alpha) treatment of human cancer. Cancer Immunol Immunother. 2005;54(1):1-10.
140. Wills RJ. Clinical pharmacokinetics of interferons. Clinical pharmacokinetics. 1990;19(5):390-9.
141. Glue P, Fang JW, Rouzier-Panis R, Raffanel C, Sabo R, Gupta SK, et al. Pegylated interferon-alpha2b: pharmacokinetics, pharmacodynamics, safety, and preliminary efficacy data. Hepatitis C Intervention Therapy Group. Clinical pharmacology and therapeutics. 2000;68(5):556-67.
142. Holsti LR, Mattson K, Niiranen A, Standertskiold-Nordenstam CG, Stenman S, Sovijarvi A, et al. Enhancement of radiation effects by alpha interferon in the treatment of small cell carcinoma of the lung. Int J Radiat Oncol Biol Phys. 1987;13(8):1161-6.
143. Parmar S, Platanias LC. Interferons: mechanisms of action and clinical applications. Curr Opin Oncol. 2003;15(6):431-9.
144. Schmidt J, Jager D, Hoffmann K, Buchler MW, Marten A. Impact of interferon-alpha in combined chemoradioimmunotherapy for pancreatic adenocarcinoma (CapRI): first data from the immunomonitoring. Journal of immunotherapy. 2007;30(1):108-15.

145. Rocha FG, Hashimoto Y, Traverso LW, Dorer R, Kozarek R, Helton WS, et al. Interferon-based Adjuvant Chemoradiation for Resected Pancreatic Head Cancer: Long-term Follow-up of the Virginia Mason Protocol. Ann Surg. 2016;263(2):376-84.
146. Baskar R, Dai J, Wenlong N, Yeo R, Yeoh KW. Biological response of cancer cells to radiation treatment. Front Mol Biosci. 2014;1:24.
147. Eric J. Hall AJG. Radiobiology for the Radiologist. 7th ed. Lippincott Williams & Wilkins2006.
148. Hall EJ. Cancer caused by x-rays--a random event? Lancet Oncol. 2007;8(5):369-70.
149. Picozzi VJ, Pisters PW, Vickers SM, Strasberg SM. Strength of the evidence: adjuvant therapy for resected pancreatic cancer. Journal of gastrointestinal surgery : official journal of the Society for Surgery of the Alimentary Tract. 2008;12(4):657-61.
150. The 5 R's Of Fractionation 2017 [Available from: http://ozradonc.wikidot.com/the-5-r-s-of-fractionation.
151. HERON PJF. 5-Fluorouracil 2017 [updated 17 June 2009. Available from: http://www.oncoprof.net/Generale2000/g09_Chimiotherapie/Complements/g09-gb_comp11.html.
152. Longley DB, Harkin DP, Johnston PG. 5-fluorouracil: mechanisms of action and clinical strategies. Nat Rev Cancer. 2003;3(5):330-8.
153. Ghoshal K, Jacob ST. Specific inhibition of pre-ribosomal RNA processing in extracts from the lymphosarcoma cells treated with 5-fluorouracil. Cancer Res. 1994;54(3):632-6.
154. Santi DV, Hardy LW. Catalytic mechanism and inhibition of tRNA (uracil-5-)methyltransferase: evidence for covalent catalysis. Biochemistry. 1987;26(26):8599-606.
155. Patton JR. Ribonucleoprotein particle assembly and modification of U2 small nuclear RNA containing 5-fluorouridine. Biochemistry. 1993;32(34):8939-44.
156. Samuelsson T. Interactions of transfer RNA pseudouridine synthases with RNAs substituted with fluorouracil. Nucleic Acids Res. 1991;19(22):6139-44.
157. Carrico CK, Glazer RI. Effect of 5-fluorouracil on the synthesis and translation of polyadenylic acid-containing RNA from regenerating rat liver. Cancer Res. 1979;39(9):3694-701.
158. Alfred Gilman Sr. LSG. Pharmacological Basis of Therapeutics. Alfred Gilman Sr. LSG, editor.
159. Siddik ZH. Cisplatin: mode of cytotoxic action and molecular basis of resistance. Oncogene. 2003;22(47):7265-79.
160. Kelland LR, Sharp SY, O'Neill CF, Raynaud FI, Beale PJ, Judson IR. Mini-review: discovery and development of platinum complexes designed to circumvent cisplatin resistance. J Inorg Biochem. 1999;77(1-2):111-5.
161. Kelland LR. Preclinical perspectives on platinum resistance. Drugs. 2000;59 Suppl 4:1-8; discussion 37-8.
162. Pinto AL, Lippard SJ. Binding of the antitumor drug cis-diamminedichloroplatinum(II) (cisplatin) to DNA. Biochim Biophys Acta. 1985;780(3):167-80.
163. Roberts JJ, Friedlos F. Quantitative estimation of cisplatin-induced DNA interstrand cross-links and their repair in mammalian cells: relationship to toxicity. Pharmacol Ther. 1987;34(2):215-46.

164. Momparler RL. Optimization of cytarabine (ARA-C) therapy for acute myeloid leukemia. Exp Hematol Oncol. 2013;2:20.
165. Mini E, Nobili S, Caciagli B, Landini I, Mazzei T. Cellular pharmacology of gemcitabine. Ann Oncol. 2006;17 Suppl 5:v7-12.
166. Gandhi V, Plunkett W. Modulatory activity of 2',2'-difluorodeoxycytidine on the phosphorylation and cytotoxicity of arabinosyl nucleosides. Cancer Res. 1990;50(12):3675-80.
167. Huang P, Chubb S, Hertel LW, Grindey GB, Plunkett W. Action of 2',2'-difluorodeoxycytidine on DNA synthesis. Cancer Res. 1991;51(22):6110-7.
168. Heinemann V, Xu YZ, Chubb S, Sen A, Hertel LW, Grindey GB, et al. Cellular elimination of 2',2'-difluorodeoxycytidine 5'-triphosphate: a mechanism of self-potentiation. Cancer Res. 1992;52(3):533-9.
169. Heinemann V, Xu YZ, Chubb S, Sen A, Hertel LW, Grindey GB, et al. Inhibition of ribonucleotide reduction in CCRF-CEM cells by 2',2'-difluorodeoxycytidine. Mol Pharmacol. 1990;38(4):567-72.
170. Baker CH, Banzon J, Bollinger JM, Stubbe J, Samano V, Robins MJ, et al. 2'-Deoxy-2'-methylenecytidine and 2'-deoxy-2',2'-difluorocytidine 5'-diphosphates: potent mechanism-based inhibitors of ribonucleotide reductase. J Med Chem. 1991;34(6):1879-84.
171. Heinemann V, Schulz L, Issels RD, Plunkett W. Gemcitabine: a modulator of intracellular nucleotide and deoxynucleotide metabolism. Semin Oncol. 1995;22(4 Suppl 11):11-8.
172. Ruiz van Haperen VW, Veerman G, Boven E, Noordhuis P, Vermorken JB, Peters GJ. Schedule dependence of sensitivity to 2',2'-difluorodeoxycytidine (Gemcitabine) in relation to accumulation and retention of its triphosphate in solid tumour cell lines and solid tumours. Biochem Pharmacol. 1994;48(7):1327-39.
173. Pourquier P, Gioffre C, Kohlhagen G, Urasaki Y, Goldwasser F, Hertel LW, et al. Gemcitabine (2',2'-difluoro-2'-deoxycytidine), an antimetabolite that poisons topoisomerase I. Clin Cancer Res. 2002;8(8):2499-504.
174. Jiang PH, Motoo Y, Sawabu N, Minamoto T. Effect of gemcitabine on the expression of apoptosis-related genes in human pancreatic cancer cells. World J Gastroenterol. 2006;12(10):1597-602.
175. Hill R, Rabb M, Madureira PA, Clements D, Gujar SA, Waisman DM, et al. Gemcitabine-mediated tumour regression and p53-dependent gene expression: implications for colon and pancreatic cancer therapy. Cell Death Dis. 2013;4:e791.
176. Federico C, Morittu VM, Britti D, Trapasso E, Cosco D. Gemcitabine-loaded liposomes: rationale, potentialities and future perspectives. Int J Nanomedicine. 2012;7:5423-36.
177. Houghton JA, Cheshire PJ, Morton CL, Stewart CF. Potentiation of 5-fluorouracil-leucovorin activity by alpha2a-interferon in colon adenocarcinoma xenografts. Clin Cancer Res. 1995;1(1):33-40.
178. Iacopino F, Ferrandina G, Scambia G, Benedetti-Panici P, Mancuso S, Sica G. Interferons inhibit EGF-stimulated cell growth and reduce EGF binding in human breast cancer cells. Anticancer Res. 1996;16(4A):1919-24.

179. Pfeffer LM, Dinarello CA, Herberman RB, Williams BR, Borden EC, Bordens R, et al. Biological properties of recombinant alpha-interferons: 40th anniversary of the discovery of interferons. Cancer Res. 1998;58(12):2489-99.
180. Decatris M, Santhanam S, O'Byrne K. Potential of interferon-alpha in solid tumours: part 1. BioDrugs. 2002;16(4):261-81.
181. Santhanam S, Decatris M, O'Byrne K. Potential of interferon-alpha in solid tumours: part 2. BioDrugs. 2002;16(5):349-72.
182. Wang L, Wu WZ, Sun HC, Wu XF, Qin LX, Liu YK, et al. Mechanism of interferon alpha on inhibition of metastasis and angiogenesis of hepatocellular carcinoma after curative resection in nude mice. J Gastrointest Surg. 2003;7(5):587-94.
183. Ma JH, Patrut E, Schmidt J, Knaebel HP, Buchler MW, Marten A. Synergistic effects of interferon-alpha in combination with chemoradiation on human pancreatic adenocarcinoma. World J Gastroenterol. 2005;11(10):1521-8.
184. Ruszczak Z, Schwartz RA. Interferons in dermatology: biology, pharmacology, and clinical applications. Adv Dermatol. 1997;13:235-88.
185. Houghton JA, Morton CL, Adkins DA, Rahman A. Locus of the interaction among 5-fluorouracil, leucovorin, and interferon-alpha 2a in colon carcinoma cells. Cancer Res. 1993;53(18):4243-50.
186. Murphy BR, Rynard SM, Einhorn LH, Loehrer PJ. A phase II trial of interferon alpha-2A plus fluorouracil in advanced renal cell carcinoma. A Hoosier Oncology Group study. Invest New Drugs. 1992;10(3):225-30.
187. Lee KH, Lee JS, Suh C, Lee YS, Min YI, Ahn SH, et al. Combination of 5-fluorouracil and recombinant interferon alpha-2B in advanced gastric cancer. A phase I study. Am J Clin Oncol. 1992;15(2):141-5.
188. Paquette RL, Hsu NC, Kiertscher SM, Park AN, Tran L, Roth MD, et al. Interferon-alpha and granulocyte-macrophage colony-stimulating factor differentiate peripheral blood monocytes into potent antigen-presenting cells. J Leukoc Biol. 1998;64(3):358-67.
189. Matikainen S, Sareneva T, Ronni T, Lehtonen A, Koskinen PJ, Julkunen I. Interferon-alpha activates multiple STAT proteins and upregulates proliferation-associated IL-2Ralpha, c-myc, and pim-1 genes in human T cells. Blood. 1999;93(6):1980-91.
190. Marrack P, Kappler J, Mitchell T. Type I interferons keep activated T cells alive. J Exp Med. 1999;189(3):521-30.
191. Kanai R, Wakimoto H, Cheema T, Rabkin SD. Oncolytic herpes simplex virus vectors and chemotherapy: are combinatorial strategies more effective for cancer? Future Oncol. 2010;6(4):619-34.
192. Ghosh A, Nayak R, Shaila MS. Inhibition of replication of rinderpest virus by 5-fluorouracil. Antiviral Res. 1996;31(1-2):35-44.
193. Toyoizumi T, Mick R, Abbas AE, Kang EH, Kaiser LR, Molnar-Kimber KL. Combined therapy with chemotherapeutic agents and herpes simplex virus type 1 ICP34.5 mutant (HSV-1716) in human non-small cell lung cancer. Hum Gene Ther. 1999;10(18):3013-29.
194. Heise C1 S-JA, Williams A, McCormick F, Von Hoff DD, Kirn DH. ONYX-015, an E1B gene-attenuated adenovirus, causes tumor-specific cytolysis and antitumoral efficacy that can be augmented by standard chemotherapeutic agents. Nat Med 1997 Jun;3(6):639-45. 1997.

195. Khuri FR, Nemunaitis J, Ganly I, Arseneau J, Tannock IF, Romel L, et al. a controlled trial of intratumoral ONYX-015, a selectively-replicating adenovirus, in combination with cisplatin and 5-fluorouracil in patients with recurrent head and neck cancer. Nat Med. 2000;6(8):879-85.
196. Reid T, Galanis E, Abbruzzese J, Sze D, Andrews J, Romel L, et al. Intra-arterial administration of a replication-selective adenovirus (dl1520) in patients with colorectal carcinoma metastatic to the liver: a phase I trial. Gene Ther. 2001;8(21):1618-26.
197. Galanis E, Okuno SH, Nascimento AG, Lewis BD, Lee RA, Oliveira AM, et al. Phase I-II trial of ONYX-015 in combination with MAP chemotherapy in patients with advanced sarcomas. Gene Ther. 2005;12(5):437-45.
198. Nemunaitis J, Cunningham C, Tong A, Post L, Netto G, Paulson AS, et al. Pilot trial of intravenous infusion of a replication-selective adenovirus (ONYX-015) in combination with chemotherapy or IL-2 treatment in refractory cancer patients. Cancer Gene Ther. 2003;10(5):341-52.
199. D K. Clinical research results with dl1520 (Onyx-015), a replication-selective adenovirus for the treatment of cancer: what have we learned? Gene Ther 2001;8:89–98. 2001.
200. Jordan Sell AO, Eric Jensen, Edward Greeno, Masato Yamamoto, Julia Davydova. Evaluating the Efficacy of Combination Cancer Treatment: Oncolytic Adenovirus and 5FU Chemotherapy. 2016;Volume 24, Supplement 1, pS167, May 2016.
201. S L. Die Mischiarnei. Klin Wochenschr. 1927;6: 1077-1085.
202. Tallarida RJ. An overview of drug combination analysis with isobolograms. J Pharmacol Exp Ther. 2006;319(1):1-7.
203. Tallarida RJ. Quantitative methods for assessing drug synergism. Genes Cancer. 2011;2(11):1003-8.
204. Tallarida RJ. Drug Combinations: Tests and Analysis with Isoboles. Curr Protoc Pharmacol. 2016;72:9 19 1-.
205. Chou TC. Theoretical basis, experimental design, and computerized simulation of synergism and antagonism in drug combination studies. Pharmacol Rev. 2006;58(3):621-81.
206. Chou TC, Talaly P. A simple generalized equation for the analysis of multiple inhibitions of Michaelis-Menten kinetic systems. J Biol Chem. 1977;252(18):6438-42.
207. Chou TC. On the determination of availability of ligand binding sites in steady-state systems. J Theor Biol. 1977;65(2):345-56.
208. TC C. Comparison of the mass-action law with the power law, the probit

law and the logit law in dose-effect analysis. Pharmacologist. 1977;19:165.
209. TC C. The median-effect principle and the combination index for quantitation

of synergism and antagonism, in Synergism and Antagonism in Chemotherapy. Academic Press, San Diego. 1991(pp 61–102).
210. Wasim L, Chopra M. Panobinostat induces apoptosis via production of reactive oxygen species and synergizes with topoisomerase inhibitors in cervical cancer cells. Biomed Pharmacother. 2016;84:1393-405.

211. Chou TC, Talalay P. Quantitative analysis of dose-effect relationships: the combined effects of multiple drugs or enzyme inhibitors. Adv Enzyme Regul. 1984;22:27-55.
212. Chou TC, Motzer RJ, Tong Y, Bosl GJ. Computerized quantitation of synergism and antagonism of taxol, topotecan, and cisplatin against human teratocarcinoma cell growth: a rational approach to clinical protocol design. J Natl Cancer Inst. 1994;86(20):1517-24.
213. Franken NA, Rodermond HM, Stap J, Haveman J, van Bree C. Clonogenic assay of cells in vitro. Nat Protoc. 2006;1(5):2315-9.
214. Hall E. **Radiobiology for the radiologist**1973.
215. Tsvetkova EV, Asmis TR. Role of neoadjuvant therapy in the management of pancreatic cancer: is the era of biomarker-directed therapy here? Curr Oncol. 2014;21(4):e650-7.
216. Goldstein D, El-Maraghi RH, Hammel P, Heinemann V, Kunzmann V, Sastre J, et al. nab-Paclitaxel plus gemcitabine for metastatic pancreatic cancer: long-term survival from a phase III trial. J Natl Cancer Inst. 2015;107(2).
217. Andtbacka RH, Kaufman HL, Collichio F, Amatruda T, Senzer N, Chesney J, et al. Talimogene Laherparepvec Improves Durable Response Rate in Patients With Advanced Melanoma. J Clin Oncol. 2015;33(25):2780-8.
218. Matthew O.Olda. Trisha Wise-Draper CLW, Balveen Kaur, TheodorosTeknosa. The current status of oncolytic viral therapy for head and neck cancer. World Journal of Otorhinolaryngology-Head and Neck Surgery. 2016(2):84-9.
219. Davydova J, Yamamoto M. Oncolytic adenoviruses: design, generation, and experimental procedures. Curr Protoc Hum Genet. 2013;Chapter 12:Unit 12 4.
220. Davydova J, Le LP, Gavrikova T, Wang M, Krasnykh V, Yamamoto M. Infectivity-enhanced cyclooxygenase-2-based conditionally replicative adenoviruses for esophageal adenocarcinoma treatment. Cancer Res. 2004;64(12):4319-27.
221. Leitner S, Sweeney K, Oberg D, Davies D, Miranda E, Lemoine NR, et al. Oncolytic adenoviral mutants with E1B19K gene deletions enhance gemcitabine-induced apoptosis in pancreatic carcinoma cells and anti-tumor efficacy in vivo. Clin Cancer Res. 2009;15(5):1730-40.
222. Bhattacharyya M, Francis J, Eddouadi A, Lemoine NR, Hallden G. An oncolytic adenovirus defective in pRb-binding (dl922-947) can efficiently eliminate pancreatic cancer cells and tumors in vivo in combination with 5-FU or gemcitabine. Cancer Gene Ther. 2011;18(10):734-43.
223. Cherubini G, Kallin C, Mozetic A, Hammaren-Busch K, Muller H, Lemoine NR, et al. The oncolytic adenovirus AdDeltaDelta enhances selective cancer cell killing in combination with DNA-damaging drugs in pancreatic cancer models. Gene Ther. 2011;18(12):1157-65.
224. Hart LS, Yannone SM, Naczki C, Orlando JS, Waters SB, Akman SA, et al. The adenovirus E4orf6 protein inhibits DNA double strand break repair and radiosensitizes human tumor cells in an E1B-55K-independent manner. J Biol Chem. 2005;280(2):1474-81.
225. Khanna KK, Jackson SP. DNA double-strand breaks: signaling, repair and the cancer connection. Nat Genet. 2001;27(3):247-54.

226. Boyer J, Rohleder K, Ketner G. Adenovirus E4 34k and E4 11k inhibit double strand break repair and are physically associated with the cellular DNA-dependent protein kinase. Virology. 1999;263(2):307-12.
227. Williams BR. PKR; a sentinel kinase for cellular stress. Oncogene. 1999;18(45):6112-20.
228. Kalbasi A, June CH, Haas N, Vapiwala N. Radiation and immunotherapy: a synergistic combination. J Clin Invest. 2013;123(7):2756-63.
229. Golden EB, Apetoh L. Radiotherapy and immunogenic cell death. Semin Radiat Oncol. 2015;25(1):11-7.
230. Hill R, Li Y, Tran LM, Dry S, Calvopina JH, Garcia A, et al. Cell intrinsic role of COX-2 in pancreatic cancer development. Mol Cancer Ther. 2012;11(10):2127-37.
231. Cascinu S, Scartozzi M, Carbonari G, Pierantoni C, Verdecchia L, Mariani C, et al. COX-2 and NF-KB overexpression is common in pancreatic cancer but does not predict for COX-2 inhibitors activity in combination with gemcitabine and oxaliplatin. Am J Clin Oncol. 2007;30(5):526-30.
232. Bramson JL, Hitt M, Addison CL, Muller WJ, Gauldie J, Graham FL. Direct intratumoral injection of an adenovirus expressing interleukin-12 induces regression and long-lasting immunity that is associated with highly localized expression of interleukin-12. Hum Gene Ther. 1996;7(16):1995-2002.
233. Seetharam S, Staba MJ, Schumm LP, Schreiber K, Schreiber H, Kufe DW, et al. Enhanced eradication of local and distant tumors by genetically produced interleukin-12 and radiation. Int J Oncol. 1999;15(4):769-73.
234. Lohr F, Hu K, Haroon Z, Samulski TV, Huang Q, Beaty J, et al. Combination treatment of murine tumors by adenovirus-mediated local B7/IL12 immunotherapy and radiotherapy. Mol Ther. 2000;2(3):195-203.
235. Ono HA, Le LP, Davydova JG, Gavrikova T, Yamamoto M. Noninvasive visualization of adenovirus replication with a fluorescent reporter in the E3 region. Cancer Res. 2005;65(22):10154-8.
236. Yamamoto M, Alemany R, Adachi Y, Grizzle WE, Curiel DT. Characterization of the cyclooxygenase-2 promoter in an adenoviral vector and its application for the mitigation of toxicity in suicide gene therapy of gastrointestinal cancers. Mol Ther. 2001;3(3):385-94.
237. Davydova J, Gavrikova T, Brown EJ, Luo X, Curiel DT, Vickers SM, et al. In vivo bioimaging tracks conditionally replicative adenoviral replication and provides an early indication of viral antitumor efficacy. Cancer Sci. 2010;101(2):474-81.
238. Azzi S, Hebda JK, Gavard J. Vascular permeability and drug delivery in cancers. Front Oncol. 2013;3:211.
239. Goel S, Duda DG, Xu L, Munn LL, Boucher Y, Fukumura D, et al. Normalization of the vasculature for treatment of cancer and other diseases. Physiol Rev. 2011;91(3):1071-121.
240. De Bock K, Cauwenberghs S, Carmeliet P. Vessel abnormalization: another hallmark of cancer? Molecular mechanisms and therapeutic implications. Curr Opin Genet Dev. 2011;21(1):73-9.

241. Kim MS, Zhong Y, Yachida S, Rajeshkumar NV, Abel ML, Marimuthu A, et al. Heterogeneity of pancreatic cancer metastases in a single patient revealed by quantitative proteomics. Mol Cell Proteomics. 2014;13(11):2803-11.
242. Patricia Adamo CMC, Christopher P Neal,Vilas Mistry, Karen Page, Ashley R Dennison, John Isherwood, Robert Hastings, JinLi Luo, David A Moore, Pringle J Howard, Martins L Miguel, Catrin Pritchard, Margaret Manson, and Jacqui A Shaw. Profiling tumour heterogeneity through circulating tumour DNA in patients with pancreatic cancer. Oncotarget. 2017 8(50): 87221–87233.
243. Siurala M, Bramante S, Vassilev L, Hirvinen M, Parviainen S, Tahtinen S, et al. Oncolytic adenovirus and doxorubicin-based chemotherapy results in synergistic antitumor activity against soft-tissue sarcoma. Int J Cancer. 2015;136(4):945-54.
244. Raki M, Sarkioja M, Desmond RA, Chen DT, Butzow R, Hemminki A, et al. Oncolytic adenovirus Ad5/3-delta24 and chemotherapy for treatment of orthotopic ovarian cancer. Gynecol Oncol. 2008;108(1):166-72.
245. Alonso MM, Gomez-Manzano C, Jiang H, Bekele NB, Piao Y, Yung WK, et al. Combination of the oncolytic adenovirus ICOVIR-5 with chemotherapy provides enhanced anti-glioma effect in vivo. Cancer Gene Ther. 2007;14(8):756-61.
246. Majumdar S, Aggarwal BB. Methotrexate suppresses NF-kappaB activation through inhibition of IkappaBalpha phosphorylation and degradation. J Immunol. 2001;167(5):2911-20.
247. Cai WZ, Schaffer PA. Herpes simplex virus type 1 ICP0 plays a critical role in the de novo synthesis of infectious virus following transfection of viral DNA. J Virol. 1989;63(11):4579-89.
248. Liu ZQ, Kunimatsu M, Yang JP, Ozaki Y, Sasaki M, Okamoto T. Proteolytic processing of nuclear factor kappa B by calpain in vitro. FEBS Lett. 1996;385(1-2):109-13.
249. Oeckinghaus A, Hayden MS, Ghosh S. Crosstalk in NF-kappaB signaling pathways. Nat Immunol. 2011;12(8):695-708.
250. Inoue H, Tanabe T, Umesono K. Feedback control of cyclooxygenase-2 expression through PPARgamma. J Biol Chem. 2000;275(36):28028-32.
251. Karakhanova S, Mosl B, Harig S, von Ahn K, Fritz J, Schmidt J, et al. Influence of interferon-alpha combined with chemo (radio) therapy on immunological parameters in pancreatic adenocarcinoma. Int J Mol Sci. 2014;15(3):4104-25.
252. Loi S. Host antitumor immunity plays a role in the survival of patients with newly diagnosed triple-negative breast cancer. J Clin Oncol. 2014;32(27):2935-7.
253. Kotoula V, Chatzopoulos K, Lakis S, Alexopoulou Z, Timotheadou E, Zagouri F, et al. Tumors with high-density tumor infiltrating lymphocytes constitute a favorable entity in breast cancer: a pooled analysis of four prospective adjuvant trials. Oncotarget. 2016;7(4):5074-87.
254. Fridman WH, Zitvogel L, Sautes-Fridman C, Kroemer G. The immune contexture in cancer prognosis and treatment. Nat Rev Clin Oncol. 2017;14(12):717-34.
255. Tang C, Wang X, Soh H, Seyedin S, Cortez MA, Krishnan S, et al. Combining radiation and immunotherapy: a new systemic therapy for solid tumors? Cancer Immunol Res. 2014;2(9):831-8.

256. Weichselbaum RR, Liang H, Deng L, Fu YX. Radiotherapy and immunotherapy: a beneficial liaison? Nat Rev Clin Oncol. 2017;14(6):365-79.
257. Demaria S, Golden EB, Formenti SC. Role of Local Radiation Therapy in Cancer Immunotherapy. JAMA Oncol. 2015;1(9):1325-32.